

19th DOE/NRC NUCLEAR AIR CLEANING CONFERENCE

SESSION 4

**FILTERS, FILTER TESTING**

TUESDAY: August 19, 1986  
CHAIRMEN: H.J. Ettinger  
R.C. Scripsick  
Los Alamos Scientific Lab.

THE EFFECTS OF HIGH RELATIVE HUMIDITIES ON HEPA FILTER MEDIA  
B. Normann

HEPA-FILTER BEHAVIOR UNDER HIGH HUMIDITY AIRFLOWS  
C.I. Ricketts, V. Ruedinger, J.G. Wilhelm

CALIBRATION TESTS OF A LASER FLUORESCENT PARTICLE SPECTROMETER  
Ph. Mulcey, P. Pybot, J. Vendel

A NEW LIGHT SCATTERING SPECTROSCOPY TECHNIQUE FOR RAPID ASSESSMENT OF  
FILTER MEDIA  
Y.W. Kim

HEPA FILTRATION AND MONITORING SYSTEM FOR AN UNDERGROUND NUCLEAR  
WASTE REPOSITORY  
P.S. Parthasarathy, J. Shome

MEASUREMENTS OF REMOVAL EFFICIENCIES PERFORMED ON POWDER METAL AND  
FIBER METAL CARTRIDGES TO BE USED IN URANIUM ENRICHMENT FACILITIES  
AND GLOVEBOX EXHAUST DUCTS  
H.-G. Dillmann, W. Bier, G. Linder, K. Schubert

EXPERIMENT ON A MULTILAYER TYPE AIR FILTER FOR THE FILTRATION OF  
SODIUM AEROSOL  
N. Otake, O. Nozaki

DEVELOPMENT AT THE KARLSRUHE NUCLEAR RESEARCH CENTER (KfK) OF  
REMOTELY OPERATED FILTER HOUSINGS AND FILTER ELEMENTS FOR  
REPROCESSING PLANTS  
K. Jannakos, H.J. Becka, G. Potgeter, J. Furrer

OPENING COMMENTS OF SESSION CO-CHAIRMAN SCRIPSICK

This session promises to be a truly global look at the status of filter performance research, and the development of filter test methods. We have papers from Japan and Germany on the performance of high efficiency filters, and papers from Sweden and France on filter testing. As at the 18th Conference in Baltimore, the work being carried out in West Germany on extreme condition filter performance is well represented. We were reminded earlier this year of the importance of such filtration studies with an airborne radioactive material release from the Chernobyl plant. There are predictions that indicate that thousands of extra cancer cases may result from this release. High efficiency air filtration systems are often the last barrier to such releases. The proper design and operation of these filtration systems to a large extent depend on our understanding of filter performance, and the application of meaningful filter performance tests. The presentation of papers from United States and France on filter testing, as well as the activity in this area in Great Britain and Australia, indicates a worldwide interest in filter performance testing. Designing a meaningful performance test requires a broad understanding of filter performance. During this session I will be interested to hear from our speakers how they designed their filter test systems and how they used information on filter performance to design these systems. I will also be interested to hear what information the filter performance authors will have for those performing filter testing. We expect to hear about new and novel methods from the experts in filter testing and in filter performance.

## 19th DOE/NRC NUCLEAR AIR CLEANING CONFERENCE

### THE EFFECTS OF HIGH RELATIVE HUMIDITIES ON HEPA FILTER MEDIA.

Bård Normann  
Studsvik Energiteknik AB  
S-611 82 Nyköping  
Sweden

#### Abstract

The effects of high relative humidities and water on HEPA glass fiber filter media have been investigated.

The experiments also comprised exposure to pure steam for some hours at elevated temperature.

After exposure samples of filter media were dried and tested with respect to particle penetration and tensile strength.

The penetration measurements were carried out with DOP aerosols. The results showed a tendency to increased penetration when exposed to high humidities at elevated temperature.

The tensile strenght of the filter material decreased to about 40 percent of its original value after being exposed to flowing steam for 4 - 5 hours.

As expected the media lost their tensile strength in flowing steam (100 degr C) the strength decreased almost to zero.

Exposure for a few hours to approximately 100 percent humidified airstream at ambient temperatures did not cause any significant changes in the particle retention ability.

The strength was also unaffected by high humidities at ambient temperatures.

No damage to the fibres could be seen on examination in a scanning electronic microscope.

#### I. Introduction

The introduction of combined carbon- and HEPA filters in the offgas and emergency systems in Swedish nuclear power stations has reduced the folding height considerably.

The depth, or folding height, of the filter, se Figure 1, has thus been reduced from between 200 and 300 mm to about 70 mm, for the HEPA part of a combined filter.

This results in a decrease in the bending strength and thus a reduced tolerance with regard to higher pressure drops. A considerable increase in the pressure drop and reduced structural strength have also been observed across particle filters after loading to high humidities and then drying them;

this occurred in the filter material. Steam leakage, either small or large amounts in boiling water reactors, increases the risk for filter failures (3).

The aim with the work reported here (according to (4)) has been to gain a better understanding for the risk of filter failure in triple filters, or other similar installations; and also to determine the causes for filter failure as well as the effects of humidity on

- the structural strength of the type of HEPA filter incorporated in triple filters
- the penetration of DOP aerosol
- the structure of the filter material

## II. Test programme

### Types of material and filters

Two different filter material which are currently of interest for HEPA filters were studied. The materials are used as the filter medium in the off-gas and accident ventilation systems in Swedish nuclear power stations.

Both materials are glass fibre and are said to be resistant to damp, that is to say they can resist 100 % relative humidity during operation.

The fibres have been treated so as to resist the growth of bacteria, to be flame resistant and to withstand continual operation at 120°C.

One full scale HEPA filter, 610 x 610 mm was tested. It was intended for the triple filter installation, see Figure 1.

The filter comprised 70 pleats with aluminium separators and a pleat depth of 67 mm. The filter packet was housed in a plywood frame and neopren rubber glue was used as the filler material.



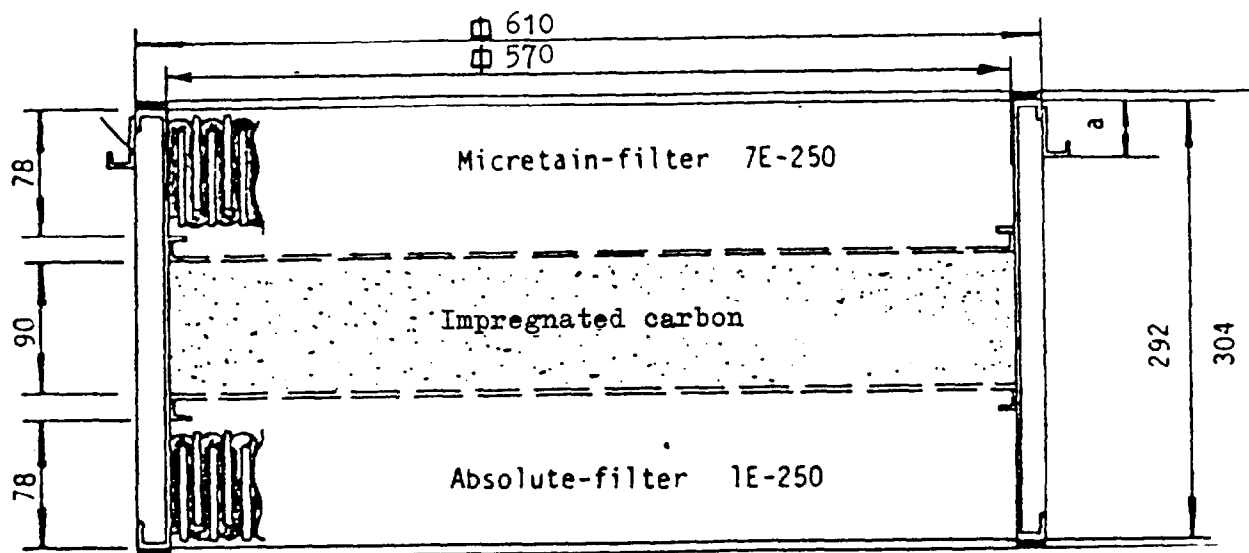


Figure 1. Exempel of a triple filter, manufacturer Camfil. Measurements in mm.

#### Test of filter material

Test were performed with filter material in damp air at between about 50 and 100 % RH in the temperature region 20 to 100°C, including pure steam.

The following material properties were studied

- the increase in penetration as a function of exposure to steam
- changes in the fracture strength as a function of time for steam exposure
- structural changes after exposure in moist air and steam.

## 19th DOE/NRC NUCLEAR AIR CLEANING CONFERENCE

### Tests of filter material

Test environment	Material	
	type 1	type 2
Varying humidity at ambient temperatures	x	
Moisture at elevated temperatures	x	
Moisture att 100°C	x	x
Condensed steam	x	
Water saturated	x	x
DOP	x	x
Mechanical strength	x	x

### Full scale filter tests

Tests performed on full scale HEPA filters:

1. Week-long tests at about 90 % RH.
2. 3 day tests at about 100 % RH.
3. Tests with water saturated filters.

### III. Test and measurement equipment

#### Tests of filter material

The equipment shown in Figure 2 was used to perform the material tests in moist air and steam. The temperature, humidity and flow rate can all be controlled.

In order to prevent condensation that part of the equipment containing flowing steam or a mixture of steam and air is insulated.

Temperature and flow rate regulation is manual, based on resistance control and valves. The temperature is measured using a wet and dry bowl mercury thermometer. The flow rate is measured using a Fisher & Porter rotameter.

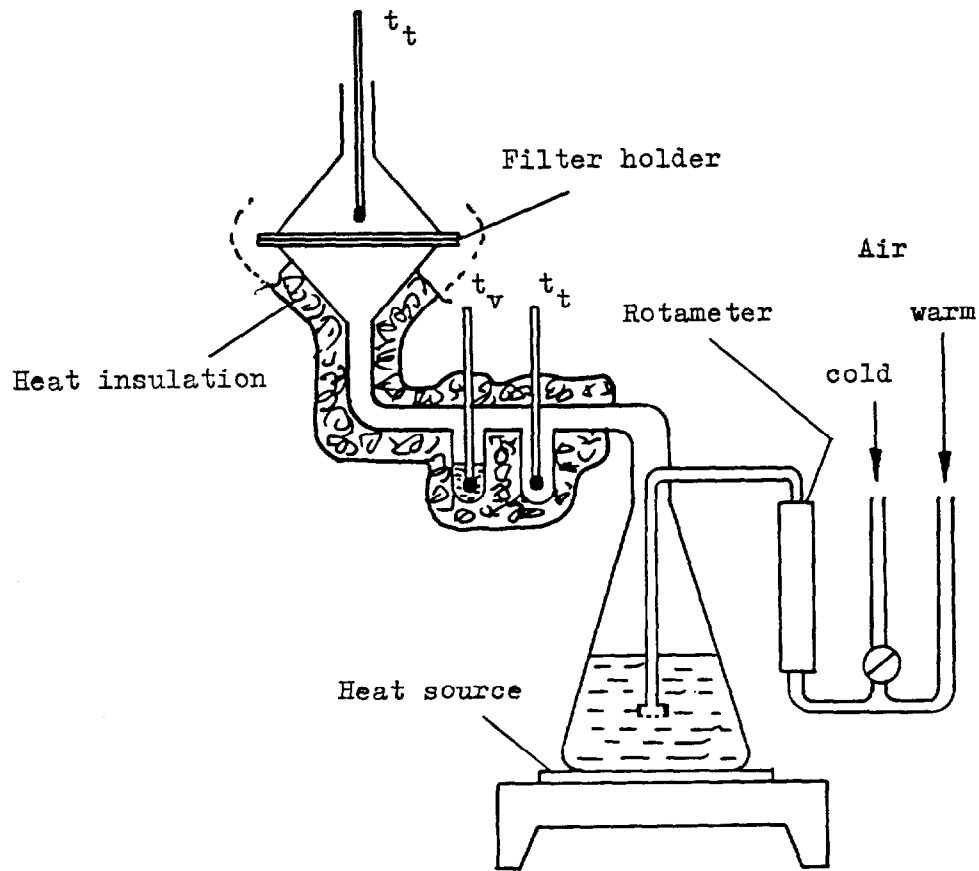


Figure 2. Apparatus for exposing filter material to varying temperatures and pressures.  $t_t$  and  $t_v$  are the dry and wet temperatures respectively.

The mechanical strength tests, Figure 3, are performed in air in which the flow rate can be increased successively until failure occurs.

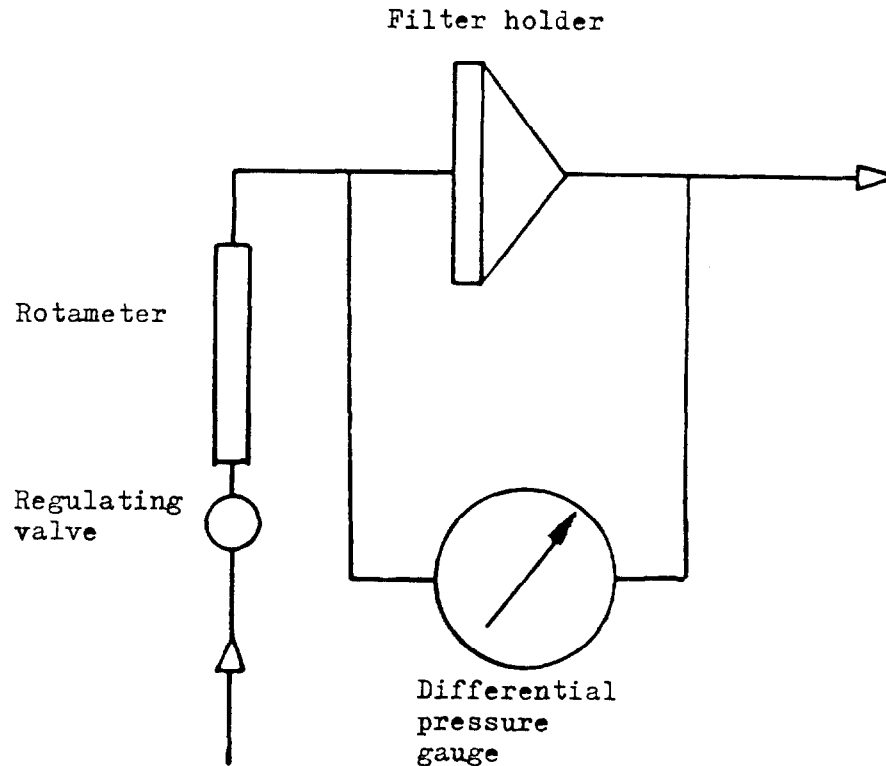


Figure 3. Apparatus for measuring the pressure drop and failure pressure across filter material.

#### Full scale filter test

The full scale tests of HEPA filters has been carried out in a rig in which the correct humidity and temperature can be attained and maintained automatically.

### IV. Results

#### Filter material

#### Tests in moist air and water at room temperature

A number of measurements of the pressure drops at high humidities and room temperature are shown in Table 1 and Figure 4. The results show that the pressure drop is almost constant up to about 90 % RH. Above that there is a marked increase, Figure 4.

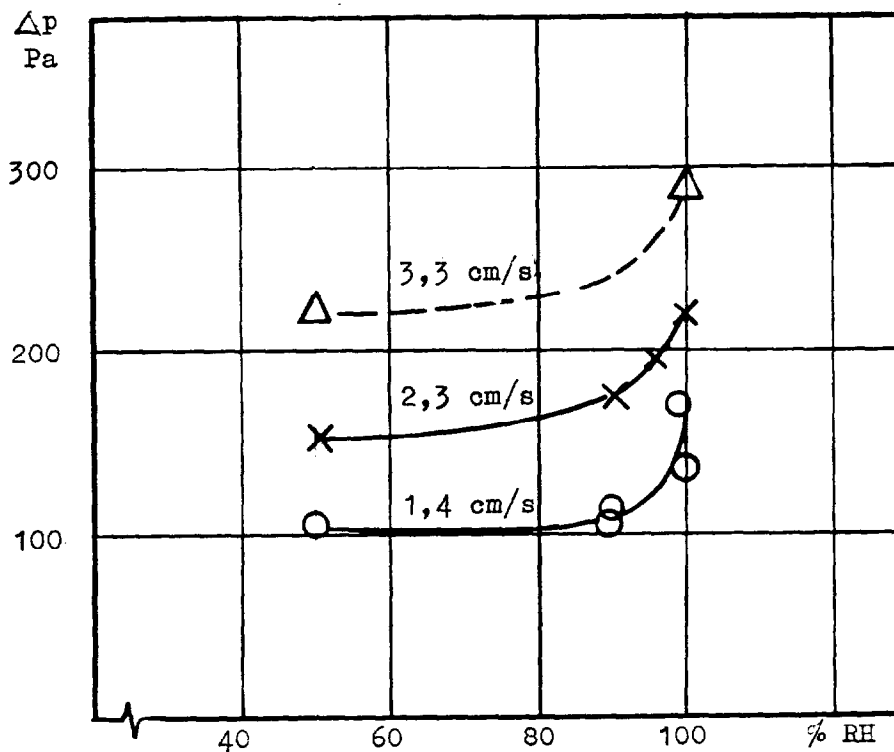


Figure 4. Pressure drop as a function of relative humidity for filter material type 1.

These tests, and tests in which the filter material is wetted in the ionized water for 6 days, show that no signs of change in the material structure could be seen using Scanning Electron Microscopy (SEM).

#### Material tests in moisture at elevated temperatures

Two tests at approximately 85 and 90 % RH at 85°C were carried out using material type 1. One test lasted 2 hours and the other one hour.

It is difficult to determine from the SEM micrograph, Figure 12, whether there is any damage to the fibres as a result of the relatively high humidity and temperature. On the other hand the mechanical strength has been affected.

# 19th DOE/NRC NUCLEAR AIR CLEANING CONFERENCE

Table 1. Pressure drop across filter material, type 1, exposed to flowing air.

Rel hum %	t°C l/min	Flow rate	v cm/s	ΔP mm vp
~90	20	-	1.43	10.8
50	20	14	1.41	10.4
50	20	23	2.32	15.6
50	20	32.5	3.28	22.4
95	20	22.5	2.32	16.8
100	20	13.4	1.35	13.8
100	20	22.4	2.30	22.0
100	20	27.8	2.80	28.4
90	20	13.4	1.35	11.2
90	20	13.4	1.35	13.8
90	20	13.4	1.35	10.8
90	20	14.6	1.47	10.8
97	20	13.4	1.35	16.8

Table 2. Mechanical strength after exposure to pure steam at 100°C. The material samples were dried prior to "pressure testing".

Pressure drop kPa at 28 l/min	Steam flow rate min	Failure pressure kPa
<u>Material 1</u>		
4.75	0	100
4.70	60	67
4.70	160	35
4.60	300	35
4.60	360	18
<u>Material 2</u>		
4.80	0	85
4.70	130	55
4.60	300	27

Tests in pure steam

Tests in pure steam, 6 in all with 2 types of material, were performed with a flow rate of approximately 13 l steam per minute. This gives a flow rate through the material of 1.3 cm/s, which corresponds to about 50 % of the flow rate through the filter during normal operations.

Measurement of the pressure drop after the material has dried does not show any significant difference between new material and material exposed to steam at 100°C, see Table 2.

Tests of mechanical strength

Tests of the mechanical strength have been carried out using material exposed to pure steam at 100°C. After drying, the specimens were mounted in a circular holder, diameter 42 mm, tilted with the means for measuring pressure and flow rate, see Figure 3.

The results, Figure 5 and Table 2, show that the fracture strength decreases markedly when the material is exposed to flowing steam for some time.

Both types of material had a reduction in failure pressure from about 1 bar to between 0.3 and 0.4 bar after drying.

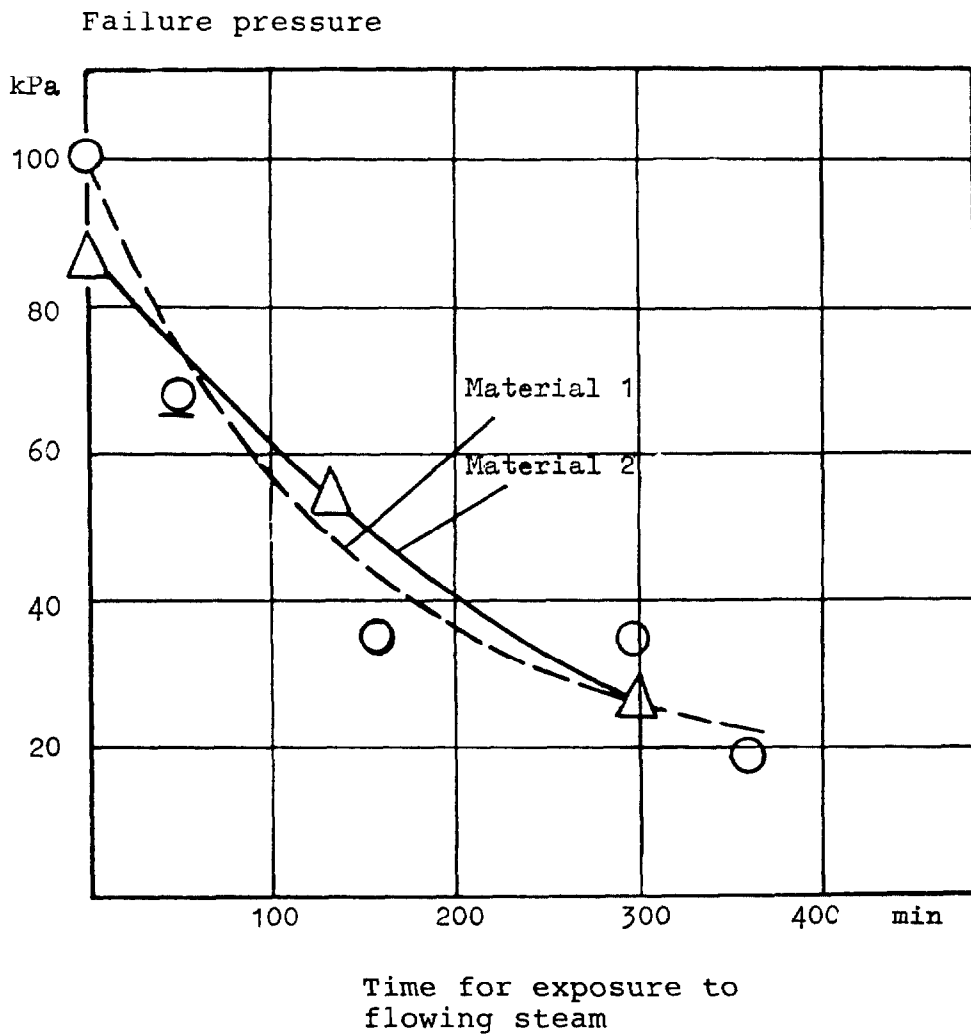


Figure 5. Filter material 1 and 2 mechanical strength sample after exposure to steam at 100°C and a flow rate of approximately 1.3 cm/s. The point 68 kPa/50 min is at about 90°C. The material was dried at about 50°C after exposure to the steam.



Penetration measurements

The tests were performed with DOP on filter material exposed to pure steam at 100°C. A poly dispersive aerosol and particle counter were used for the tests.

The flow rate for the penetration tests was 5.3 cm/s, which is about twice as high as during normal operation.

The filter material was dried in an oven at 50 - 60°C before measurements were made.

The results from the DOP tests indicate that there was an increased penetration, after the filter material had been exposed to pure steam at 100°C for some time, see Table 3 and Figure 6.

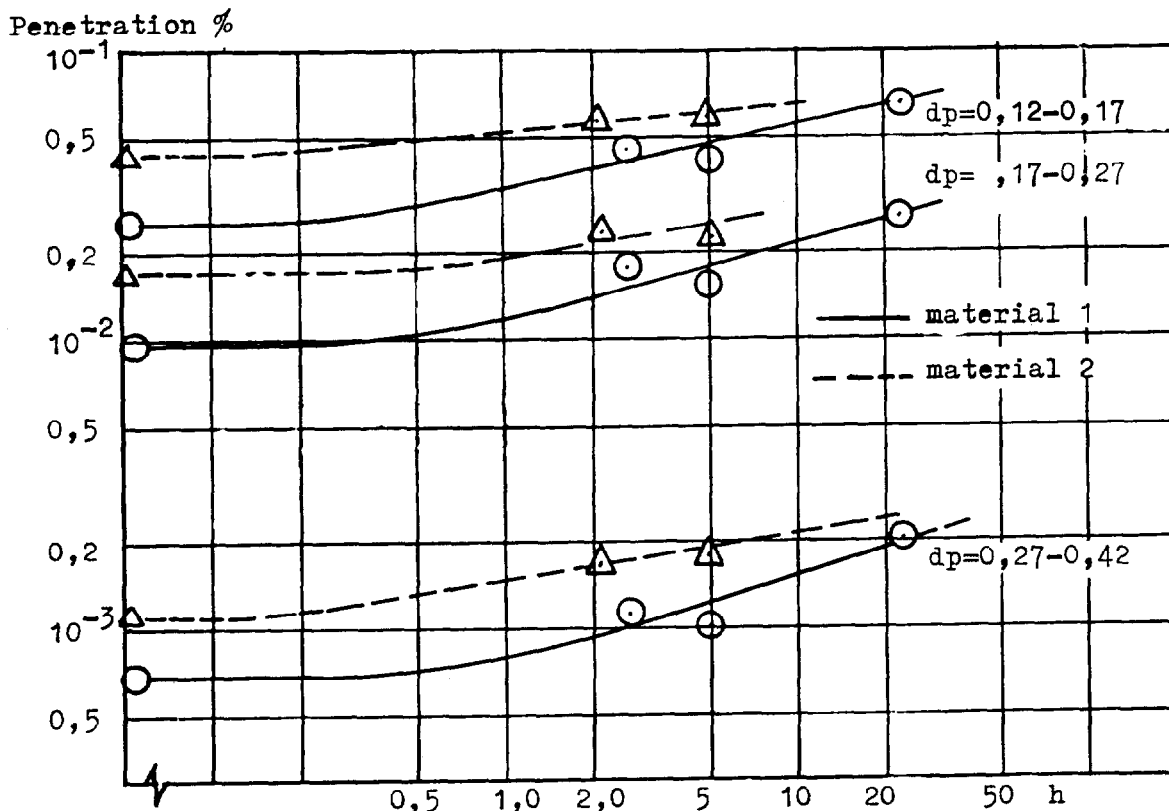


Figure 6. Increase in penetration measured after exposure to steam at 100°C and a flow rate of approximately 2 cm/s.  $dp$  in the diagram indicates the particle diameter during the penetration test.

### Shape changes

During exposure to the 100°C steam the material specimens had been mounted horizontally; the steam flowed from below. After a while the material deformed into an upturned hemisphere.

The height of the hemisphere increased with time, and was between 5 and 15 mm after 300 minutes exposure to the steam. The diameter of the specimens was 150 mm.

### Tests in condensed steam

Two tests were performed in condensed steam. 100°C steam flowing towards the filter ( $\sim 0.5$  cm/s) down stream from which cold air flowed. Thus the steam condensed in the material. Cracks appeared in the material during this test.

However after drying the remaining parts were mechanically tested and examined using SEM.

The fracture strength of 42 mm circle was about 0.2 - 0.4 bar, compared with 1.0 bar for new material. The results are comparable with these obtained in pure steam.

The SEM micrographs however do not indicate any notable changes in the structure of the material, Figure 11.

### Full scale filters

#### Tests in moisture at room temperature

The filter was run for a week with 90 % RH at ambient temperatures, and a further 3 days at 100 %. Measurements showed that there was no difference in the pressure drop before or after the prolonged exposure.

#### Tests in water saturated filters

The pressure drop across the water saturated filter as a function of the flow rate is shown in Figure 7. The filter was mounted horizontally and the air flowed from above it.

It can be seen that the pressure drop at 400 m<sup>3</sup> air/hour is about five times larger with water than without water. The pressure drop across a dry filter is about 200 Pa

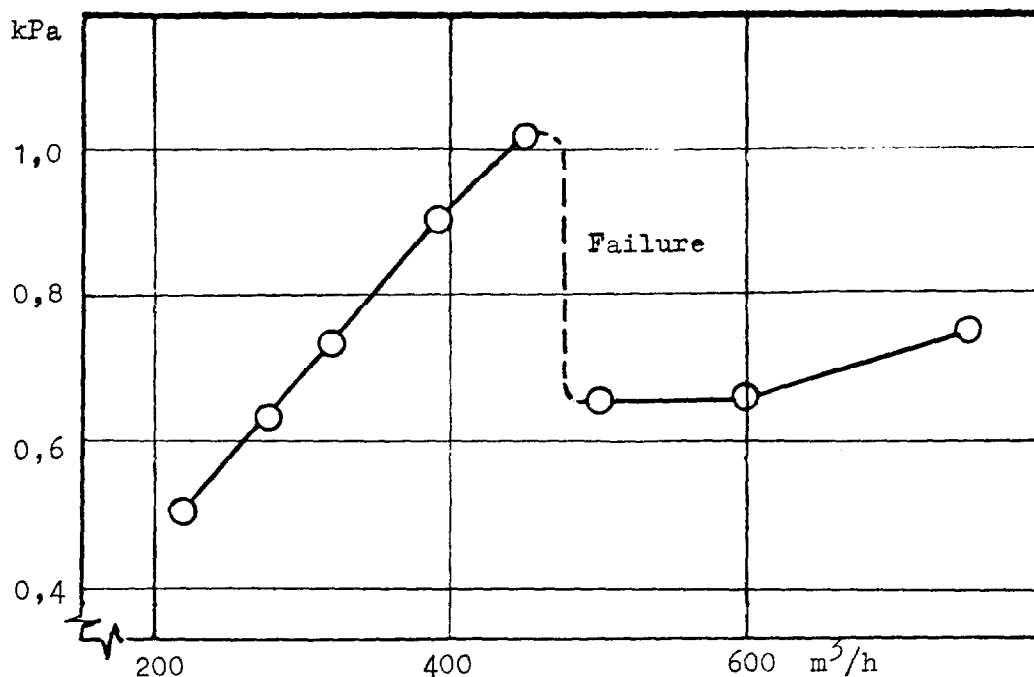


Figure 7. HEPA-filter "triple" design pressure drop after the filter was loaded with water.

During this test the filter contained about 7 l water. The water remained on the horizontal surfaces of the filter during the initial stage of the test.

At about  $450 \text{ m}^3/\text{h}$  and a pressure drop of more than 1 kPa the filter failed, Figure 8. This test shows partly that the material does not allow large amounts of condensate to pass through and partly that this in its turn increases the loading until it exceeds the failure level of the filter at moderate flow rates. As a comparison a standard HEPA filter, bed depth 294 mm, will survive 2.5 kPa or about 250 mm water.

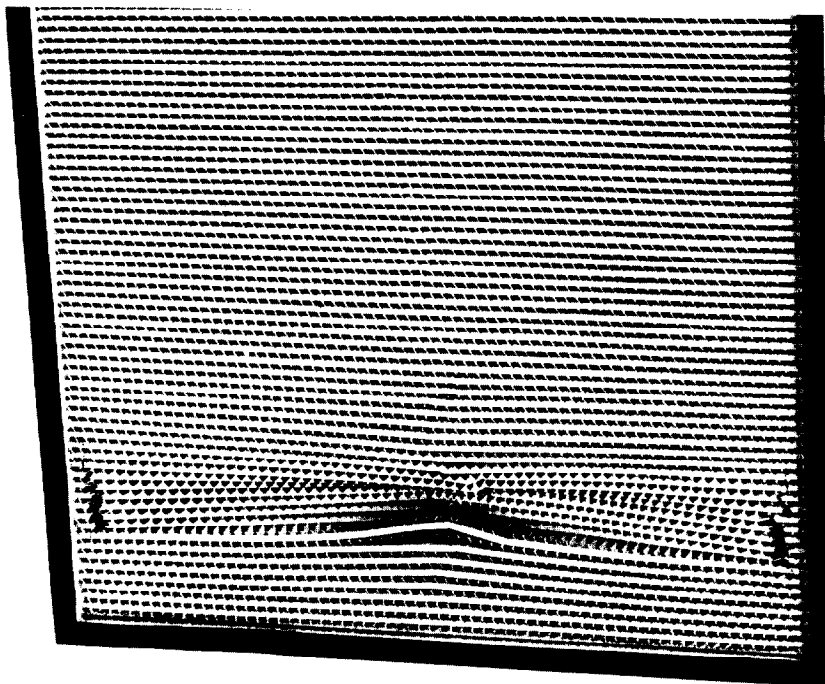


Figure 8a

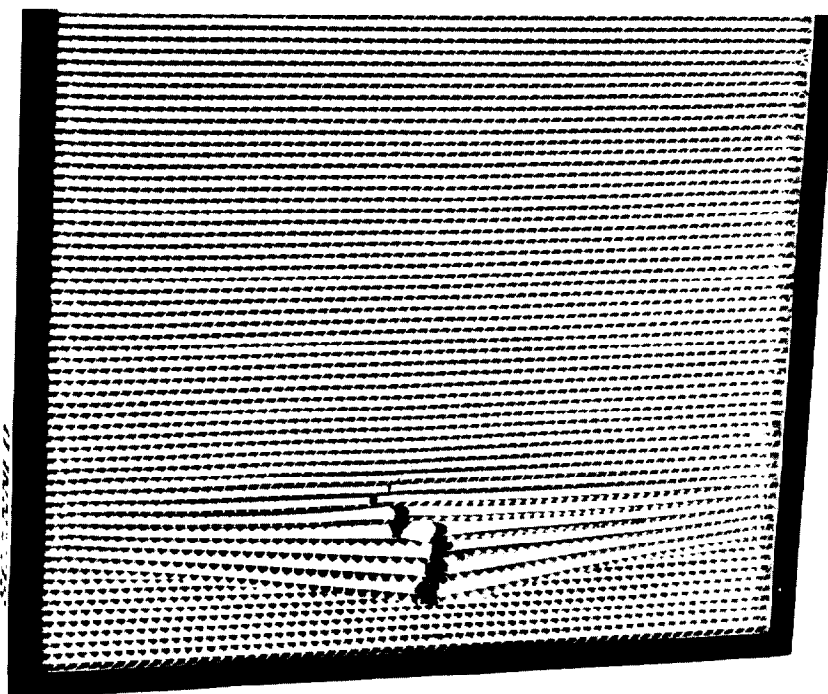


Figure 8b

Figure 8. Failure in HEPA-filter after loading with water and exposure to flowing air. Figure 8a upstream and 8b downstream from the filter.

## 19th DOE/NRC NUCLEAR AIR CLEANING CONFERENCE

### V. Comments

The following conclusions can be drawn from the results of the filter material tests in moist air and water:

#### Moisture at room temperature

Moist air,  $\leq 100\%$  RH, at about  $20^{\circ}\text{C}$  not had any noticeable effect on the filter material after short exposure times (hours).

#### Super-saturated air

When super-saturated air flows through the filter material at ambient temperatures and condensation occurs, the pressure drop increases significantly and the material can thus be temporarily overloaded. Overloading and material failure have occurred in boiler water power plants (3).

As noted in (5) an increase has been observed in the penetration during exposure to moisture at ambient temperatures.

#### Moisture at elevated temperatures

It has been found that HEPA filter material can almost completely lose its strength at high moisture levels and temperatures,  $85 - 90^{\circ}\text{C}$ . Exposure to moisture in the region  $20 - 85^{\circ}\text{C}$  has not been studied. However it is probable that the reduction in strength starts at temperatures lower than  $85^{\circ}\text{C}$ . The mechanical tests were performed after the material had been dried.

Moist and warm material has an almost negligible strength in this temperature region.

#### Steam and condensation at $100^{\circ}\text{C}$

In this environment the filter material is considerably weakened and can fail due to its own weight or in a minimal stream of air.

Filter material which is in practice also partially clogged by dust will probably absorb a larger amount of condensation. It will thus probably "blow" apart in a much less aggressive environment with regard to moisture and temperature even at low flow rates or pressures (6).

#### Moisture/water, long term exposure

Figure 13 shows deposits on the fibres. The test has not been repeated. However the fact that high moisture levels at moderate temperatures,  $20 - 40^{\circ}\text{C}$ , have an adverse effect on the material cannot be excluded.

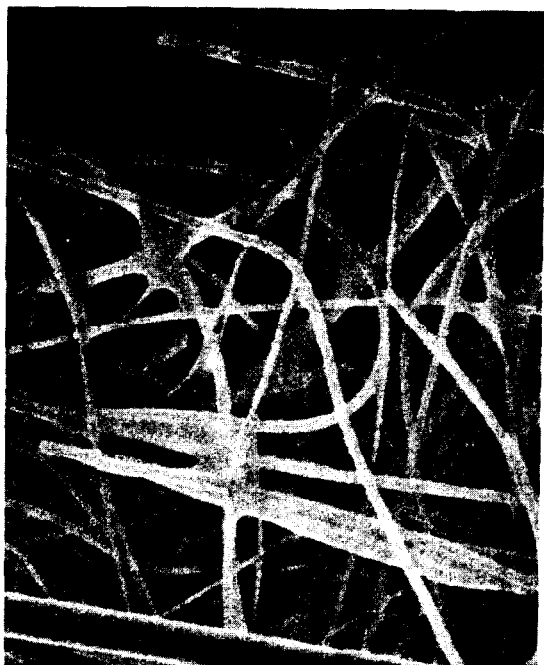


Figure 9. Reference Specimen, new filter material, type 1. Magnification x 2 000.

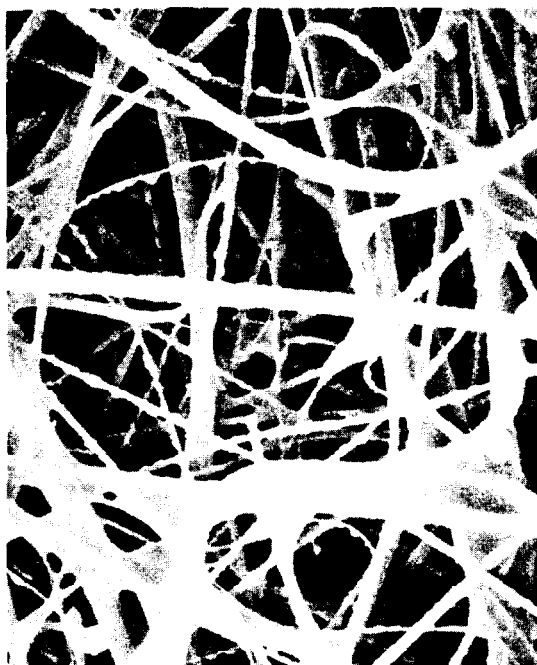


Figure 10. Filter material soaked in water for 6 days. The reason for the deposit on the fibres is uncertain.



Figure 11. Material type 1 after exposure to condensed steam for 2 h.



Figure 12. Material type 1 after exposure to an air steam mixture 85 % RH at 85°C for 2 h.

## 19th DOE/NRC NUCLEAR AIR CLEANING CONFERENCE

### Full scale filters

As expected the thinner HEPA filter has only moderate resistance to the pressure increase caused by water or condensation.

During prolonged operation with moisture levels of about 100 % an increasing quantity of condensed water can form a layer of water on the surface of the filter.

The filter material is very compact which results in the water remaining in the fibres. This in turn can result in an excessive load and ultimately to filter failure.

It should however be pointed out that the carbon filter in triple and combination filters, in which HEPA filters are usually used, are much stronger because of their plate design.

### VI. Future work

It is important to note the difference between the effect of moisture/condensation at ambient temperatures and at temperatures around 100°C.

In the current work the filter material has been exposed to moisture or water at various temperatures and pressures.

It has thus been shown that the mechanical strength of the filter material was considerably reduced after it had been exposed to moisture at higher temperatures.

The tests were only conducted on the HEPA part of the triple filter.

Since the triple filter is strengthened by the perforated plates which surround the carbon bed, a number of complementary tests of complete triple filters are planned. These tests will be performed at high pressures and temperatures, and also with air steam mixtures.

The work has been commissioned by the Swedish Radiation Protection Institute and will be performed in collaboration with Kernforschungszentrum, Karlsruhe, where there is a rig for testing at high temperatures and pressures (8)

# 19th DOE/NRC NUCLEAR AIR CLEANING CONFERENCE

Table 3. Penetration through the filter material after exposure to flowing steam.

Exposure time h	Particle size, $\mu\text{m}$			Average
	0.12-0.17	0.17-0.27	0.27-0.42	
<u>Material type 1</u>				
0	0.0254	0.0093	0.00066	0.0117
2.67	0.0449	0.0177	0.00112	0.0212
5.0	0.0419	0.0153	0.00103	0.0194
23.0	0.0648	0.0262	0.00202	0.0310
<u>Material type 2</u>				
0	0.0433	0.0171	0.00110	0.0205
2.17	0.0583	0.0246	0.00170	0.0282
5.0	0.0585	0.0227	0.00181	0.0277

## REFERENCES

1. NEA Group of Experts CSNI, Report on Air Cleaning in Accident Situations, Febr 1984.
2. RÜDINGER, V RICKETTS, C J and WILHELM, J, G Limits of HEPA-Filter Application under High-Humidity conditions. 18th DOE Conf, Baltimore, Aug 1984.
3. Normann, B Iodine and Particle Filter systems in Nuclear Power Stations, Functional requirements and tests. Studsvik Report NW-83/431 (1983) (In Swedish).
4. National Institute of Radiation Protection, Order Project SSI P271-84, Particulate filters at high humidity, 1984-05-15.
5. DAVIS, R J et al The effects of Moisture on the Character and Filtration of  $\text{UO}_2$ -Stainless steel Aerosols. Symposium, New York, Aug 1968. Treatment of Airbourne Radioactive Wastes.
6. NORMANN, B, WIKTORSSON, C Projekts on filter testing in Sweden. 18th DOE Nuclear Waste Management and Air Cleaning Conference.
7. Nationalinstitute of Radiation Protection Project SSI P313-85, Tests of Carbon/Particulate filters in accident situations.
8. RÜDINGER, V, ARNITZ, T H, RICKETS, C I and WILHELM, J G Bora - a Facility for Experimental Investigation of Aircleaning during Accident Situations.



19th DOE/NRC NUCLEAR AIR CLEANING CONFERENCE

DISCUSSION

SCRIPSICK: The penetration measurements that you showed seem rather high, going up to about 0.05% penetration. Is that normal for this type of filter system?

NORMANN: Not for the system, but maybe for the filter media. I can not give you any explanation for this high penetration at the moment. The tests were done with a polydisperse aerosol and the penetration of 0.05 percent refers to very small particles. The penetration decreases with increasing particle size.

SCRIPSICK: My experience with nuclear grade filters suggests that penetration is fairly high, even with the 0.12 to 0.17 m aerosol.

NORMANN: Yes, I noticed that and will look it over. You can see that we have an increase from lower humidity to higher.

WILHELM: Would you indicate the upstream and downstream side of the filter? Is the upstream side the HEPA filter or the prefilter?

NORMANN: In operation, the upstream side is the prefilter, and then you have the carbon filter, and after that you have the HEPA filter.

WILHELM: Our experience has been that small particles pass the prefilter and pass on to the HEPA filter. Now, if the small particles absorb iodine, this iodine will deposit on the HEPA filter but it won't stay there long because it leaves the HEPA filter by oxidation and desorption and will be released. We experienced that in our hot cell work. If you use only a prefilter in front of the carbon filter, I think you won't have good removal efficiency for iodine.

NORMANN: I have not heard about this before. The prefilter is to protect the HEPA filter. When they designed and constructed the filters, I think they divided them into two parts, iodine and particles. No particles stayed in the carbon, all particles stayed in the HEPA, and no iodine reached the HEPA filter. That was the philosophy in Sweden at the beginning.

HEPA-FILTER BEHAVIOR UNDER HIGH HUMIDITY AIRFLOWS\*

C.I. Ricketts, V. Ruedinger, J.G. Wilhelm

Kernforschungszentrum Karlsruhe GmbH  
Laboratorium für Aerosolphysik und Filtertechnik  
Postfach 3640, D-7500 Karlsruhe 1  
Federal Republic of Germany

Abstract

A loss-of-coolant accident could threaten the integrity of the HEPA filters in the air cleaning systems of a nuclear power reactor with airflows of high humidity, elevated temperature, and greater than design flow rate. It is important that filter reliability be assured during accident situations since a loss of filter integrity could result in a loss of containment.

A review of the literature concluded that existing countermeasures are either not being fully taken advantage of or are not preventing humidity related filter failure in, for the most part, routine service. The development of filters with greater pack stability and structural strength was judged to be necessary for accident conditions that would involve high humidity airflows.

The average failure differential pressure at 1700 m<sup>3</sup>/h for three commercial filter designs under conditions of high air humidity at 50 °C were found to lie between 0.7 and 7.6 kPa. The modes and mechanisms of structural failure were determined for wooden frame deep pleat filters, the design with the most potential for improvement. Initial tests of prototype filter units with a glass fiber medium reinforced by fiber glass cloth proved that structural limits could be increased to a least 10 kPa even with significant decreases in the lateral stability of the filter pack. A similar test of a prototype filter equipped with a special arrangement of the separators and a conventional glass fiber medium showed that pack stability could be maintained during fog conditions that cause failure of conventional glass fiber filters within several hours.

Initial investigations of the water vapor sorption characteristics of glass fiber filter media at 25 °C showed that a dust loading can increase the adsorbed water content in a filter medium by up to a factor of 50 at 97 % r.h.

\* Work performed under the auspices of the Federal Ministry of the Interior under Contract No. SR 290/1.

## I. Introduction

Despite the advanced stage of development and the high levels of performance exhibited by today's commercial High Efficiency Particulate Air (HEPA) filters, reports of moisture related filter failure in nuclear facilities, for the most part during routine service, still appear persistently in the literature /1-7/. The susceptibility of glass-fiber HEPA filters to deteriorations in performance resulting from exposure to humid airflows remains an undesirable and only partially mitigated filter characteristic. As part of the barrier between contaminated zones and the ambient environment, the relatively fragile HEPA filters must be depended upon to perform at design specifications not only during normal operations but also under abnormal operating conditions.

Steam released by a Loss of Coolant Accident (LOCA) /8,9/ or water sprays activated during a fire /9,10/ or LOCA /5,11/ could introduce large quantities of moisture at elevated temperature into the air cleaning systems of a nuclear facility. Filter reliability during such accident conditions is brought into serious question by the reported occurrences of moisture-related filter failure during more routine operations.

A recent study of the literature on the topic of air cleaning in nuclear accident situations /8/ found a lack of information concerning the influence of particulate loading, long term moisture exposure, and filter aging on filter response to high humidity airflows. In a progress report on ongoing filter testing /12/ it was concluded from a literature survey that for dust loaded filters in particular, filter behavior is not documented well enough to assure filter reliability during accident conditions that would involve humid airflows.

Filter reliability depends foremost upon the preservation of filter structural integrity. Assurance of filter reliability requires that filter structural limits not be exceeded by the mechanical loads acting upon filters at their service locations. Values of filter structural limits and mechanical loads are prerequisites to the calculation of realistic safety margins for abnormal or accident conditions.

For practical reasons, the structural limits of individual components such as filters are measured in test facilities. The mechanical loads placed on components in an accident situation can be estimated by the use of computer codes that numerically model the fluid-dynamic and thermodynamic conditions that would prevail in the air cleaning system during the accident/13/. For accurate predictions from such codes, experimentally determined flow-resistance characteristics of individual components are indispensable as input data.

To realistically assess the reliability and the safety margins of in-service HEPA filters under exposure to high humidity airflow, necessitates a knowledge of filter structural limits and flow resistance characteristics under the relevant conditions of

operation, and the availability of a suitable computer code for modeling fluid-dynamic and thermodynamic transients in air cleaning systems. Should improvements in filter structural strength be judged to be necessary, the modes and mechanisms of moisture related filter failure would then also become important.

## II. Literature

### Parameters Governing the Incorporation of Water into the Filter Medium

Moisture induced deteriorations in filter performance and filter structural failure result principally from the presence of liquid water in the fiber structure of the filter medium. The incorporation of water into the filter medium from the airstream can occur by sorption, condensation, or the filtration of water droplets, depending upon the water content of the air /12/.

It is to be assumed that various parameters of the airstream and of the fiber structure influence the moisture content of the filter medium at equilibrium, as well as the rate at which the moisture content attains an equilibrium value. Among these would be the temperature, velocity, and moisture content of the airstream. Relevant characteristics of the fiber structure would include the material, the fiber diameter, the porosity, the water repellency, the particulate loading, and the drainage properties. However, the degree to which and the ranges of values for which these parameters influence the transfer of water into and out of a HEPA-filter medium remain yet largely undocumented in the literature. Summarized below are some of the investigations that have been found to be pertinent.

Sorption: Isotherms and Kinetics. For an air relative humidity,  $\phi$ , between 0 and 100 %, physical sorption is responsible for the water bound on the surfaces and in the pores of a glass-fiber filter medium. The airborne water vapor, the filter medium, and the surface-bound water correspond in the sorption process to the adsorbate, the adsorbent, and the adsorpt, respectively. One measure of the hygroscopic behavior of an adsorbent is the sorption isotherm. This is defined to be the equilibrium moisture content, at constant temperature,  $\theta$ , of a sorbent as a function of  $P_d/P_s$ , the ratio of the sorbate partial pressure to the sorbate saturation pressure, which is equal to  $\phi$  /14/. Adsorption measurements are normally made by either volumetric or gravimetric methods /15/. The units commonly used for the moisture content of the sorbent,  $\psi$ , are g H<sub>2</sub>O/100 g dry sorbent.

Brunauer et al. /16/ have classified sorption isotherms in the five major groups illustrated in Fig. 1. The characteristic shapes can provide information about the sorption phenomena involved and the ranges of  $\phi$  for which they dominate.

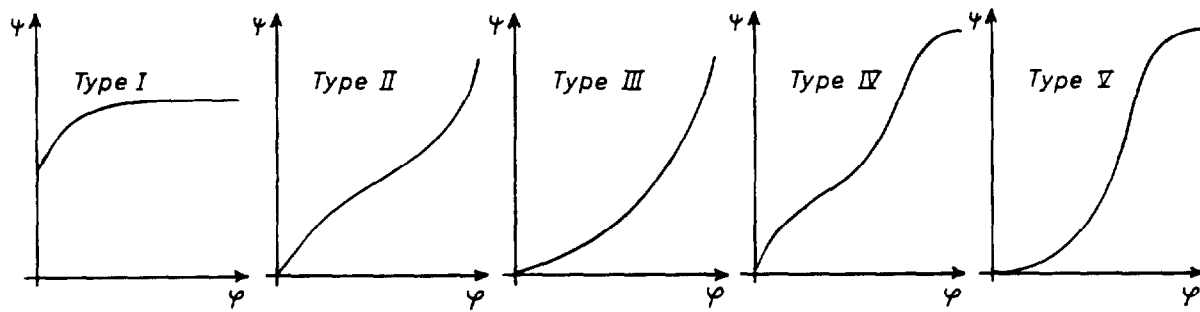


Fig. 1: Classification of Sorption Isotherms from Brunauer, Deming, Deming, and Teller /16/.

In the general case of a type-II isotherm as shown in Fig. 2, monolayer sorption, multilayer sorption, and capillary condensation dominate in respective ranges of  $\phi$  which are marked by changes in curve slope /17,18/. Due to hysteresis, the desorption curve for a given material generally exhibits a greater moisture content than the adsorption curve.

Studies by Kadlec and Dubinin /19/ of capillary condensation in microporous glass at 20 °C yielded type-IV sorption isotherms for 0-100 % r.h. with large hysteresis loops above 40 % r.h. and maximum  $\phi$  values of about 20 %. The effects of various surface and heat treatments in limiting the adsorption of water vapor on porous glass has been reported by Kawasaki and coworkers /20/. For type-II isotherms at 30 °C and up to 75 % r.h., the maximum values of  $\phi$  for untreated surfaces lay under 3 % and some were reduced by almost one-half after treatment.

Type-II adsorption isotherms for two different presumably clean, unspecified filter papers /17,21/ showed  $\phi$  at 90 % r.h. and 20 ° to be on the order of 10 % for both. For the captured particulates on slightly loaded glass-fiber sampling filters, Tierney /22/ published type-III adsorption curves that at 100 % r.h. and 22 °C show  $\phi$  values between 40 and 90 % depending upon particulate type. Capillary condensation was evident at 50 % r.h. Equivalent type-III isotherms for the loaded filters themselves displayed a maximum of 8 % for  $\phi$ . Clean filters exhibited no apparent adsorption of water vapor. Type-II isotherms from Hofmann /23/ for a number of clean and slightly loaded HEPA filters at 97 % r.h. and 20.5 °C had values of  $\phi$  equal to 2 and 8 %, respectively. The maximum  $\phi$  due to hysteresis for the dust loaded filter units was a factor of 10 greater than that of the clean units. Capillary condensation began to dominate at 70 % r.h. with clean and at 60 % r.h. with loaded units.

These studies illustrate that  $\phi$  at equilibrium can significantly depend on current and prior  $\phi$  as well as the structure or composition of the glass or particulate adsorbent. Less well documented are effects of other parameters. For a given value of  $\phi$ , the moisture content of an adsorbent generally decreases with increasing temperature /17,21/. Although adsorption can be mea-

sured for an adsorbent in an airstream /14/, it is probable only for large, yet uninvestigated values of  $\phi$  and superficial velocity that the amount of adsorbed water in capillaries could be influenced aerodynamically.

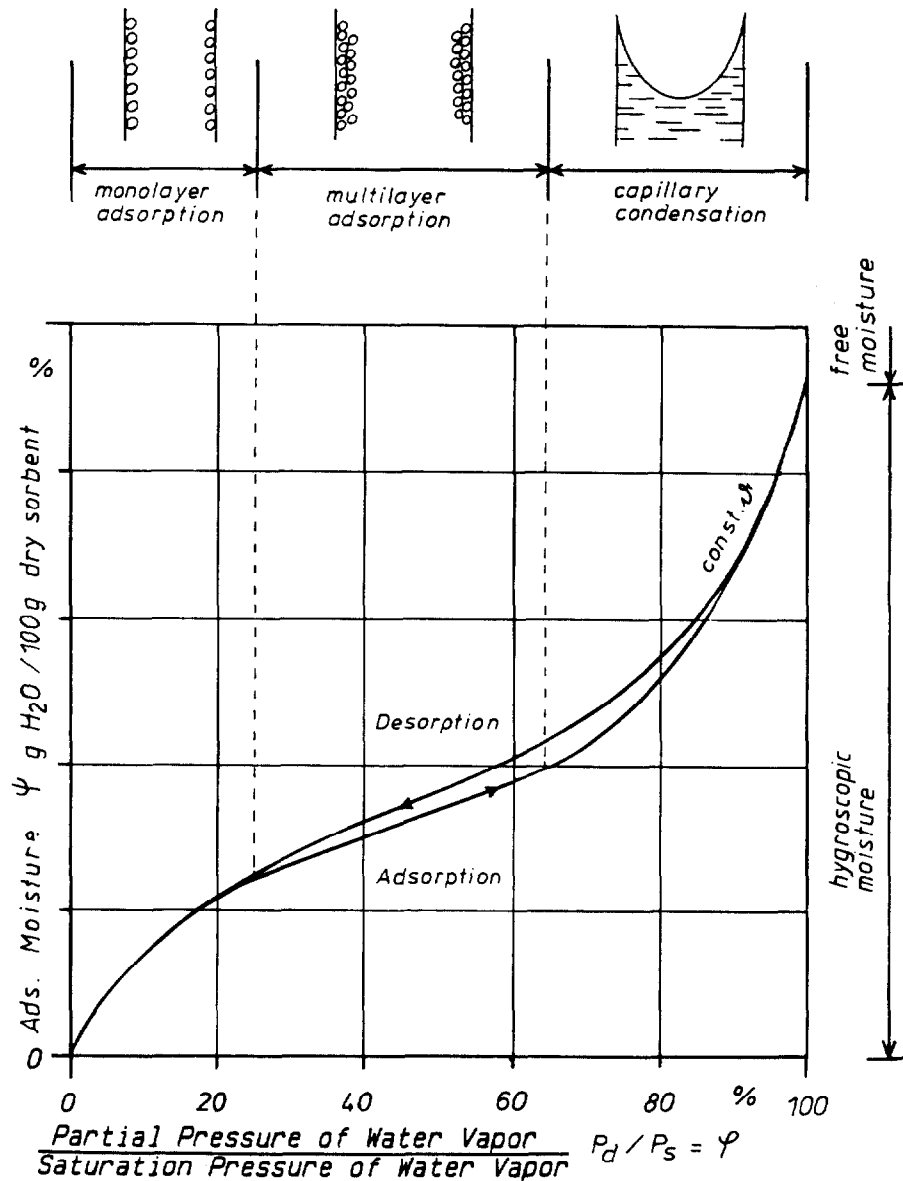


Fig 2: Type-II Sorption Isotherm and Sorption Phenomena /18/.

In addition to the equilibrium values of  $\phi$ , sorption kinetics (see 24), in particular the rates at which equilibrium is attained at constant  $\phi$ , are also relevant. However, even sorption kinetics in general have been topics of very few published experimental investigations. The rate of physical sorption usually increases with temperature / 25/ and most likely with increasing

velocity of an adsorbate through a porous adsorbent. The influence of  $\phi$  and the surface properties and structure of glass fibers on sorption kinetics do not appear to have been investigated yet.

Condensation. Condensation of airborne water vapor onto filter fibers as free water will occur during any time that the dew-point temperature of the air exceeds the temperature of the fibers or at  $\phi = 100\%$  r.h., both unstable states in an airstream. Practically, these two special cases can exist in an air cleaning system for short periods of time and only under transient conditions. Nevertheless, saturation of a filter medium by condensation cannot be ruled out. The amount of water incorporated and the rate of incorporation would then depend upon the rate and duration of condensation as well as the water repellency, drainage characteristics, and capillary structure of the filter medium. The airstream velocity would also become important in the rate of water transfer from the downstream side of the filter medium back to the airstream by reentrainment.

Droplet Filtration. For airstreams with a water content above that corresponding to 100% r.h., filtration of entrained water droplets by the filter will also lead to the incorporation of free water into the filter medium. The rate and extent of water incorporation are dependent upon the duration of exposure to the droplet flow and also the concentration and size distribution of the droplets. Additional factors include the filtration efficiency as well as the other filter medium parameters and the airstream velocity as noted above for the case of condensation.

For filter units in continuous service, Burchsted /9/ proposed for the water content of the filter medium a maximum allowable value of 25 g of  $H_2O$  per  $m^2$  of filter medium surface area, said to correspond to a liquid water content in the airstream of 24 g of  $H_2O/m^3$  of air, at design flow rate and equilibrium conditions. Since these values took increased water retention due to dust loads and filter aging into account, values twice as large were said to be permitted for clean new filters at equilibrium. The recommended maximum diameter of airborne water droplets allowed to reach HEPA-filter units in continuous service was given as 1  $\mu m$ . In comparison with curves from Ruedinger /12/ for  $\Delta P$  as a function of air humidity, the value of 24  $g/m^3$  seems to be somewhat high.

#### The Effects of Moisture on Filter Performance and Construction Materials

Moisture degrades the performance of HEPA-filter units through detrimental changes in the properties of filter construction materials, especially those of the glass-fiber filter medium. Surveys of reports that deal with the moisture effects on filters have appeared elsewhere /8,9,12/ and altogether draw upon such a large number of sources that the brief summary presented here will at times refer to these surveys rather than directly to each original publication.

Filter Medium. The presence of moisture in a clean glass-fiber HEPA-filter medium can effect an increase in the pressure drop /26,27/ and the weight /28/ as well as a decrease in the tensile strength /12,8,29/ and the filtration efficiency /30/ of the medium. The degree to which these changes occur has been shown to increase with decreases in the water repellency of the filter medium /26-28/. Factors which can significantly reduce the water repellency include dust loading /26,27/, aging /31/, creasing /31/, and gamma radiation /27/ of the medium. How water repellency is influenced by moisture exposure time and temperature remains yet unknown. A number of studies have shown that the surfaces of glass fibers can slowly dissolve in water solutions (see 32 and his citations 96, 107, and 103). To what extent the organic binder and water proofing agents inhibit this process also remains yet to be determined.

Increases in pressure drop from about 0.5 to 4 and 4.6 kPa at 100 % r.h. and 30 °C after 7 h were reported by Jones for specimens from filter units loaded during, respectively, 7 and 48 months of service /27/. In one test, Peters measured a maximum of 10 kPa for a clean water repellent sample after 22 h in a wet steam flow at 100 °C and design flow rate /26/. Both authors found a tendency toward more rapid and greater increases in  $\Delta P$  as well as lower values of water repellency for dust-loaded filter papers. Filter medium samples measured by Schwalbe in steam-air mixtures at 65 °C and 4.5 times rated flow showed in one case a maximum value of 2.5 kPa after 12 min of exposure. A non water repellent sample burst at 3.8 kPa after 5 minutes. After 2 h the weight increase due to water loading of the undamaged samples ranged between 64 and 460 % /28/.

Published decreases in tensile strength of clean wet samples of filter medium compared to dry ones have ranged from 35 to 70 % /12,29/. Tests of wet dust-loaded specimens do not seem to have been reported. Decreases of up to 35 % in the tensile strength of clean, dry samples were measured by Jones /27/ after exposure to  $5 \times 10^7$  rad. Similar doses of gamma radiation were also found to reduce the relative water repellency of equivalent samples by up to 100 times. Reductions in tensile strength of up to 60 % /33/ and 70 % /31/ for new dry filter media have been attributed to the creases formed in folding the media during filter manufacture. Values for similar samples from used filters showed decreases of up to 80 % /31/. Water repellencies of both new and used media were determined to be 40-60 % lower for samples that contained creases. Aging has accounted for decreases in tensile strength of up to 5 % for unfolded and up to 26 % for folded dry specimens from filters taken out of normal service /31/. Water repellency also decreased due to aging by some 20 % for those samples without creases and 40 % for those with. Although such deteriorations in tensile strength and water repellency represent more extreme cases and are not necessarily cumulative they provide an outline of the challenges posed to the integrity of filter media in service.

Storage of samples of HEPA-filter media up to 48 h at 100 % r.h. and 80 °C have led to increases of up to one order of magnitude in the penetration by  $U_2O$ -stainless steel aerosols /30/. This



was attributed to an increase in effective fiber diameter due to a drawing together of small filters into wetted bundles with filtration characteristics of larger fibers. Here also, water repellent media showed less susceptibility to moisture effects. Similar decreases in the filtration efficiencies for the same aerosols in humid as compared to dry airflows at a 5-cm/s superficial velocity were presumed to be due to moisture-induced shrinkage of agglomerates into more penetrating sizes. A laser spectrometer was used by Deworm /34/ at 20 °C and 100 % r.h. to measure the penetration of DOP, NaCl, and uranine aerosols with diameters of 0.09-0.3  $\mu\text{m}$  through clean HEPA filter units. In spite of the questionableness of using a liquid or a water soluble aerosol at high humidities, results for all three aerosols were of the same order of magnitude and showed an average decrease of some 45 % in penetration in comparison with values at 26 % r.h. Possible explanations for the results were not discussed. Ensinger has reported on the development of a method which will employ a  $\text{TiO}_2$  aerosol to measure HEPA filtration at high humidities /35/. This method should fill a large gap in knowledge for actual filtration behavior of full-size filter units during accident situations.

Filter Construction Materials. The effects of moisture on filter construction materials other than the filter medium can include the corrosion of aluminum separators /31,38/ or metal frames /9/. Also reported have been the softening of asbestos separators /9,36/, the swelling of wooden frames, and the separation of pack adhesives from wooden frames /12,37,38/. The availability of suitable corrosion resistant materials such as stainless steel and surface treated aluminum or steel make the prevention of these types of deteriorations primarily matters of cost and of procurement specifications.

HEPA-Filter Units. The principal reported undesirable effects of humid airflow on full-sized filter units are differential pressure increases and structural failure /9,12/, both attributed to water in the filter medium. Ruedinger /12/ published curves for equilibrium differential pressure as a function of air relative humidity and liquid moisture content at design flow rate and 50 °C. Values as large as 9 kPa for clean filters exposed to fog and 7.5 kPa for service loaded filters subjected to saturated airflow were observed. Filter  $\Delta P$  as a function of accumulated water mass in clean filter units exposed to water aerosols at 20 °C have been reported by Fenton /39/. In one case the differential pressure rose up to 1.5 kPa at reduced flow rate after 27 h and corresponded to a mass of 3.4 kg of water in the medium and the asbestos separators of the filter. At approximately 97 % r.h. and 20 °C Hofmann /40/ found the  $\Delta P$  of a slightly loaded filter to be 300 % greater than that of a clean unit. Stratmann used a liquid water aerosol to load 11 clean HEPA filters of various types up to 1.2 kPa /38/. The time required varied between 4 and 40 h. Two additional filter units investigated showed little increase in  $\Delta P$ . Steam-air mixtures at 3 times the design flow rate and 80 °C were used by Jones /41/ to test model filters constructed with filter medium removed from full-size filters following service periods of 4-13 months. The  $\Delta P$  of one filter increased to 6 kPa after less than 5 min. of exposure. Collins and

coworkers /42/ demonstrated the effect of pleat orientation to water entrained airstreams on  $\Delta P$  by tests of two filters, in tandem with respective prefilters, exposed to water droplets of 1 to 10- $\mu$ m diameter at initial flow rates of close to 1700 m<sup>3</sup>/h. The differential pressure of the filter in the upward vertical flow, despite exposure to 40 % less entrained moisture, had an initial-flow-rate equivalent  $\Delta P$  twice as large as the filter in the horizontal flow. Other authors have measured filter  $\Delta P$  increases in humid airflows ranging from some Pa to several kPa /see 12/ often without repeatable or comparable results.

The wide variations in the extent and rate of reported  $\Delta P$  increase can be attributed to the difficulties encountered in the accurate measurement and control of high humidities in an airstream, as well as the extreme sensitivity of filter  $\Delta P$  at air humidities close to and above saturation. The ranges and strong influences of dust loading and water repellency on the incorporation of water into the filter medium also contribute to the inconsistency of published results. Tests performed at other than constant flow rate also make comparisons difficult. A reasonable judgment is that values of  $\phi$  from 95 to 100 % r.h. at  $\theta \leq 50$  °C can lead to differential pressures of up to 5 kPa across dust loaded filters at design flow rate in less than 24 hours of exposure. Likewise, airstreams with liquid moisture contents of about 10 g/m<sup>3</sup> can produce similar  $\Delta P$  across clean filter units despite the use of a water repellent medium. These values for design flow rates may still be subject to some revisions. Corresponding values of  $\Delta P$  and humidity for filters in vertical airstreams or with horizontally oriented pleats or at higher than design flow rates require further investigation.

The structural limits for a total of 7 HEPA filters given by various authors and compiled in one literature survey /12/ lay between 0.6 and 2.5 kPa. Ruedinger reported differential pressures at failure which ranged between 1.7 and 9 kPa for 15 deep-pleat filters /12/. Analyses of the modes and respective underlying mechanisms of structural failure were discussed for filters with wooden frames and those with metal frames and pack-to-frame sealants of glass fiber.

Documentation of moisture damage to deep-pleat filters with elastomeric /12,36,38/ and glass fiber /12/ sealants as well as to separatorless /43/ and mini-pleat V-type filters /38,43/ have been published. The reported loosening of the filter pack /12,38,43/ and the transverse tearing of folds close to the top or bottom of the pack /12/ resemble damages sustained by filters during high temperature exposure /44/ or during handling and shipment /45,46/. The ruptures at the downstream ends of the pleats in the medium during exposure to humid airflow /12/ have also been observed for filters under high differential pressure /33,47/, at high temperature /44/, and after shipment /36,46/. The occurrence of the same failure modes under such different conditions serves to point out the locations of structural weakness and instability in deep-pleat filters. A similar argument can be made for the mini-pleat V-type filters which in general are structurally weaker than the wooden frame deep-pleat filters /38,43,47/.

### Countermeasures

An important measure taken to counter many of the effects of moisture on HEPA-filter units was the development of water-repellent glass-fiber filter medium. However, dust loading, creasing, radiation, and aging of the medium can compromise the effectiveness of present water repellency treatments, as noted previously.

Metal fiber demisters located upstream of HEPA filters have been shown to be effective in protecting new, clean and slightly loaded filters from damage by water entrained airstreams /see review in 8,12/. Reported structural failures of dust loaded test filters at less than 100 % r.h. /12/ confirm the need for air heaters downstream of the demister to lower the relative humidity of the air upstream of the filter as, for example, in the standard design concept of Standby Gas Treatment Systems (SGTS) /48/. As active components however, heaters require external power and control systems and are therefore subject to failure.

The reliability and safety margins of HEPA filters downstream of demisters could be greatly increased by filters that would, in a dust loaded condition and in the case of a heater malfunction, withstand the temperatures, flow rates, and air humidities to be expected /8/ downstream of the demister during a LOCA. Filters with stainless steel /49/ or polycarbonate /50/ microfibers have been shown to fulfill such a requirement. These filter types however, are still restricted in practice to special applications such as containment venting or acid environments due to size or temperature limitations and costs.

For general nuclear applications, it appears at present that further improvements in HEPA-filter performance during exposure to humid airflow will have to be made with media of glass fiber. The moderate cost, high filtration efficiency, low flow resistance, large surface area per unit volume, reasonable degree of chemical inertness, and fair resistance to radiation, elevated temperature, and fire, form a combination of characteristics for glass fiber which no other material can presently match.

### Conclusions

The literature survey has shown that the incorporation of water into the glass fiber medium is an adverse phenomena associated with the exposure of HEPA filters to high humidity airflows. Water in the filter medium leads to an increase in differential pressure and to deteriorations in filter pack stability and in filter medium performance characteristics, especially the tensile strength. The mechanical load on the filter is thus increased at the same time that the structural strength is decreased. The end result is that filter structural failure can occur for unacceptably low values of  $\Delta P$ , even at design flow rates.

If it is reasonable to assume that existing countermeasures are for the most part being effectively utilized, then the persistent reports of filter failure in normal operations indicate that the effects of humid airflows on filter performance have only

been moderated and not yet eliminated by these countermeasures. Filters loaded with dust in service still remain particularly prone to failure and the subject of all too few investigations. The development of filters with greater pack stability and strength is seen to be necessary if containment of airborne radioactive material is to be maintained during accident situations involving high humidity airflows at elevated temperature and greater than design flow rates.

Once filter structural integrity can be assured, removal efficiency tests of filter units under high humidity should be conducted with an appropriate aerosol. To be able to mathematically model or to minimize the increase in differential pressure, additional systematic investigations of water transfer into and out of the filter in terms of airstream and filter medium parameters need to be carried out.

### III. Experimental Investigations

#### Filter Structural Tests

Test Apparatus, Parameters, Filters (Commercial). The filter test facility TAIFUN located at Karlsruhe Nuclear Research Center was used to determine the structural limits of 610x610x292-mm commercial HEPA filters during exposure to high humidity airflows of 1700 m<sup>3</sup>/h in tests which lasted between 2 and 200 h each. The structural limit of a test filter was considered to be the differential pressure at which the first visible structural damage to the filter medium appeared on the downstream side of the filter. Descriptions of the test facility, instrumentation, and general experimental procedures have been reported elsewhere /12/.

The new and dust-loaded commercial filters tested were nuclear grade and contained water repellent glass fiber media. Three principal filter designs have been investigated so far. These include:

- deep pleat filters with an elastomeric sealant and a wooden frame for service at < 120 °C,
- deep pleat filters with a seal of packed glass fiber and a metal frame for service at < 250 °C, and
- mini pleat V-type filters with an elastomeric sealant and a wooden frame for service at < 120 °C.

Approximately 35 filters have been tested at 50 °C. An additional 4 filters each were tested at 20 and at 80 °C to evaluate possible influences of temperature on filter behavior.

Most loaded filters in a test group of 21 had pretest pressure drops of 1 to 2 kPa at 1700 m<sup>3</sup>/h after 12-18 months of continuous service in a laboratory building in which radioactive iodine is the primary airborne contaminant. Four mini - pleat

## 19th DOE/NRC NUCLEAR AIR CLEANING CONFERENCE

filters tested had average differential pressures of 0.6 kPa at design flow rate following removal from up to 12 months of active service in a decommissioned reactor building currently used as a containment safety test facility /51/. All loaded filters had served with prefilters in exhaust air ventilation systems and had been mounted in individual caissons or banks through which the vertical airflow was upward into the horizontal upstream face of the filter /52/. None of the filters showed measurable residual levels of radioactivity at the time of the humidity tests.

During a test the air humidity was increased in steps from about 50 % r.h. until either structural failure occurred or an equilibrium  $\Delta P$  at 100 % r.h. was attained. The test filters that remained undamaged at saturation were then exposed to an airstream with a liquid water content of some 10 g/m<sup>3</sup> and consequently failed within a few hours. The removal efficiency of most test filters was measured for a 0.7- $\mu$ m DOP aerosol before and after each test at high humidity.

Test Results. The results of the structural tests of commercial filters are summarized in Table 1. For new clean filters, the filter design can be seen to greatly affect the average  $\Delta P$  at failure. If an average value for the AP and CN filters, 4 kPa, is compared to one for the RNF and DPF types, 0.9 kPa, it is noted that the structural limits of the mini pleat design are only 1/4 of those for the deep pleat design. The use of a packed glass-fiber seal instead of an elastomeric one in deep-pleat filters can account for a decrease of almost 50 % in the average structural limit. This is seen by comparison of the average for clean AP and CN filters, 4 kPa, to the VM value of 2.2. The 50-mm pack depth of the special RNFS filters accounted for no more than a 17 % increase in average  $\Delta P$  at failure compared to the loaded RNF filters with the standard 20-mm depth.

A greater influence on average structural limit is exerted by the humidity itself. Comparison of the values of Table 1 with those obtained for equivalent filters procured from the same manufacturers and then tested with dry air at high flow rates /47/, show that prolonged exposure to moisture can reduce the differential pressure at structural failure by 60 to 90 %. For instance, the value of 3.4 kPa for clean CN filters is only 15 % of the average value of 23 kPa reported for tests with dry air.

The effect of dust loading on the average  $\Delta P$  at failure for the deep pleat AP & AN<sup>+</sup> and CN filters appears here to be insignificant. This is not the case for the mini-pleat RNF filters where the average failure  $\Delta P$  of the loaded filters is twice that of the clean ones. This effect can be partially explained if a loading of dust can increase the wet tensile strength of an uncreased filter medium, as discussed later.

+ The difference between the AP and AN filters (from the same manufacturer) was in materials; the AP type had a particle board and the AN a plywood frame. Test results for these 2 types are considered to be independent of this difference and therefore comparable.

## 19th DOE/NRC NUCLEAR AIR CLEANING CONFERENCE

Table 1: Structural limits of commercial 610x610x292-mm glass fiber HEPA filters tested under high air humidities at 1700 m<sup>3</sup>/h and 50 °C.

Filter		Structural Test Results				
Design	Manf.	Test	No. of	Range of $\Delta P$	Std.	Average $\Delta P$
Pack / Flow Rate (m <sup>3</sup> /h)	Code	Cond.	Tests	at Failure	Dev.	at Failure
Frame / Serv. Temp. (°C)				(kPa)	(kPa)	(kPa)
Deep Pleat (270 mm) / 1700 Al. Separators  Wood / < 120	AP	new	4	2.5 - 5.9	1.4	4.6
	AN	loaded	7	4.1 - 6.3	0.8	5.0
	CN	new	5	1.8 - 5.9	1.6	3.4
	CN	loaded	11	0.9 - 5.7	1.4	3.3
	DN*	new	2	6.3 - 9.0	1.9	< 7.6
Deep Pleat (270 mm) / 1700 Al. Separators  Metal / < 250	VM	new	3	1.2 - 3.3	1.1	2.2
Mini Pleat (20 or 50 mm) / 1700 V Panels  Wood / < 120	RNF	new	2	0.8 - 1.4	0.4	1.1
	RNF	loaded	4	1.4 - 3.6	0.9	2.3
	RNFS	loaded	3	2.5 - 3.4	0.3	2.7
Mini Pleat (25 mm) / 3000 V Panels  Wood / < 120	DPF	new	2	0.4 - 0.9	0.4	0.7

\*  $\Delta P$  is that by first visible damage on downstream face of filter. Filters had probably failed sooner within pack at lower  $\Delta P$ .

The most important effect of a dust loading on the structural failure of any filter type is to lead to structural failure at lower air humidities than those for clean filters. The dust loading and its characteristics determine the degree to which this happens. For the dust and loadings involved here, 15 of 23 loaded filters failed at  $\phi \leq 100$  % r.h. The average value of  $\phi$  at failure was 97 % r.h. after an average exposure time of 21 h. Two deep pleat filters that failed at 80 % r.h. in less than 3 h represented the lowest values of  $\phi$  and exposure time. Only 1 of 18 clean filters failed at  $\phi \leq 100$  % r.h. and it was later determined to have had an only partially water repellent medium. Clean filters in general failed after an average of < 10 h in airflows with moisture contents of some 10 g/m<sup>3</sup>.

Documentation, Modes, and Mechanisms of Structural Failure

Loss of Tightness in the Filter Pack. Typical structural damage caused by humid airflow through wooden frame deep pleat filters is shown in Figs. 3-5. Two different modes of failure can be seen. One results in ruptures along the creases in the downstream ends of the pleats of the filter medium. Consequences of the second are horizontal tears in the sides of pleats, which normally extend through the depth of the filter so that the damage is also visible on the upstream ends of the pleats.

Damage to the filter medium of 610x610x292-mm deep pleat filters caused by humid airflows.

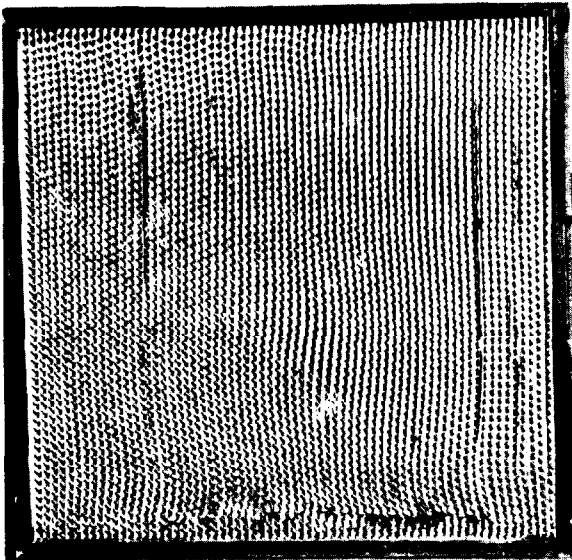
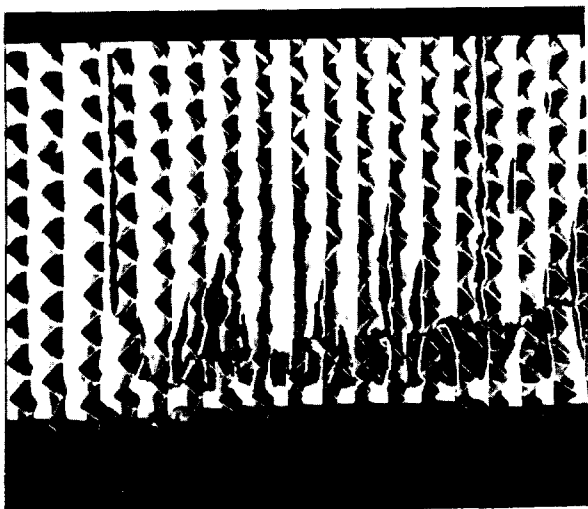


Fig. 3: Ruptured and torn downstream ends of pleats.

Fig. 4: Close-up of downstream ruptured ends of pleats.

Fig. 5: Close-up of play and torn upstream ends of pleats.

3.



4.



5.

Structural limits varied among filter manufacturers by about 50 % for both the deep pleat and mini pleat designs. This is observed in comparisons of results for AP & AN with those of CN filters and of results for RNF with those of DPF filters. The value of 7.6 kPa listed for the DN filters is probably somewhat higher than the actual value. These filters, outfitted with a webbing of glass fiber between the ends of the separators and the filter medium, likely failed earlier within the pack than on the downstream filter face monitored during tests.

The influence of temperature between 20 and 80 °C on the  $\Delta P$  at failure remains inconclusive due to the limited number of tests performed at other than 50 °C, the relatively large scatter in results as well as the weak effect anticipated. There is some circumstantial evidence to suggest that airflows with large and numerous fluctuations in humidity and differential pressure can play a role in structural failure. A tendency toward failure with less service time and at lower  $\Delta P$  may be expected for such cases. Both moisture cycling and temperature remain topics for further study.

One mechanism which contributes to both failure modes is the loosening of the filter pack. An example of the resulting play between adjacent pleats of the filter medium is evident in Fig. 5. Every filter tested sustained a loss in pack tightness which at zero flow rate resulted in an average of 20 mm of total play on the downstream filter face. The amount of play in the filters tested ranged from 10-40 mm. Service history or dust loading had no effect on the average value but considerably accelerated the relaxation process. Several loaded filters showed 10 mm of play within 1 h of exposure to airflow with  $\phi \leq 80$  % r.h.

The geometrical configuration of adjacent separators which makes the relaxation possible is illustrated in Fig. 6. In the lower detail is the most adverse arrangement of the peaks on adjacent separators. Under the combined effects of differential pressure, moisture, and exposure time the filter medium takes on the corrugated form of the separators. This results in a loss of tightness in the pack and the creation of play which allows those pleats that are internally pressurized to grow in width.



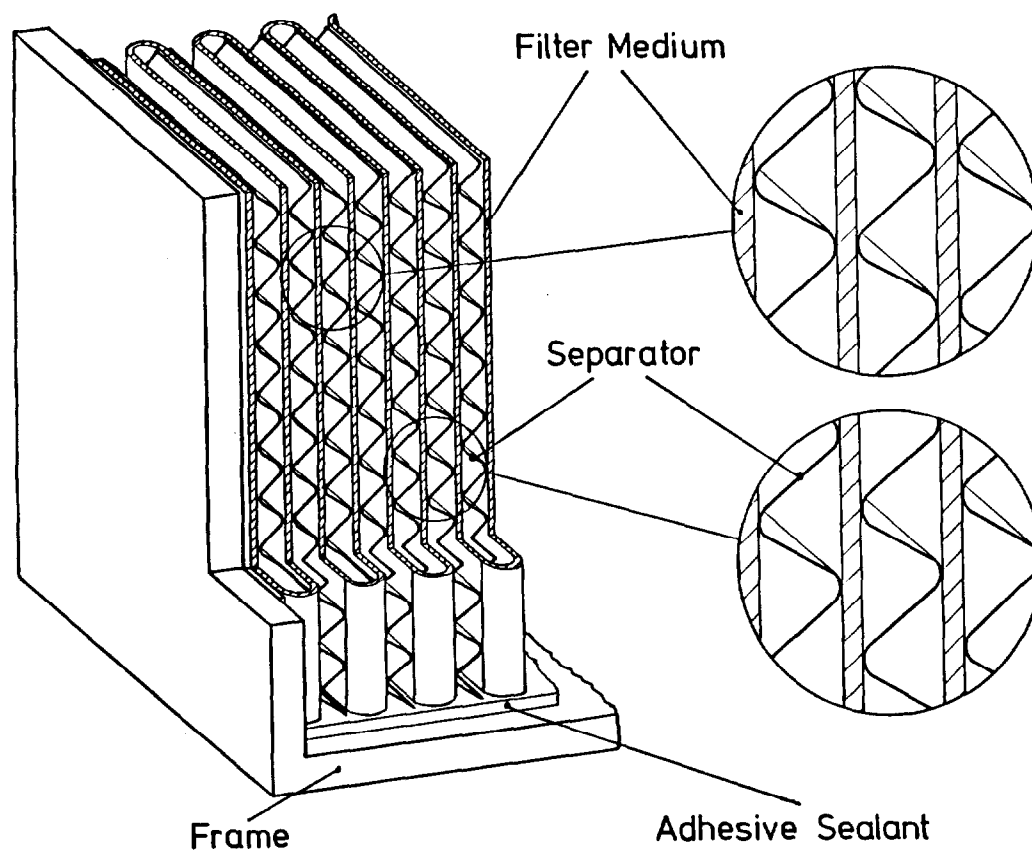


Fig. 6: Two extreme cases for the arrangement of adjacent separators in a deep pleat HEPA-filter pack.

This increase in pleat width is a second mechanism for both failure modes. For the downstream ends of the pleats, any increase in width can have several adverse consequences, one of which is greater circumferential tensile stresses in the filter medium /12/. Additionally, contact and interaction between the edge of the separator and the end of the pleat become possible by a movement of the pleat end into the edge of the separator during swelling /54/ or a movement of the then loosely bound separator into the pleat end after swelling.

Ruptures in the Downstream Ends of the Pleats. Quantitative knowledge of the effects of wetness, creases, prior moisture exposure, and dust loading on filter medium strength are needed to evaluate the extent to which decreases in strength contribute to ruptures and tears in the filter medium. Consequently, samples of filter medium were removed from a total of 40 new, loaded and humidity tested 610x610x292-mm filters for testing according to DIN 53 857 Part 2. These tensile strength tests were performed with wet and dry specimens 50 x 250 mm in size using a ZWICK Model 1425 testing machine. To thoroughly saturate the wet specimens, they were submerged in water and conditioned for 1-2 h in a vacuum chamber at an absolute pressure of 5 kPa and at the temperature of the prior filter humidity test, usually 50 °C. Dry specimens were tested at 20 °C. The average values of tensile strength and of elongation at rupture are listed in Table 2 for groups of samples classified by filter manufacturer and by filter service and test histories.

Results are presented for specimens oriented in the cross direction of the filter medium as well as in the machine direction, with and without the creases caused by pleating. Analysis of the averages in the machine direction for all filter types, excluding those of the prototype MP filter, show that acting alone wetness caused a 60 % decrease in tensile strength, creases 45 %, humidity-test moisture exposure with subsequent drying 40 %, and dust loading (for creased samples) 5 %. If the decreases are assumed to be cumulative the residual tensile strength can be calculated to be 13 % of the value for a new uncreased filter paper. The residual value for AN and CN filters after pleating, loading, high humidity exposure (& drying), and wetting is a comparable, yet even lower, 7 %. That for the single, only partially water repellent CN filter was 3.5 %. This indicates that the effects of these factors acting together can be greater than the sum of their individual effects acting alone. The cumulative effect of the above 4 factors on elongation was to decrease the values for AP (& AN) and CN filters by 40 and 80 %, respectively.

It is noted for CN filters that dust loading brought about an avg. 35 & 70 % increase, resp., in tensile strength of uncreased dry and wet specimens without prior high humidity exposure. This effect was reduced for wet and dry samples after exposure to high humidities during filter testing. Creased, loaded, CN dry samples without humidity exposure exhibited no increase in tensile strength; probably because folded creases do not load during service (see Figs. 8,9). Similar wet loaded samples showed, as yet inexplicably, a 45 % larger residual strength than wet clean ones. However, creases, humidity exposure (& drying), and wetting produced equal and the lowest values, in both clean and loaded samples.

Table 2: Results of tensile strength tests of filter medium samples removed from new and humidity tested HEPA filters.

Samples of Filter Media			Tensile Strength (kN/m)						Elongation (m/m %)			
Manf. Code	Pretest Cond.	No. of Filters Sampled	XD <sup>+</sup>	Dry MD <sup>++</sup> (w/o fold)		MD (w/fold)	XD	Wet MD (w/o fold)		MD (w/fold)	Dry MD (w/fold)	Wet MD (w/fold)
AP	cl./new	1	0.92	1.08		0.33	0.63	0.86		0.24	0.29	0.30
AP	cl./h-t.	3	0.47	1.03		0.20	0.37	0.72		0.13	0.22	0.20
AN	cl./new	1	0.52	0.83		0.42	0.35	0.63		0.25	0.31	0.26
AN	ld./h-t.	6	0.56	0.85		0.19	0.28	0.40		0.06	0.29	0.30
CN	cl./new	3	0.57	0.87		0.38	0.14	0.20		0.11	0.51	0.47
CN	cl./h-t.	5	0.34	0.50		0.17	0.14	0.20		0.07	0.29	0.32
CN*	cl./h-t.	1	0.26	0.49		0.13	0.02	0.03		0.03	0.36	0.32
CN	ld.	1	0.82	1.08		0.36	0.25	0.32		0.16	0.34	0.40
CN	ld./h-t.	10	0.56	0.81		0.21	0.17	0.21		0.06	0.36	0.37
DN	cl./new	2	0.37	0.81		0.31	0.06	0.14		0.05	0.35	0.42
DN	cl./h-t.	3	0.64	0.83		0.29	0.13	0.17		0.09	0.43	0.45
VM	cl./new	1	0.69	1.05		0.58	0.13	0.20		0.16	0.58	0.48
VM	cl./h-t.	1	0.41	0.74		0.31	0.21	0.44		0.17	0.47	0.50
MP**	cl./new	1	10.3	14.7		14.7	6.9	11.8		11.6	1.52	1.52
MP**	cl./h-t.	1	9.8	16.0		15.5	7.4	12.9		11.4	1.91	1.50

<sup>+</sup>cross direction  
cl. = clean filter

<sup>++</sup>machine direction  
h-t. = humidity tested filter

\*partially water repellent medium  
ld. = loaded filter

\*\*Lydair 255LW1 medium

# 19th DOE/NRC NUCLEAR AIR CLEANING CONFERENCE

In addition to exhibiting the lowest values of tensile strength and of elongation to rupture, the ends of the pleats are also more vulnerable to wetting by liquid water. This was observed both during the conditioning of wet samples for tensile tests and during water repellency tests on samples from the same 40 filters. An apparatus equivalent to the Q101 Water Repellency Indicator of MIL-F-0051079B was used to test 10 creased and 10 uncreased samples from each filter. With the exception of the one partially water repellent filter medium (value of 2 kP), and filters from one manufacturer who makes no claim to meet the military standard, the averages for uncreased samples from the other 34 filters all exceeded the 5 kPa minimum value. The results for creased samples were significantly different; only for new untested filters were water repellency values above 5 kPa evident. Average values for loaded and humidity tested filters in the groupings of Table 1 ranged between 1 and 4 kPa. A number of filters, particularly loaded humidity tested ones, showed consistent values of zero for creased samples and hydrophilically absorbed water along the creases within 1 sec after initial contact with a water surface.

The loosening of the filter pack and swelling of the pleats together with the results of the tensile strength and water repellency tests provide strong evidence as to why the downstream ends of the pleats are so prone to rupture in high humidity airflows.

Given values for the total amount of play in the pack,  $x_p$ , the tensile strength across the wet ends of the pleats, and the failure differential pressure, the validity of Equation (1),

$$\sigma_c = \frac{r \cdot \Delta P}{d} \quad , \quad (1)$$

which was proposed /53/ and qualitatively confirmed /47/ by Ruedinger for dry swollen pleats, can be checked for wet swollen pleats of lesser width. In Equation (1),  $\sigma_c$  is the circumferential tensile stress in the pleat end,  $r$  the radius of a downstream pleat end,  $\Delta P$  the differential pressure across the filter, and  $d$  the thickness of the filter medium. If it is assumed that up to 1/4 of the total play is at any one time available to any one pleat for room to swell, then the maximum radius of a swollen pleat end is approximated by

$$r \approx r_0 + \frac{x_p}{8} \quad , \quad (2)$$

where  $r_0$  is the average initial radius of the downstream pleat ends before the humidity test. For the filters tested, the calculated values of  $r$  ranged from 3-7 mm and the recorded values from 2-10 mm. These calculated values of  $r$ , based on the amount of play in the filter pack at failure, were used because the video-recorded values were available for only some few cases. How well Equation (1) predicts the circumferential stresses in the pleat end is seen in Fig. 7 where the actual structural limits of 26 filters tested are plotted against respective calculated

structural limits. This diagram for new and loaded deep pleat 610x610x292-mm wooden frame filters from 3 different manufacturers indicates with a correlation coefficient of 0.56 a qualitative confirmation of Eq. (1). The slope of the linear regression curve fit to the points is seen to be a factor of 3.5 smaller

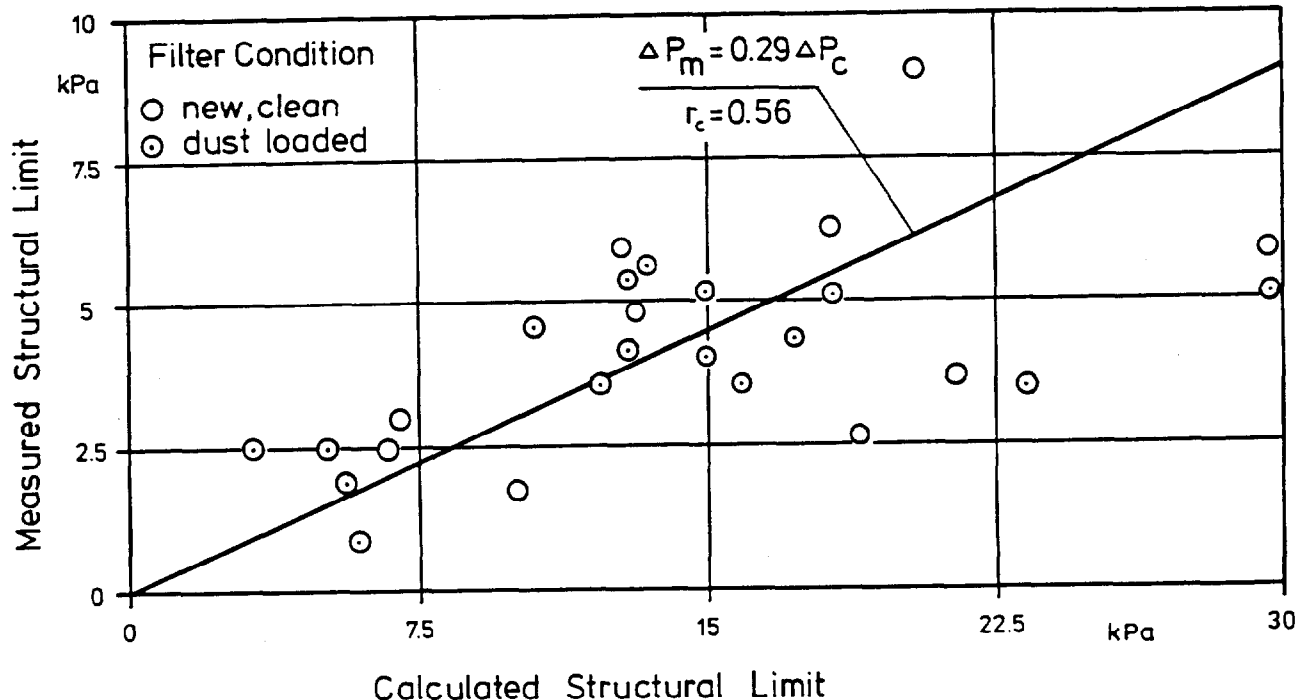


Fig. 7: Comparison of the measured to the calculated differential pressure at structural failure for the case of a wet swollen pleat end.

than the value needed for a quantitative confirmation. One explanation for this is that Eq. (1) does not take into account the additional stresses in the pleat end caused by any contact and interaction with the enclosed separator.

Damage caused by such contact is shown in Fig. 8. Here, the upstream side of pleat ends removed from the downstream face of clean and dust loaded filters after humidity tests are shown. The small gap between separators and filter medium, typically 0-3 mm in commercial filters, is illustrated in Fig. 9 by similar photos taken of dust loaded pleat ends after humidity tests. The horizontal white lines are the creases in the end of the pleat whereas the vertical ones indicate the areas of contact between the sides of the pleats and the separators during service.

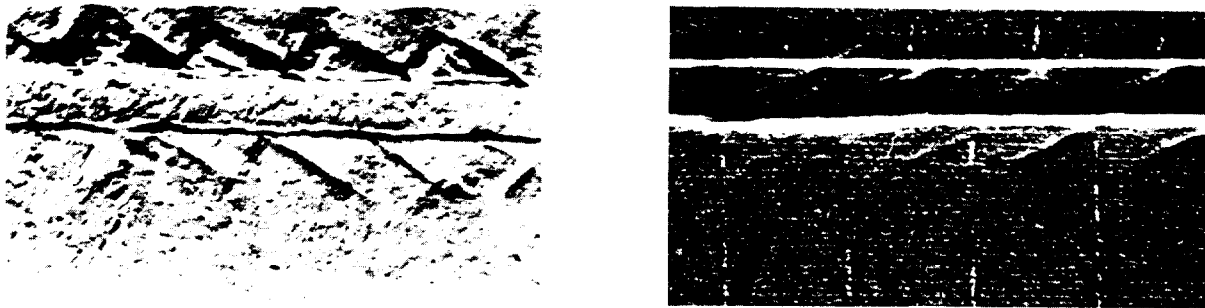


Fig. 8. Damage caused to downstream pleat end of clean (l.) and dust loaded (r.) filter medium by contact with the edge of an aluminum separator during humidity test.

The black intervals by which each vertical line fails to fully intersect with a horizontal line is a record of how large the gap between separator edge and pleat end was during service. The photo on the right in Fig. 9 shows the edge of an aluminum separator at the position it was in with respect to the pleat end during service and the subsequent humidity test. These four photos illustrate how separators can threaten filter medium integrity and how little relative movement is required to bring the edges of the separators into contact with the filter medium. They also explain why Equation (1) does not fully account for all the stresses in the pleat ends during filter exposure to humid airflows.

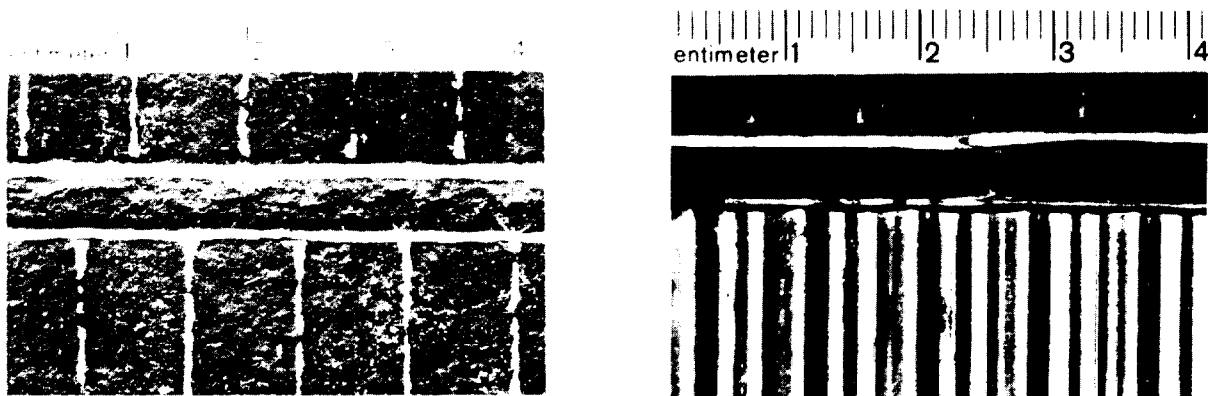


Fig. 9. Record of the gap between the edge of separators and the ends of pleats during service for two dust loaded HEPA filters.

#### Tears in the Filter Medium Along the Sides of the Pleats.

The loosening of the filter pack also leads to the tears observed in the filter medium along the sides of the pleats, frequently for the full depth of the filter. These tears were found to run parallel to the edge of the adhesive on the medium, within 30 mm of the frame on both the top or the bottom of the filter pack. The number of pleats damaged per filter ranged from 3 to 50 for the 7 new and the 9 loaded filters that exhibited this failure mode. A filter

pack that is no longer tight leaves the pleat room, not only for swelling but also for movement and thus subjected to the influence of the aerodynamic forces in the airstream.

The pleats in a pack loosened by humidity and differential pressure can have two degrees of freedom in movement. One is a lateral motion made possible by the play between the pleats. The second is a relative lateral motion of the upstream end of a pleat with respect to the downstream end. The potential for this relative motion to occur is increased by the 8-mm, or 40 %, greater amount of average total play measured on the upstream side of the filters tested. Tears in the upstream ends of pleats were observed to appear twice as frequently and sooner than on the downstream side, and in some cases sooner than the rupture of the swollen downstream ends of pleats.

A plausible explanation for the locations of these tears is evident if the side of a swollen pleat is modeled as a beam with fixed ends and a distributed load, and without the support provided by the adjacent downstream separator. The maximum stresses are found to occur at the top and bottom of the pleat and for a conventional filter medium, ruptures can be expected for a  $\Delta P < 1$  kPa. This simple model does not take into account any residual support from the separators or any fatigue factor due to pleat movements. For several filters under test, lateral oscillations with an amplitude of up to 5 mm and a frequency of about 1/60 Hz have been observed among the downstream ends of the pleats /55/.

These tears then can be attributed to the longitudinal stresses in the sides of the pleats, stresses normally present due to filter  $\Delta P$ , but increased by the swelling and movement of the pleats and by decreases in the rigid support of adjacent separators. Moisture and the fatigue due to pleat movement reduce the ability of the filter medium to withstand these increased stresses. This failure mode requires more study before a suitable model can be developed and verified.

#### First Improvements in Filter Structural Strength Under Humid Airflows

Several options are available to improve filter construction and thus prevent structural damage to glass-fiber HEPA filter units in humid airflows. An increase in the tensile strength of the filter medium or in the stability of the filter pack are two principal ones. Measures to protect the ends of the pleats from contact with the separators constitute a third option.

Tests of Prototype Filters with Glass Fiber Medium. Initial tests of 3 deep pleat 610x610x292-mm prototype filters which incorporated some of these countermeasures have been carried out. A glass fiber filter medium<sup>+</sup> reinforced by a fiber glass cloth was used to fabricate<sup>++</sup> 1 filter with a wooden frame and an elasto-

<sup>+</sup> Grade 255LW1 from Lydall Inc. (See Table 2 for tensile strengths.)

<sup>++</sup> Manufacturer: Mitchell Cotts Air Filtration Ltd.

## 19th DOE/NRC NUCLEAR AIR CLEANING CONFERENCE

meric adhesive and 1 filter with a metal frame and a ceramic adhesive. Each was tested with high humidity airflow in the manner described for the structural tests of the commercial HEPA filters.

Under fog conditions and despite a resultant 80 mm of play in the pack, the wooden frame filter sustained without damage a differential pressure of 10 kPa, the maximum  $\Delta P$  of the test facility at 1700 m<sup>3</sup>/h. Filter DOP filtration efficiency after the humidity test and drying of the filter was measured to be 99,98 % compared with a value of 99,99% before the test. The metal frame filter, with a maximum 60 mm of resultant play, withstood a 5-kPa differential pressure for 2 h before the ceramic adhesive separated abruptly from the frame at 7 kPa. These results represent, by factors of 2-3, increases in failure differential pressure above the values for respective commercial filters given in Table 1. This improvement was achieved with only an increase in the tensile strength of the filter medium, without any attempt to minimize the loosening of the pack.

To evaluate one possible method to minimize the loosening of the filter pack, 1 prototype filter with a wooden frame, conventional glass fiber medium, and special aluminum separators was also tested in an airflow which had a liquid moisture content of some 10 g/m<sup>3</sup>. These separators were formed such that the corrugations were slightly inclined to the direction of the airflow and were installed so that the corrugations on adjacent separators were not parallel but instead skew with respect to each other. This filter failed at a differential pressure of 9 kPa during exposure to the fog conditions, but more importantly, the play in the filter pack was limited to < 5 mm. This represented less than 6% of the final play exhibited by the wooden frame filter with the reinforced medium.

That the increase in filter structural strength and the minimization of the resultant play in the pack were achieved by two different means, indicates the potential for even greater improvement in filter strength in a combination of the two. Tests of prototype filters with both the reinforced filter medium and the special separators are planned for the near future.

### Initial Investigations of Adsorption Phenomena

To investigate the effects of dust loading, humidity, exposure, and fiber material on the water vapor adsorption characteristics of HEPA filters, samples were removed from a total of 14 new and humidity tested filters and used to determine the adsorption isotherms for the filter media. Preparation of the 100-mg samples consisted of drying them at 65 °C and an absolute pressure of 100 Pa for 48 h. With a discontinuous gravimetric method /56/, the adsorbed moisture contents at 25 °C were established after an equilibration time of 14 d. The 7 different values of relative humidity between 32 and 97 % r.h. were established with an uncertainty of  $\leq 1.5$  % r.h. by solutions of salt-saturated water.

The range of adsorption isotherms for samples from 9 clean glass fiber filters is shown in Fig. 10. This range is bounded



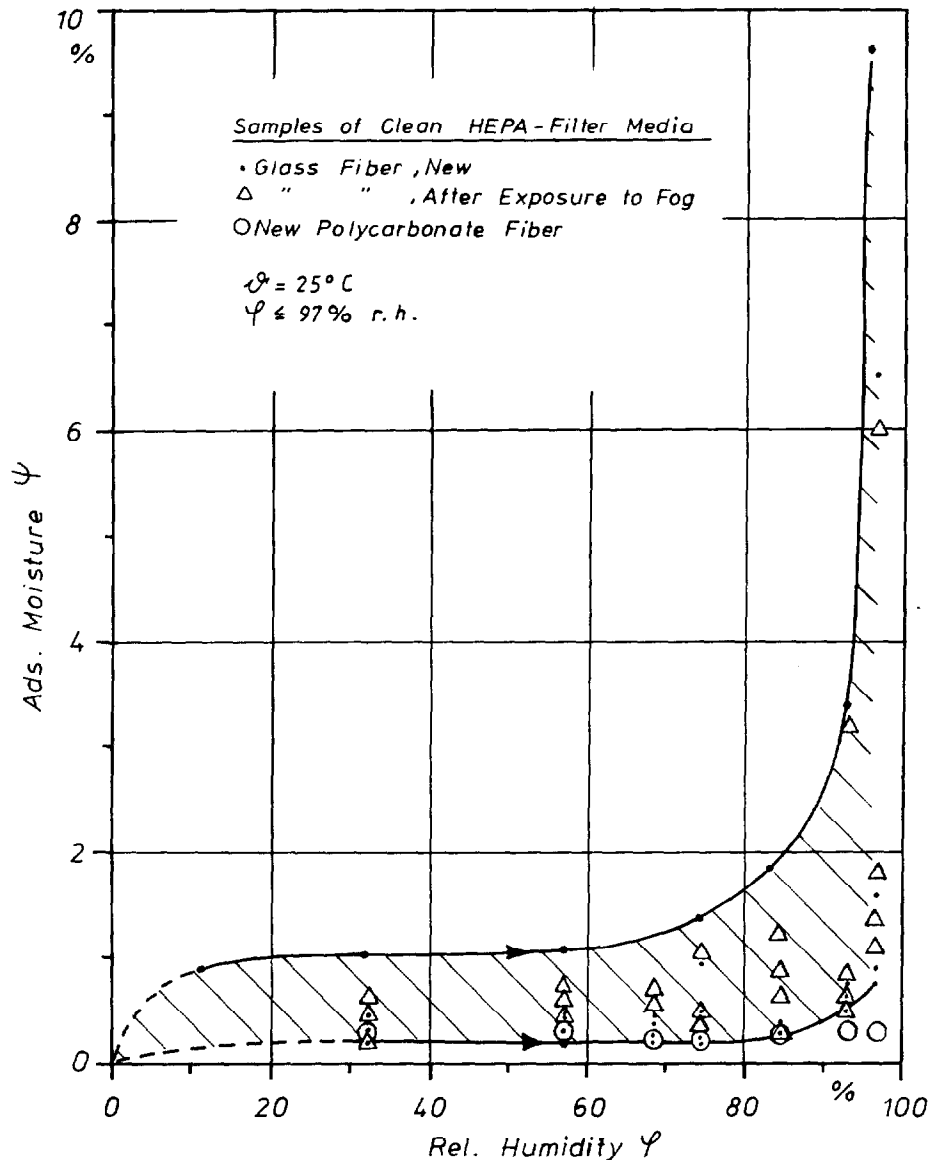


Fig. 10: Range of adsorption isotherms for media removed from 10 clean, new and humidity tested HEPA filters.

by points on isotherms for 3 new filter media, because points on the top curve represent the higher respective values for two intersecting isotherms. The curves of 2 other new and 4 humidity tested filters all lie within this range. No significant influence from fog exposure on adsorption is evident for the clean glass fiber filters sampled. The values of  $\psi$  at 97 % r.h. are noted to vary by 1 order of magnitude for the media tested so far. Only the points for the new polycarbonate microfiber medium<sup>+</sup> /50/ show no increase in moisture content up to 97% r.h. It is also of interest to note that the sorption isotherm for the partially water repellent medium lies at the bottom of this range with nothing in

<sup>+</sup> Manufacturer: Carl Freudenberg, Weinheim, FRG.

particular to distinguish it from those of the water repellent media.

When compared to that of Fig. 10 the range of isotherms for 4 dust loaded glass fiber filter media in Fig. 11 shows clearly the effects of dust loading on  $\psi$ . At 97 % r.h. the amount of adsorbed moisture can be a factor of 5-50 greater

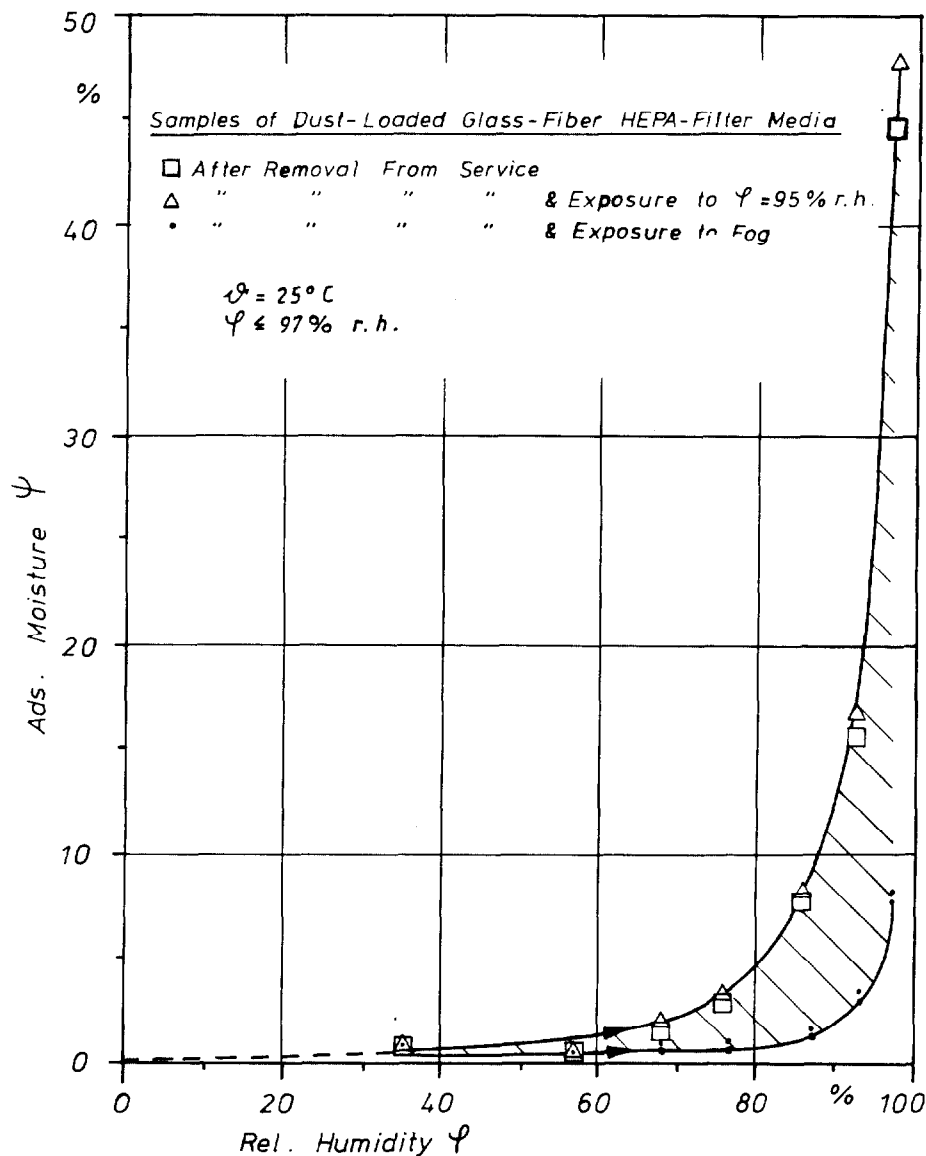


Fig. 11: Range of adsorption isotherms for media removed from 4 dust loaded HEPA filters.

in a dust loaded as compared to a clean filter medium. The two media, with  $\psi$  values presumably reduced through exposure to fog conditions, show maximum values of  $\psi$  corresponding approx. to the

## 19th DOE/NRC NUCLEAR AIR CLEANING CONFERENCE

equivalent  $\phi$  of the most hygroscopic clean media. Comparison of the points for the dust loaded filter without prior high humidity exposure, to those of a filter humidity tested with up to 95 % r.h. show no significant difference. This suggests that for the type of dust involved here,  $\phi > 95$  % r.h. is required to change the structure of the adsorbing surfaces enough to alter the hygroscopic properties of the dust loaded filter medium. This is somewhat unexpected given that values of  $\phi$  as low as 80 % r.h. normally alter the dust loaded fiber structure enough to reduce the  $\Delta P$  of a loaded filter almost to that of a new filter /12/.

These results are still preliminary and require further study and investigation. Sorption kinetics and the effects of temperature and fiber diameter on adsorption isotherms are also topics pending the analysis of already recorded experimental data.

### IV. Conclusions

Despite the many threats posed by high humidity airflows to the structural integrity of commercial glass fiber HEPA filters, studies of the modes and mechanisms of structural failure can lead to significant and cost effective improvements in filter structural strength. As a result, the reliability and safety margins of filters exposed to moisture, particularly in accident situations, can be increased considerably. The preliminary results obtained for the 3 new prototype filters need to be extended and verified for filters with combined improvements and also for filters with dust loads and radiation exposure.

Once structural integrity is assured, tests to evaluate filtration efficiencies at air humidities up to 100% r.h. can be carried out. Studies of the incorporation of water into the filter medium should be continued in order to minimize humidity related increases in filter differential pressure and to model filter  $\Delta P$  as a function of airstream and filter medium parameters in support of computer code accident analyses. The need for an international, stringent test standard for the qualification of HEPA-filter units under high humidity airflows also provides an important item on the agenda for future work.

### Acknowledgements

The authors wish to express their appreciation to Messrs. H. Leibold, E. Demmer, and U. Geckle for their valuable contributions to the filter test program and to Mr. H.-G. Dillmann who kindly made possible the use of the TAI FUN test facility. Thanks are also due to Mr. W. Wolf of the Federal Institute for Nutrition in Karlsruhe for the adsorption isotherm data and related consultations.

V. References

- / 1/ Carbaugh, E.H.  
A Survey of HEPA-Filter Experience,  
CONF-820 833 (1983) p. 790 ff.
- / 2/ Glissmeyer, J.A.; Mishima, J., and Bamberger, J.A.  
Prototype Firing Range Air Cleaning System,  
CONF-840 806 (1985) p.846 ff.
- / 3/ Moeller, D.W. and Sun, L-S.C.  
Failures in Air-Cleaning, Air-Monitoring, and Ventilation  
Systems in Commercial Nuclear Power Plants, 1978 - 1981,  
Nuclear Safety, 24 (3) (1983) p. 352 ff.
- / 4/ Moeller, D.W.  
Failures in Air-Monitoring, Air-Cleaning, and Ventilation  
Systems in Commercial Nuclear Power Plants (Jan. 1, 1975 -  
June 30, 1978),  
Nuclear Safety, 20 (2) (1979) p. 176 ff.
- / 5/ Moeller, D.W.  
Current Challenges in Air-Cleaning at Nuclear Facilities,  
Nuclear Safety, 18 (5) (1977) p. 633 ff.
- / 6/ Moeller, D.W.  
Problems in Nuclear Air Cleaning Systems,  
Nuclear Safety, 16 (4) (1975) p. 469 ff.
- / 7/ Bellamy, R.R.  
Experience with High Efficiency Particulate Air Filters at  
United States Nuclear Installations,  
Proc. of Seminar on High Efficiency Aerosol Filtration in  
the Nuclear Industry, Comm. of the European Communities,  
Luxembourg (1977).
- / 8/ Air Cleaning in Accident Situations,  
Report to CSNI by an NEA Group of Experts  
ISBN 92-64-12633-3  
OECD, Paris, 1984.
- / 9/ Burchsted, C.A.; Fuller, A.B., and Kahn, J.E.  
Nuclear Air Cleaning Handbook,  
ORNL, Oak Ridge, TN, ERDA 76-21, 1976.
- /10/ Alvares, N.J. et al.  
Fire Protection Countermeasures for Containment  
Ventilation Systems,  
CONF-801 038 (1981) p. 1213 ff.
- /11/ Glibert, R.G. et al.  
Design of a PWR Gaseous Radwaste Treatment System  
Ensuring Safe Control of Gaseous Radionuclides  
Released Under Normal and Severe Conditions,  
in: Management of Gaseous Wastes From Nuclear  
Facilities, IAEA, STI/PUB/561, Vienna, 1980, p. 545 ff.

19th DOE/NRC NUCLEAR AIR CLEANING CONFERENCE

- /12/ Ruedinger, V.; Ricketts, C.I., and Wilhelm, J.G.  
Limits of HEPA-Filter Application Under  
High-Humidity Conditions,  
CONF-840 806 (1985) p. 1058 ff.
- /13/ Arnitz, Th. and Ruedinger, V.  
Untersuchungen zur Genauigkeit zweier Rechencodes zur  
Vorhersage der Störfallauswirkungen innerhalb kern-  
technischer Lüftungsanlagen,  
in: Gaseous Effluent Treatment in Nuclear Installations,  
ed. G. Fraser & L. Luykx, CEC, EUR 10580, Graham & Trotman,  
London (1986) p. 416 ff.
- /14/ Thurner, F. and Stietz, M.  
Bestimmung der Sorptionsisothermen lösungsmittel-  
feuchter Sorbienten nach der Durchströmungsmethode,  
Chem. Eng. Proc., 18 (1984) p. 333 ff.
- /15/ Kantro, D.L.; Brunauer, S., and Copeland, L.E.  
BET Surface Areas.- Methods and Interpretations,  
in: The Solid-Gas Interface, ed. E.A. Flood,  
Edward Arnold Publishers Ltd., London, 1967, p. 413 ff.
- /16/ Brunauer, S.; Deming, L.S.; Deming, W.E., and Teller, E.  
J. Am. Chem. Soc. 62 (1940) p. 1723 ff.
- /17/ Lück, W.  
Feuchtigkeit: Grundlagen - Messen - Regeln,  
R. Oldenbourg, München - Wien, 1964.
- /18/ Poersch, W.  
Sorptionsisothermen: Ihre Ermittlung und Auswertung,  
Die Stärke 11 5 (1963) p. 405 ff.
- /19/ Kadlec, O. and Dubinin, M.M.  
Comments on the Limits of Applicability of the  
Mechanism of Capillary Condensation,  
J. Colloid & Inter. Sci. 31 4 (1969) p. 479.
- /20/ Kawasaki, K.; Senzaki, K., and Tsuchiya, I.  
Adsorption Studies of Water Vapor on Porous Glass,  
J. Colloid Sci. 19 (1964) p. 144 ff.
- /21/ Krischer, O. and Kast, W.  
Die wissenschaftlichen Grundlagen der Trocknungstechnik,  
3. Auflage, 1. Bd., Springer-Verlag,  
Berlin - Heidelberg - New York, 1978.
- /22/ Tierney, G.P. and Conner, W.D.  
Hydroscopic Effects on Weight Determination of  
Particulates Collected on Glass-Fiber Filters,  
American Industrial Hygiene Association Journal,  
(August 1967) p. 363 ff.

19th DOE/NRC NUCLEAR AIR CLEANING CONFERENCE

- /23/ Hofmann, W.M.  
Feuchtigkeitsaufnahme von Schwebstofffiltern,  
Zeitschrift für Heizung, Lüftung, Klimatechnik  
und Haustechnik (HLH), 25 3 (1974) p. 77 f.
- /24/ Rachinskii, V.V.  
The General Theory of Sorption Dynamics and  
Chromotography, (translation from the Russian),  
Consultants Bureau, New York, 1965.
- /25/ Mantell, C.L.  
Adsorption,  
1st Edition, McGraw-Hill Book Co. Inc.,  
New York and London, 1945.
- /26/ Peters, A.H.  
Applications of Moisture Separators and Particulate  
Filters in Reactor Containment,  
USAEC DP-812, Savannah River Laboratory, 1962.
- /27/ Jones, L.R.  
Effects of Radiation on Reactor Confinement  
Systems Materials,  
CONF-720 823 (1972) p. 655 ff.
- /28/ Schwalbe, H.C.  
Redevelopment of the Savannah River Laboratory  
Moisture Resistance Test for Filter Paper,  
CONF-680 821 (1968) p. 86 ff.
- /29/ Belvin, W.L. et al.  
Development of New Flouride Resistant HEPA Filter  
Medium: Final Report,  
USERDA, TID-26649, Savannah River Operations Office, 1975.
- /30/ Davis, R.J. et al.  
The Effects of Moisture on the Character and  
Filtration of UO<sub>2</sub>-Stainless Steel Aerosols,  
in: Treatment of Airborne Radioactive Wastes,  
IAEA STT/PUB 195, Vienna (1968) p. 345 ff.
- /31/ Robinson, K.S. et al.  
In-Service Aging Effects on HEPA Filters,  
in: Gaseous Effluent Treatment in Nuclear Installations,  
ed. G. Fraser & L. Luykx, CEC, EUR 10580,  
Graham & Trotman, London (1986) p. 60 ff.
- /32/ Kvetoslav, R. et al.  
Methodik und Untersuchungen zur Beständigkeit von  
Mineralfasern in vitro und in vivo,  
Staub-Reinhalt. Luft 44 4 (1984) p. 169 ff.
- /33/ Horak, H.L. et al.  
Structural Performance of HEPA Filters Under  
Simulated Tornado Conditions,  
LA-9197-MS, Los Alamos National Laboratory, 1982.

19th DOE/NRC NUCLEAR AIR CLEANING CONFERENCE

- /34/ Deworm, J.P.  
Laser Particle Spectrometry for Testing HEPA  
-Filtration Systems in the Nuclear Industry,  
Filtration & Separation July/Aug. (1984) p. 254 ff.
- /35/ Ensinger, U.; Ruedinger, V., and Wilhelm, J.G.  
A Procedure to Test HEPA-Filter Efficiency Under  
Simulated Accident Conditions of High Temperature  
and High Humidity,  
CONF-840 806 (1985) p. 1036 ff.
- /36/ Gilbert, H. and Palmer, J.H.  
High Efficiency Particulate Air Filter Units,  
TID-7023, USAEC, 1961.
- /37/ Burchsted, C.A.  
Environmental Properties and Installation Requirements  
of HEPA Filters,  
in: Treatment of Airborne Radioactive Wastes,  
IEAE, STI/PUB/195, Vienna, 1968, p. 175 ff.
- /38/ Stratmann, J.  
Bericht eines Großverbrauchers von Schwebstofffiltern  
der Klasse S,  
in: Proc. Seminar on High Efficiency Aerosol  
Filtration, Comm. European Community, Luxembourg,  
(1977), p. 411 ff.
- /39/ Fenton, D.L. and Dallman, J.J.  
HEPA-Filter Loading by Simulated Combustion Products,  
Report submitted by New Mexico State University  
Mechanical Engineering Department to Los Alamos National  
Laboratory, Sept. 1982.
- /40/ Hofmann, W.M.  
Druckverlust feuchter Schwebstofffilter,  
Zeitschrift für Heizung, Lüftung, Kimatechnik und  
Haustechnik (HLH), 25 11 (1974) p. 370.
- /41/ Jones, L.R.  
High Efficiency Particulate Air (HEPA) Filter  
Performance Following Service and Radiation Exposure,  
CONF-740 807(1974) p. 565 ff.
- /42/ Collins, R.D.; Hillary, J.J., and Taylor, J.C.  
Air Cleaning for Reactors with Vented Containment,  
CONF-660 904 (1966) p. 419 ff.
- /43/ Gunn, C.A. and Eaton, D.M.  
HEPA-Filter Performance Comparative Study,  
CONF-760 822 (1977) p. 630 ff.

19th DOE/NRC NUCLEAR AIR CLEANING CONFERENCE

- /44/ Pratt, R.P.  
The Performance of Filters Under Hot Dynamic Conditions,  
in: Gaseous Effluent Treatment in Nuclear Installations,  
ed. G. Fraser & L. Luykx, CEC, EUR 10580,  
Graham & Trotman, London (1986) p. 824 ff.
- /45/ Richardson, W.J. and Palmer, J.H.  
The Installation, Handling, and Storage of High  
Efficiency Filters,  
TID-7593, USAEC, 1960, p. 182 ff.
- /46/ Thaxter, M.D.  
Condition of Commercial High-Efficiency Filters  
Upon Receipt or Installation  
TID-7593, USAEC, 1960, p. 157 ff.
- /47/ Ruedinger, V.; Ricketts, C.I., and Wilhelm, J.G.  
Versagensgrenzen und Schadensmechanismen von Schweb-  
stofffiltern unter Beanspruchung durch trockene Luft  
hoher Strömungsgeschwindigkeit,  
in: Gaseous Effluent Treatment in Nuclear Installations,  
ed. G. Fraser & L. Luykx, CEC, EUR 10580,  
Graham & Trotman, London (1986) p. 792 ff.
- /48/ NRC  
Regulatory Guide 1.52, Revision 2,  
USNRC, Washington, D.C., 1978.
- /49/ Dillmann, H.-G.  
Ergebnisbericht über Forschungs- und Entwicklungsarbeiten  
1981 des Laboratorium für Aerosolphysik und Filtertechnik,  
KfK-Bericht 3294, (1982) p. 12.
- /50/ Alken, W. et al.  
Development of a HEPA Filter with High Structural Strength  
and High Resistance to the Effects of Humidity and Acid,  
CONF-840 806 (1985) p. 1085 ff.
- /51/ HDR Sicherheitsprogramm - Gesamtprogrammphase II, PHDR  
Arbeitsbericht 05.19/84, Kernforschungszentrum Karlsruhe  
GmbH, Karlsruhe, FRG, Jan. 1984.
- /52/ Ohlmeyer, M.  
Vor-Ort-Prüfung von Schwebstofffiltern und Entnahme von  
Sorptionsmaterialproben bei Iod-Sorptionsfiltern,  
Atomenergie- Kerntechnik 40 (1982) p. 259 ff.
- /53/ Ruedinger, V. and Wilhelm, J.G.  
HEPA-Filter Response to High Airflow Velocities,  
CONF-820833 (1983) p. 1069 ff.



## 19th DOE/NRC NUCLEAR AIR CLEANING CONFERENCE

- /54/ Ruedinger, V.; Ricketts, C.I., and Wilhelm, J.G.  
Development of Glass-Fiber HEPA Filters of High  
Structural Strength Based on the Establishment of  
Failure Mechanisms,  
in: Proceedings of the 19th DOE/NRC Nuclear Air  
Cleaning Conference, Seattle, WA, Aug. 1986,  
to be published.
- /55/ Leibold, H.  
Private Communication, KfK, July 1986.
- /56/ Wolf, W.; Spieß, W.E.L. and Jung, G.  
Standardization of Isotherm Measurements,  
(COST - Project 90)  
in: Properties of Water in Foods, eds. D. Simatos,  
J.L. Multon, NATO ASI Series, Series E,  
in: Applied Sciences No. 90, Martinus Nijhoff  
Publishers, Dordrecht - Boston - Lancaster,  
1985, p. 661 ff.

### DISCUSSION

SCRIPSICK: Please comment on the potential effects  
these extreme conditions might have on penetration and please refer  
to Normann's paper.

RICKETTS: We have not yet performed filtration  
efficiency measurements on HEPA filter units under high humidity  
conditions. However, a suitable method which employs a submicron  
TiO<sub>2</sub> condensation aerosol and AAS analysis has been developed at  
Karlsruhe Nuclear Research Center and will soon be used to test full  
scale filters at air relative humidities up to 100%. Published  
measurements of filtration efficiency under high humidity conditions  
are somewhat contradictory. The work of Adams, Davis, et al. at Oak  
Ridge National Laboratory some 20 years ago seem to be the most  
credible. Tests performed on samples of filter medium with a UO<sub>2</sub>-  
stainless steel aerosol showed increases of up to 1 order of  
magnitude in penetration after exposure to 100% RH. Reference No. 30  
in our paper provides a good summary of the work at Oak Ridge. The  
measurements presented here by Mr. Normann show the same tendency  
toward increased penetration after exposure of the filter medium to  
high humidity.

ETTINGER: How does the type of dust affect the  
sorption of water and the resulting change in pressure drop  
characteristics? Would this effect be as much as an order of  
magnitude?

RICKETTS: The material constituents, the particle  
size, and the amount of dust on a filter medium greatly influence the  
hygroscopic, and hence the sorption properties of a dust-loaded

## 19th DOE/NRC NUCLEAR AIR CLEANING CONFERENCE

filter medium. A salt, such as NaCl, can be very hygroscopic whereas some materials, such as the polycarbonate microfiber filter medium investigated here, show very little if any sorption of water vapor. At relative air humidities above 95%, and temperatures less than 30°C, the absorbed moisture content for different types of dust could vary by up to 2 orders of magnitude. For the dust in our laboratory exhaust airstream, in comparison to clean filters we have measured, the differential pressures of loaded filters were greater by 1 order of magnitude at 1700 m<sup>3</sup>/hr and >97% RH. We are currently developing a mathematical model to describe filter  $\Delta P$  as a function of the amount of adsorbed water on a clean filter.

SANDOVAL: Please explain in further detail the mechanisms involved in increasing the dust loading capabilities by high humidity airflows for the filters studied.

RICKETTS: For the particular room air dust captured in the HEPA filter units that we have tested at 1700 m<sup>3</sup>/hr and 50°C, air relative humidities between 70 and 90% RH have reduced the  $\Delta P$  of dust loaded filters from 2 kPa to values as low as 0.5 kPa within several hours of exposure. This effect has also been observed by other authors for other types of filter media and captured particulates. This phenomenon has been attributed to capillary condensation in the particulate-loaded filter medium and subsequent surface tension effects which draw particles together into agglomerates. It is hypothesized that the formation of the agglomerates partially reopens the pore structure of the filter medium and thus decreases the flow resistance of the filter. For further information and other literature citations, we refer you to reference No. 12 of our paper.

ETTINGER: You talked about the fact that dust loading increased the amount of moisture which can be picked up by a filter and produce a change in pressure drop. I assume that would vary, depending upon the type of dust. What kind of material did you use, and what range would you expect, depending upon the type of dust?

RICKETTS: The amount of water adsorbed by the dust is very much dependent upon the quantity of dust on the filter medium as well as the sorption characteristics of the dust itself. The type of dust that was on the filters that we tested was essentially room air dust. These filters had been removed from the exhaust air system of a laboratory building at Karlsruhe.

ETTINGER: Do you think there would be orders of magnitude difference depending upon the type of dust and whether it is hydroscopic or hydrophilic?

RICKETTS: Yes, definitely; perhaps up to two orders of magnitude difference.

SCRIPSICK: I have a couple of questions, both relating to penetration. Dr. Normann's paper, previous to yours, indicated that there was an increase in penetration associated with humidity-conditioned filters. I am wondering if you would comment on his results and tell me if you have investigated the effect on

19th DOE/NRC NUCLEAR AIR CLEANING CONFERENCE

penetration. You mentioned that the two major problems were  $\Delta P$  and tensile strength changes. Have you looked at penetration?

RICKETTS: We haven't made penetration measurements under high humidity conditions. That is planned for the future. A colleague in our group is presently working on the development of a test method that uses a titanium dioxide aerosol that will be used to test filter efficiency under both high humidity and high temperature.

SCRIPSICK: Are you familiar with the penetration increases associated with filters exposed to high humidities in Dr. Normann's paper?

RICKETTS: There are contradictory results published in the literature. Work done at Oak Ridge National Laboratory by Mr. Davis and Mr. Adams showed an increase in penetration under high humidity conditions. There was a recent report published by Mr. DeWorm who found decreases in penetration for DOP, NaCl, and uranine aerosols. I am rather skeptical of results for aerosols that are water soluble or that are liquids, when used under high humidity conditions.

## 19th DOE/NRC NUCLEAR AIR CLEANING CONFERENCE

### CALIBRATION TESTS OF A LASER FLUORESCENT PARTICLE SPECTROMETER

Ph. Mulcey, P. Pybot, J. Vendel  
Commissariat à l'Energie Atomique

Institut de Protection et de Sécurité Nucléaire, Département de Protection  
Technique, Service de Protection des Installations Nucléaires, Section d'Etudes  
Industrielles de Protection - CEN/Saclay, 91191 GIF SUR YVETTE Cédex, France

#### Abstract

The recent development of laser particle spectrometers enables measurements of higher decontamination factors of filters than those provided by standard test methods. Specific aerosols, as fluorescent ones, increase sensibility and eliminate interference due to background aerosol leaking into the downstream sampling location. The best compromise seems to be reached with a laser fluorescent particle spectrometer.

Before using this kind of method for testing HEPA filters, we have made a calibration of such a device (Laser Fluorescent Particle Spectrometer; PMS model ASAS.XF). Fluorescent (FL) and all particle (ALL) counting modes have been investigated.

For the fluorescent particle mode the DOP solutions are tagged with fluorescent dye (Potomac Yellow) in various concentrations in order to estimate the threshold detection.

For the all particle mode, the calibration is achieved using monodispersed polystyrene latex (PSL) aerosols reselected, for the smaller dimensions (RANGE 1), by an electrostatic classifier (DMPS; TSI model 3071).

The response of the ASAS-XF spectrophotometer to DOP particles in the same size range was finally investigated, using the same electrostatic selection device, and compared to the one obtained from PSL aerosols.

#### I. Introduction

The conventional standard test methods used to perform efficiency measurements of particulate air filters suffer limitations which makes difficult, or even impossible, the control of tandem HEPA or ULPA filters.

Recent developments in the field of optical single particle counters lead to dispose of instruments performing real time measurements of aerosol size distributions over a wide size range and, by using an appropriate dilution system, over a wide concentration range (1), (2).

The use of a laser beam as a light source can allow, if coupled with a selected dye tracer, a specific detection of the test aerosol avoiding high backgrounds due to particles entering the circuit downstream of the filter.

The calibration tests performed on a laser fluorescent particle spectrometer (PMS Model ASAS-XF) using polystyrene latex (PSL) and DOP aerosols, are presented below.

## II. Aerosol Spectrometer Description

The ASAS-XF laser aerosol spectrometer is a single particle counter which allows size classification from the amplitude of the scattered light emitted by the particle when passing through the laser beam. The laser can operate either in the "ALL" mode, for which every particle is taken into account whatever fluorescent or not, or in the "FLUORESCENT" mode for which the classification is achieved for the fluorescent particles only these being detected owing to their fluorescent emission induced by excitation in the laser wavelength if the aerosol particles are tagged with an appropriate fluorescent dye.

The spectrometer is equipped with a 10 mW He-Cd TEM<sub>00</sub> mode laser tube emitting a 442 nm wavelength. The corresponding dye, which can be used with DOP aerosols, is the Potomak Yellow (excitation wavelength : 440 nm, emission wavelength : 490 nm).

The optical diagram of the instrument is shown in figure 1.

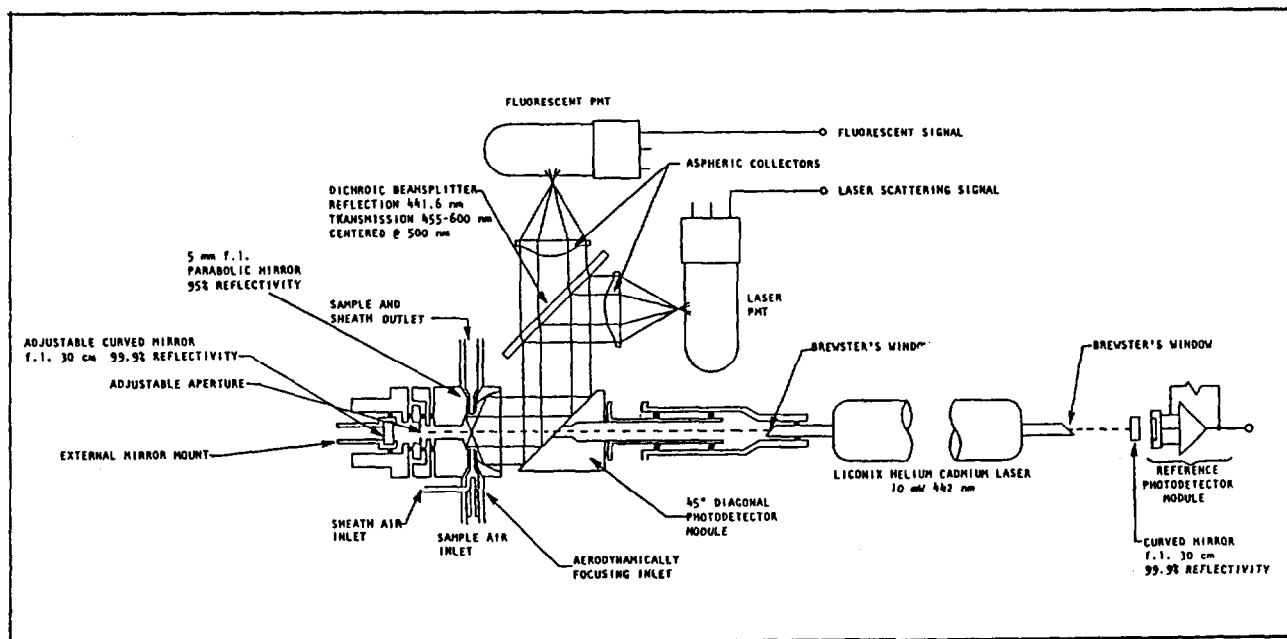


Figure 1 - ASAS-XF Optical system diagram (from Operating Manual)

The ASAS-XF airflow diagram is shown in figure 2.

## III. Calibration Tests of the Spectrophotometer

Two different series of tests were conducted :

- tests with polystyrene latex (PSL) monodispersed aerosols in order to check the initial supplier's calibration,
- tests with DOP aerosols. For some of these tests the DOP solution was tagged with Potomak Yellow.

# 19th DOE/NRC NUCLEAR AIR CLEANING CONFERENCE

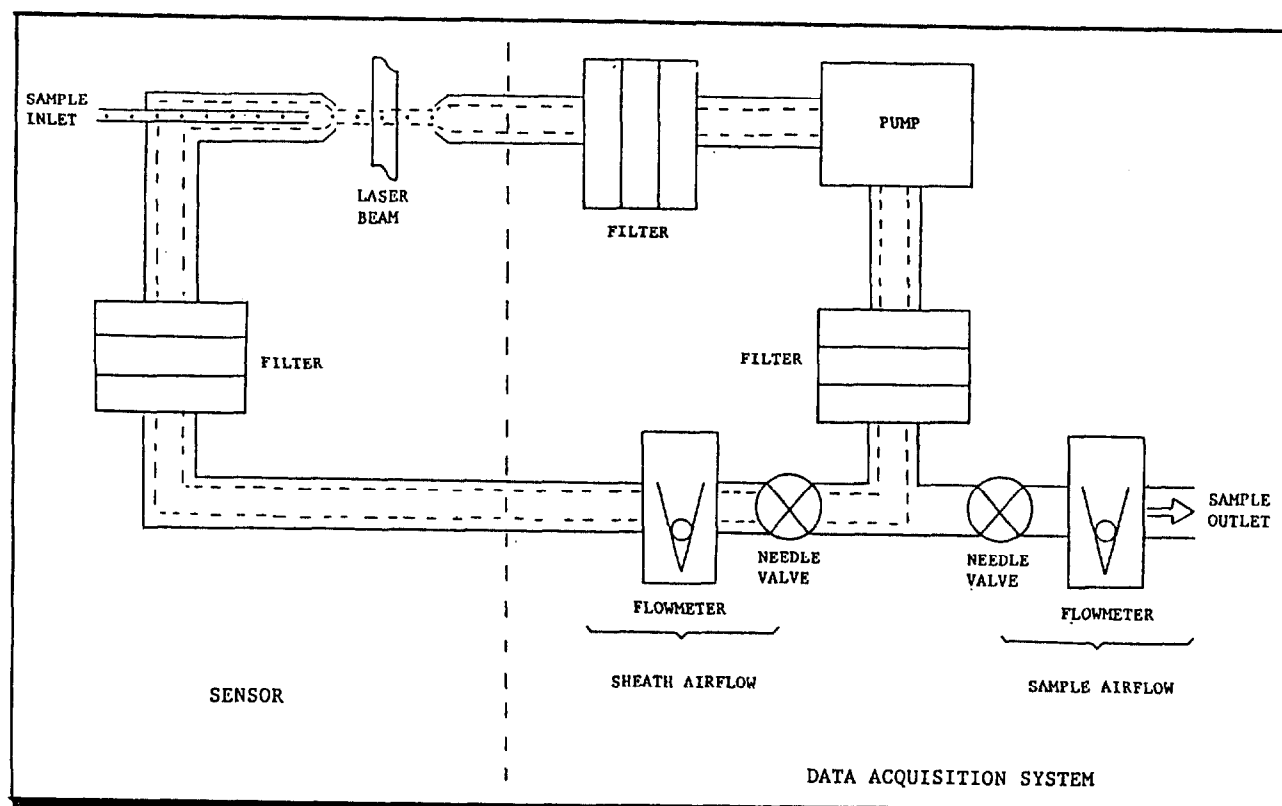


Figure 2 - ASAS-XF airflow diagram (from Operating Manual)

## Calibration tests with polystyrene latex

### Supplier's initial calibration

The ASAS-XF has two size ranges : RANGE 1 from 0.125 to 0.85  $\mu\text{m}$ ; RANGE 0 from 0.85 to 3.10  $\mu\text{m}$  each of them divided into 15 channels. The size partition is given in table I.

Table I. ASAS-XF size partition

CALIBRATION DATA			CALIBRATION DATA		
ASAS-XF (Liconix 4110 HeCd Laser [10 mW])			ASAS-XF (Liconix 4110 HeCd Laser [10 mW])		
Size Range #1 (0.125 - 0.850 $\mu\text{m}$ )			Size Range #0 (0.85 - 3.10 $\mu\text{m}$ )		
Channel	Size (microns)	Interval (microns)	Channel	Size (microns)	Interval (microns)
1	0.125 - 0.150	0.025 0.05 0.05	1	0.85 - 1.00	0.15 0.15 0.15
2	0.150 - 0.200		2	1.00 - 1.15	
3	0.200 - 0.250		3	1.15 - 1.30	
4	0.250 - 0.300		4	1.30 - 1.45	
5	0.300 - 0.350		5	1.45 - 1.60	
6	0.350 - 0.400		6	1.60 - 1.75	
7	0.400 - 0.450		7	1.75 - 1.90	
8	0.450 - 0.500		8	1.90 - 2.05	
9	0.500 - 0.550		9	2.05 - 2.20	
10	0.550 - 0.600		10	2.20 - 2.35	
11	0.600 - 0.650		11	2.35 - 2.50	
12	0.650 - 0.700		12	2.50 - 2.65	
13	0.700 - 0.750		13	2.65 - 2.80	
14	0.750 - 0.800		14	2.80 - 2.95	
15	0.800 - 0.850	0.05	15	2.95 - 3.10	0.15

## 19th DOE/NRC NUCLEAR AIR CLEANING CONFERENCE

The initial calibration delivered by the supplier from PLS aerosols is given in figure 3.

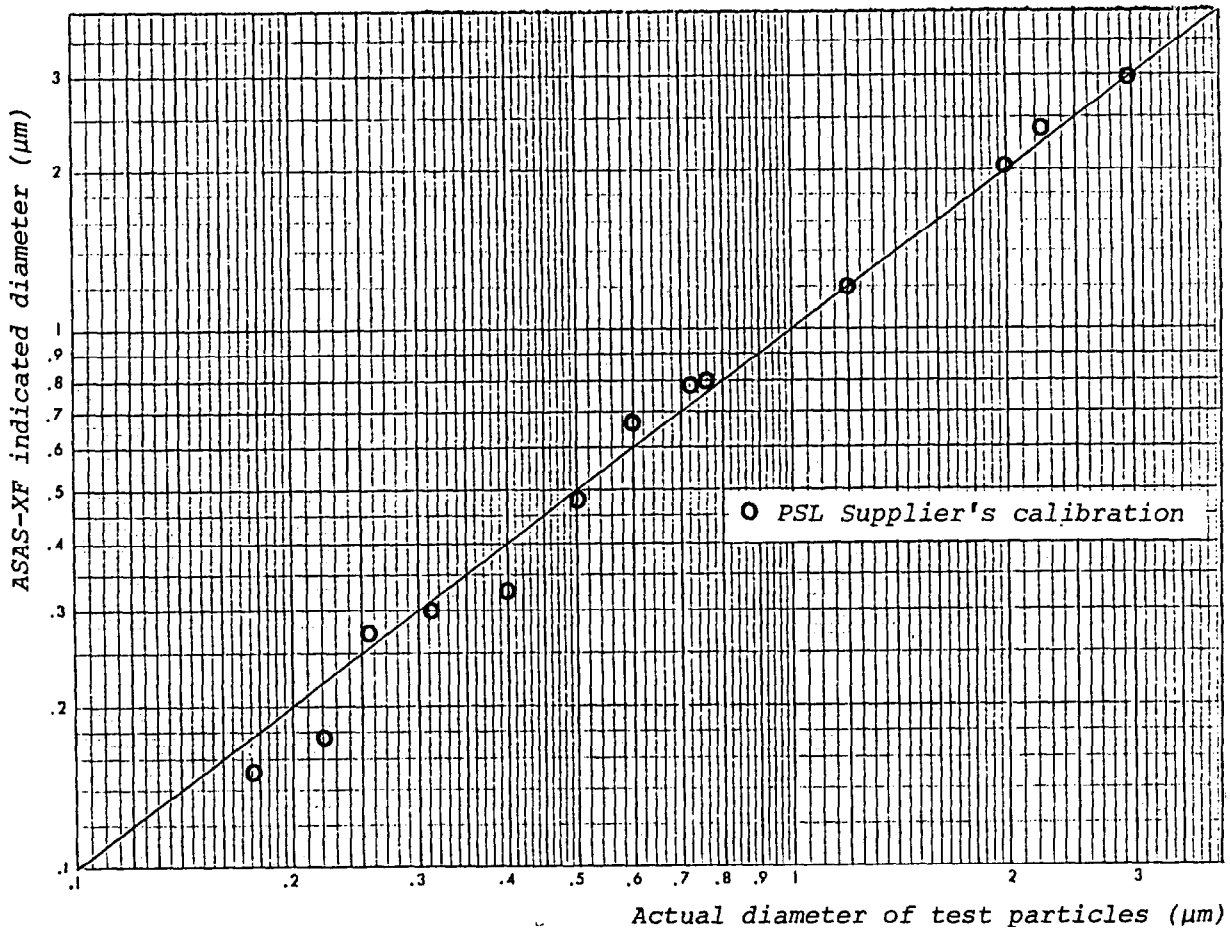


Figure 3

### Laboratory calibration

A laboratory calibration was carried out to establish the spectral response of the instrument for monodispersed aerosols. For that purpose, the PSL aerosol is reselected by means of a Differential Mobility Particle Sizer (DMPS) in order to eliminate, especially for the lower dimensions, the interfering aerosol produced by spraying and the multiplets due to coagulation of PSL particles.

The results of this calibration expressed in the form of histograms are shown in figure 4 for 0.12 μm, 0.481 μm, 0.721 μm and 3.1 μm.

The PSL aerosol sizes used for these calibration tests are the following : 0.12 μm, 0.312 μm, 0.481 μm, 0.721 μm, 0.94 μm, 1.65 μm and 3.1 μm. For the first four sizes the PSL aerosol has been reselected by means of the DMPS. The response curve of this apparatus is given in figure 5.

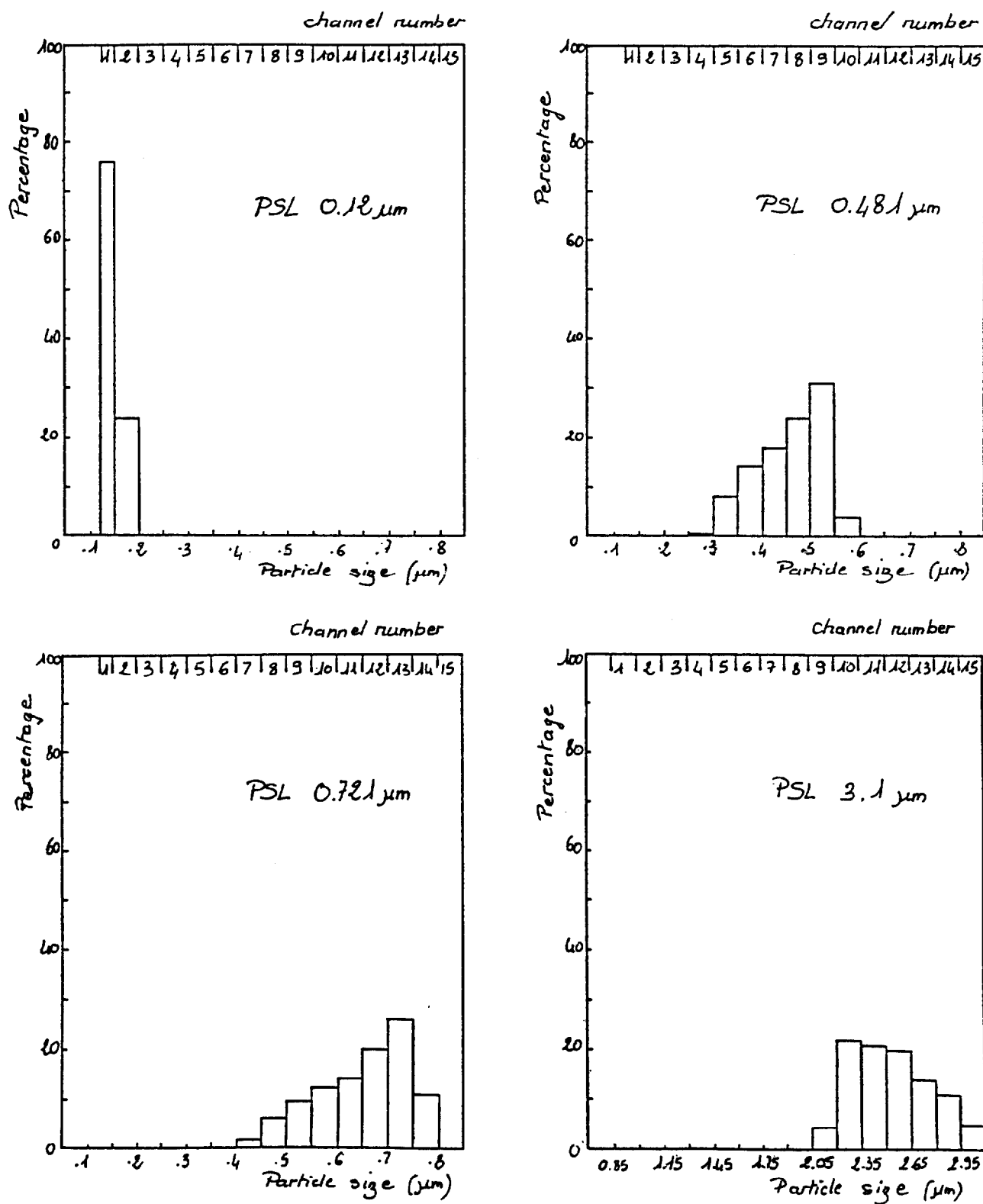


Figure 4



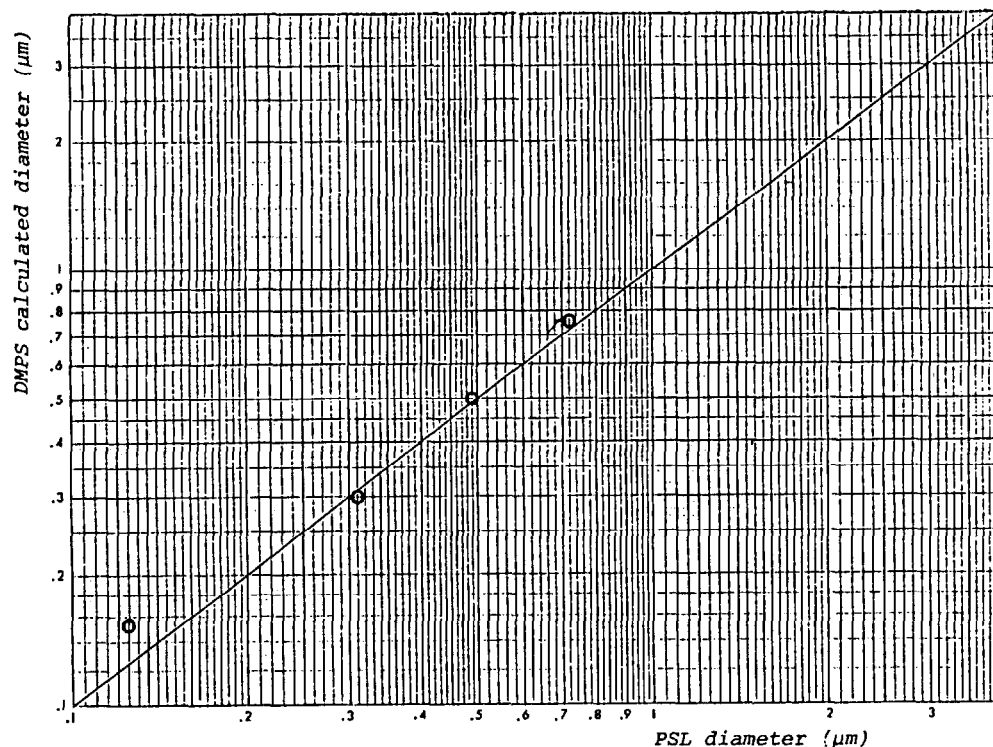


Figure 5

From these data, cumulative distributions were derived from which the mean diameter and standard deviation are calculated. The results are plotted in figure 6.

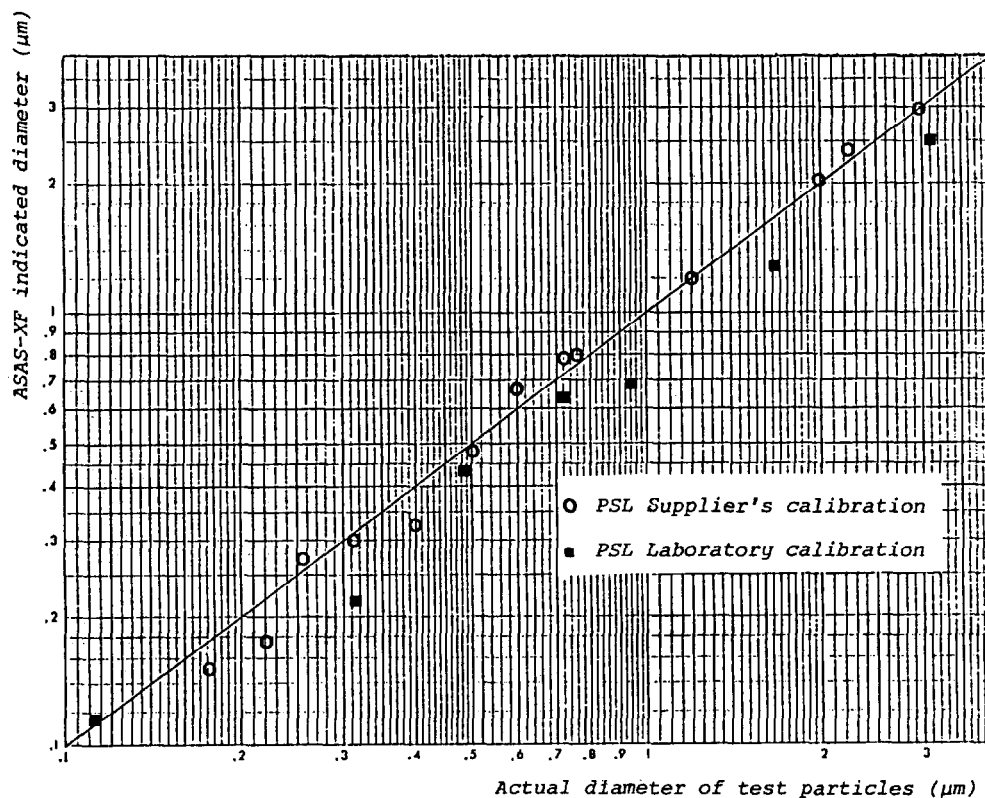


Figure 6

## 19th DOE/NRC NUCLEAR AIR CLEANING CONFERENCE

### Calibration tests with DOP

#### Fluorescent detection check

A test was conducted with a polydispersed DOP aerosol tagged with Potomak Yellow. From this test it results that the fluorescent detection has a 100% efficiency except for the very first channel. This can be explained by the low amplitude of the fluorescent emission due to the small amount of Potomak Yellow (maximum solubility in DOP : 2 g/l) contained in DOP aerosol particles of about 0.1  $\mu\text{m}$ .

#### DOP calibration tests

As for the PSL calibration tests, a polydispersed DOP aerosol was generated and then reselected by means of the DMPS. The size distributions given by the ASAS-XF for different particle sizes are illustrated in figure 7.

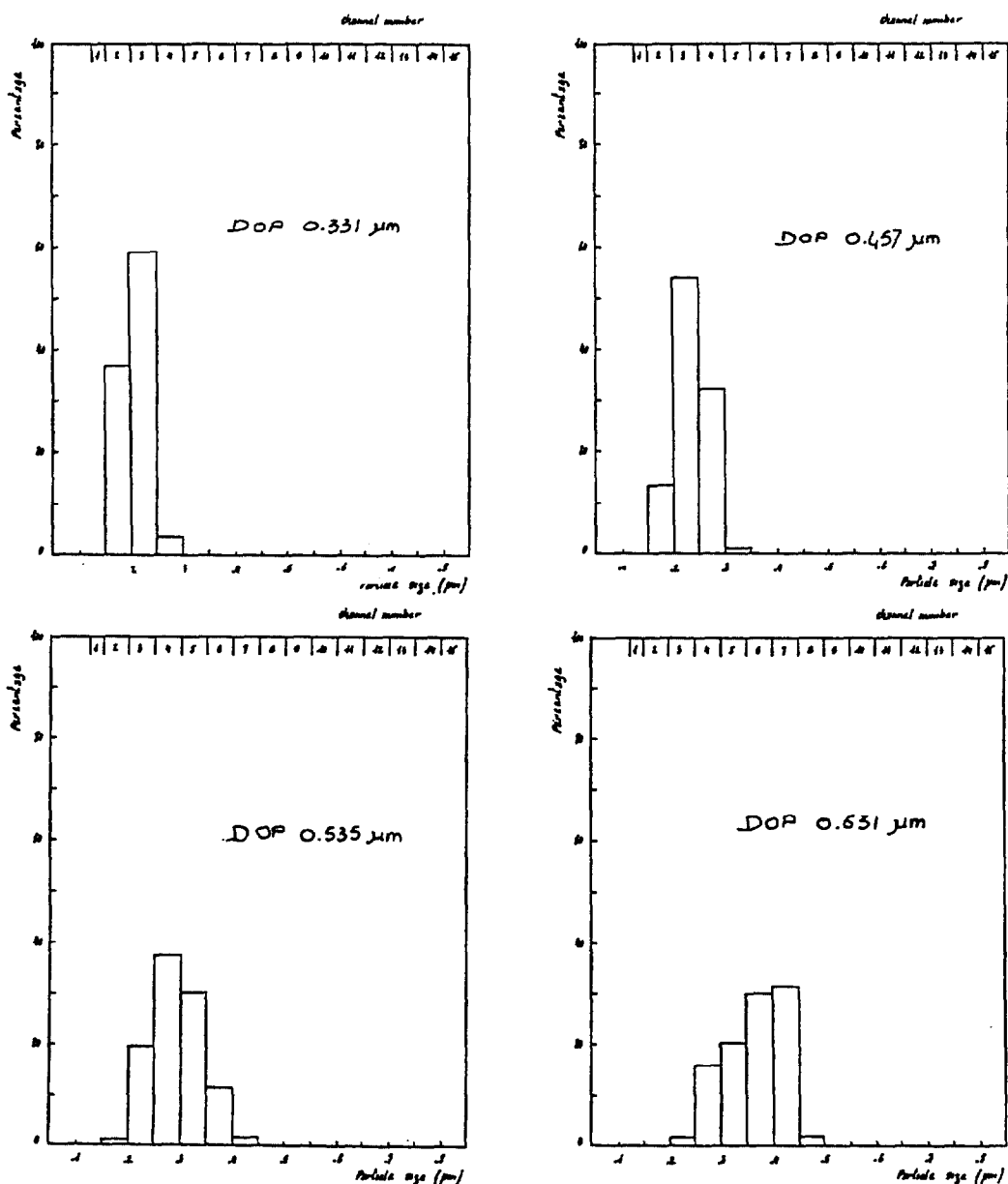


Figure 7

# 19th DOE/NRC NUCLEAR AIR CLEANING CONFERENCE

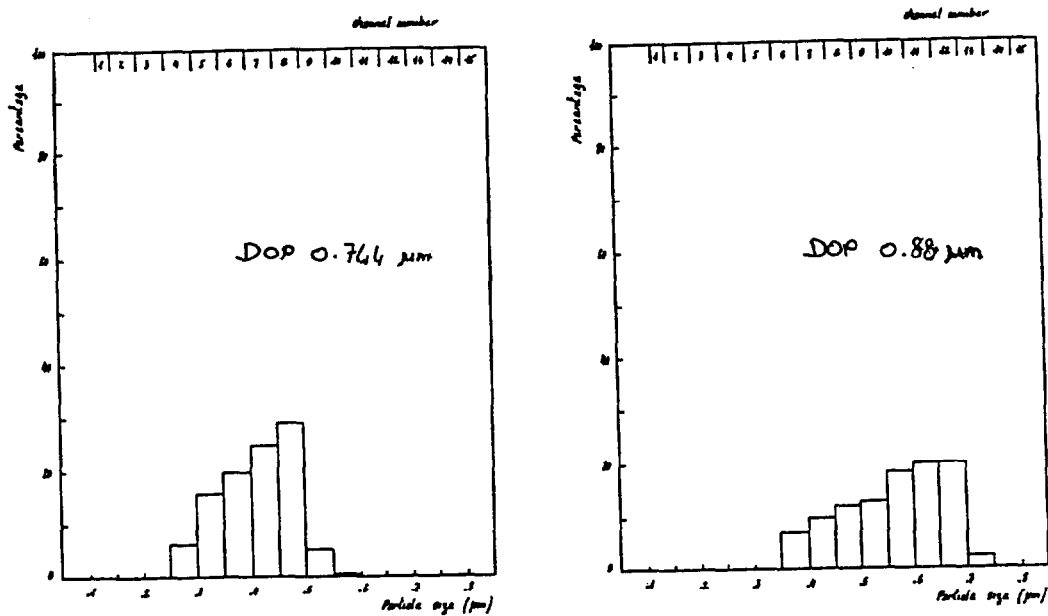


Figure 7 (followed)

Mean diameters and standard deviations were also calculated from cumulative distributions. These data are plotted in figure 8.

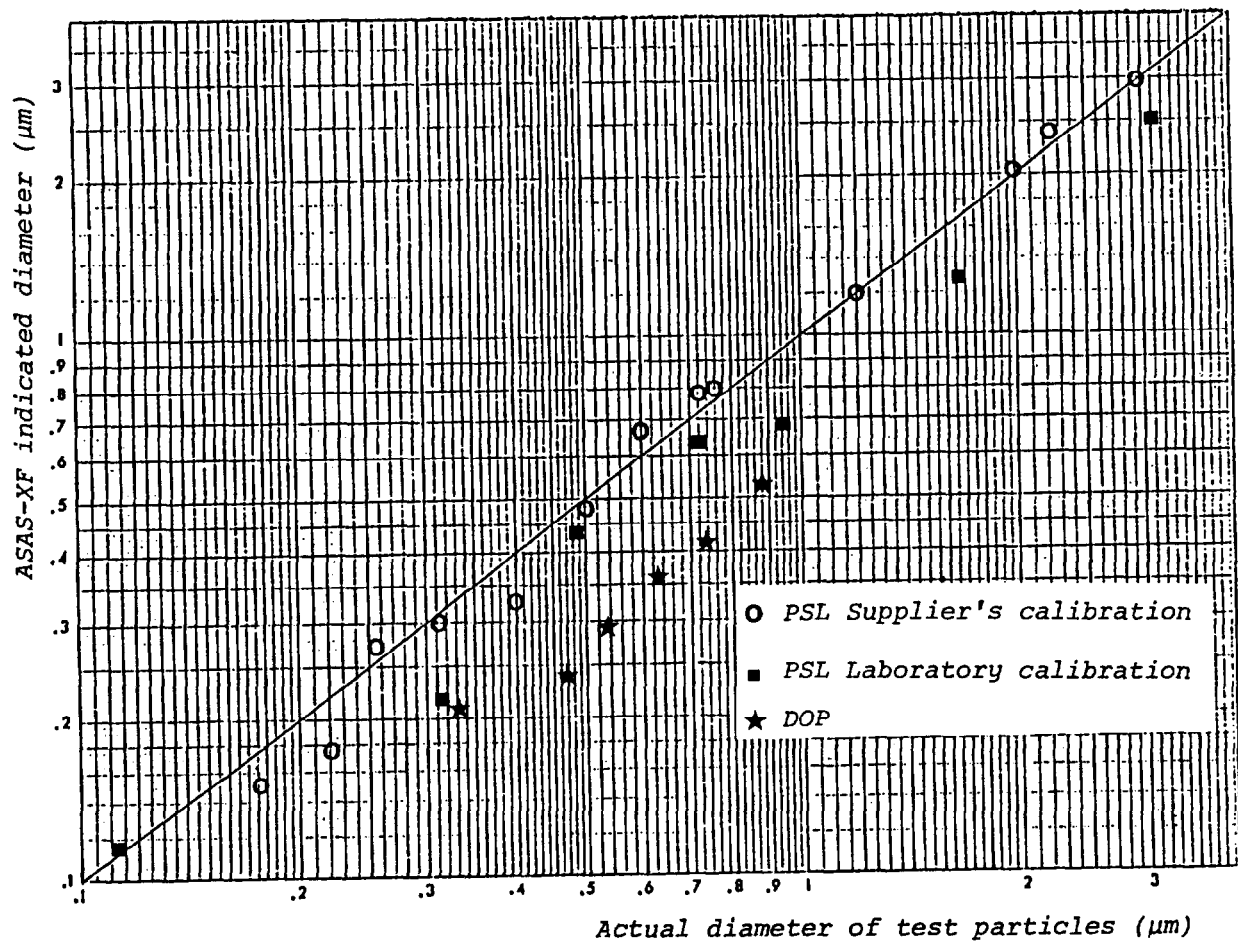


Figure 8

# 19th DOE/NRC NUCLEAR AIR CLEANING CONFERENCE

## IV. Discussion

The calibration of the ASAS-XF laser aerosol spectrometer with PSL and DOP monodispersed aerosols (all reselected by the DMPS if ranging below 0.84  $\mu\text{m}$ ) are summarized in table II.

Table II

Actual particle diameter ( $\mu\text{m}$ )	Mean particle diameter calculated from instrument indication ( $\mu\text{m}$ )	Standard deviation
0.12 (PSL)	0.13	1.09*
0.312 (PSL)	0.22	1.14*
0.481 (PSL)	0.43	1.19*
0.721 (PSL)	0.63	1.15*
0.94 (PSL)	0.68	1.26
1.65 (PSL)	1.27	1.23
3.10 (PSL)	2.50	1.11
0.331 (DOP)	0.21	1.135*
0.457 (DOP)	0.23	1.15*
0.535 (DOP)	0.29	1.18*
0.631 (DOP)	0.36	1.18*
0.744 (DOP)	0.41	1.20*
0.88 (DOP)	0.52	1.18*

\* Aerosol reselected by means of the DMPS

The results for the PSL calibration are in a good agreement with the initial calibration carried out by the supplier.

The standard deviation  $\sigma_g$  ( $\sigma_g = \frac{\text{diameter at 50\%}}{\text{diameter at 16\%}}$ ) either for PSL or DOP monodispersed aerosols is less than 1.2. This corresponds to a good spectral resolution.

On the other hand, these tests confirm previous works (3) with regard to the role played by the refractive index of the particle on the diameter measured by the instrument. As a matter of fact, the diameter indicated for DOP particles in the measurement RANGE 1 is about 50% less than the actual diameter. This is of particular importance when size distribution and spectral efficiency measurements are carried out.

## References

- (1) J.C. Elder, T.G. Kyle, M.I. Tillery and H.J. Ettinger. In place testing of tandem HEPA filter stages using fluorescent aerosols. 16th DOE Nuclear Air Cleaning Conference (1980)
- (2) J.P. Deworm. Laser particle spectrometry for testing HEPA filtration systems in the nuclear industry. Filtration and Separation. (July/August 1984)
- (3) W.C. Hinds and G. Kraske. Performance of PMS model LAS-X optical particle counter. J. Aerosol Sci. 17 n° 1 (1986)

DISCUSSION

HOLUB: Who makes the laser fluorescent particle spectrometer?

MULCEY: The manufacturer is Particle Measuring Systems, Boulder, Colorado.

ETTINGER: On your last viewgraph, where you showed the difference between polystyrene latex and DOP, did you correct DOP for index of refraction?

MULCEY: No, we did not. The data plotted on this viewgraph were directly obtained from the apparatus.

ETTINGER: Would a correction for index of refraction have brought them into closer agreement?

MULCEY: Certainly.

SCRIPSICK: A specific analysis of the difference between the responses for DOP and PSL particles of the same diameter has not been performed. This would take into account that the wavelength of our laser (He - Cd : 442 nm) is different from other's (He - Ne : 633 mn).

A NEW LIGHT SCATTERING SPECTROSCOPY TECHNIQUE  
FOR RAPID ASSESSMENT OF FILTER MEDIA

Yong W. Kim  
Professor of Physics  
Lehigh University, Bethlehem, Pa. 18015

ABSTRACT

Rapid execution of particulate filter evaluation for performance as a function of particle size is of great importance both from an applications stand point and for studies of particle removal mechanisms because any filter medium ages in the course of such testing activities. New instrumentation for essentially instantaneous determination of the particle size distribution function both upstream and downstream of a filter medium has been developed in this connection. The technique is based on real-time measurement of the light scattering loss spectrum over a wide wavelength range covering the ultraviolet to near infrared extremes. The spectrum is deconvoluted for determination of the full size distribution function in under a minute. Mineral oil drops produced by a modified Laskin generator and other atomizers are used, with concentrations varying over five orders of magnitude and particle size reaching  $0.1\text{ }\mu\text{m}$  or less on the small size end. Critical analysis of the overall methodology is presented.

I. Introduction

Small particles in suspension are encountered in a variety of situations, ranging from natural phenomena, such as volcanic events, forest fires and photochemical smog to manufacturing and basic investigations of fluid phenomena. The particle size distribution function of the suspension invariably are required in any quantitative analysis.

Of particular importance to the general program of aerosol filter evaluation is a rapid method for measuring the particle size distribution function. This is because the performance of any given filter changes as a function of its total exposure to the particle-laden gas flow. The method must also be applicable to a wide range of particle concentration because the filter efficiency as a function of particle size requires measurement of the size distribution function both on the upstream and downstream side of the filter.

In this paper, a new technique for size distribution measurement will be described, which is based on the light scattering properties of small dielectric spheres. The technique is new in that the light scattering from a suspension is observed and analyzed as a

spectroscopic phenomenon covering a continuous spectral range from 2000Å to 9000Å. In contrast, the conventional light scattering methods deal with the angular distribution of scattered intensities at one or a few selected wavelengths. As a spectroscopic process, the total scattered intensity spectrum exhibits a broad resonance structure as a result of a convolution of the light scattering cross-section and the particle size distribution function. The particle size distribution function is then obtained through deconvolution of the measured spectrum aided by the fact that the light scattering cross-section is known.

In the present implementation of the above concept of light scattering spectroscopy, measurement is made of the light scattering loss spectrum. A collimated beam of continuum light suffers a loss of intensity due to scattering as it goes through a suspension of small particles. It can be shown that the light scattering loss spectrum, when reduced to the form of the absorption coefficient, exhibits the same resonance structure as referred to earlier. The advantages of this approach are: i) the range of particle number density over which the technique can be applied can be as large as five orders of magnitude and ii) the technique is truly non-invasive, permitting in-situ applications.

In the following sections, we will describe first the basic framework of the technique in the light scattering mode. A description of the experimental implementation will then be given. The results of some measurements will be also presented, together with a critical analysis of the overall methodology.

## II. The Light Scattering Loss Spectroscopy

In the present implementation of the light scattering loss spectroscopy technique, we envision a particle suspension in a gas flow leading to, and departing from, a filter medium. A narrow, highly collimated, beam of light is directed into the suspension. The intensity of the beam is attenuated by scattering of the light from the particles and by absorption of the light by the bulk of the particles and the host gas molecules. The scattering loss alone can be determined if the incident intensity is defined to be that transmitted through the particle free gas of the same path length and gas density. The bulk absorption by the particles can also be excluded by considering the measured absorption coefficient of mineral oil, the liquid used for dispersal of the aerosol in the present experiment, but this turns out to be negligible here.

It can then be readily shown that the transmitted intensity  $I(x, \lambda)$  as affected by the scattering loss alone, is given by

$$I(x, \lambda) = I_0(\lambda) \exp[-K_f(\lambda)x] \quad (1)$$

where

$$K_f(\lambda) = \pi n \int_0^\infty R^2 Q_s(R, \lambda) f(R) dR. \quad (2)$$

$x$  denotes the length of the suspension along the beam path,  $\lambda$  the wavelength of light,  $R$  the particle radius and  $n$  the particle number density in the suspension.  $I_0(\lambda)$  is the incident intensity of light at wavelength  $\lambda$ , as defined by the intensity transmitted through the gas without particles suspended in it.  $Q_s(R, \lambda)$  is the total scattering efficiency, which is the total light scattering cross-section for a particle of radius  $R$  at wavelength  $\lambda$  expressed in units of the geometrical cross-section of the particle,  $\pi R^2$ . Derivation of eq. (1) is described in detail elsewhere.<sup>(1)</sup>

Of particular interest here is the attenuation coefficient  $K_f(\lambda)$ . It is given as a convolution of  $Q_s(R, \lambda)$  and the particle size distribution function  $f(R)$ . Here  $f(R)$  is normalized according to

$$\int_0^\infty f(R) dR = 1. \quad (3)$$

Implicit in the expression for  $K_f(\lambda)$  is that full knowledge of the index of refraction,  $m$ , for the bulk material of the particle is required because  $Q_s(R, \lambda)$  depends on it. The resonance structure mentioned earlier in the introduction pertains to the functional form of  $K_f(\lambda)$ . It comes about as a result of going in, and out of alignment, of the maxima of  $Q_s(R, \lambda)$  with the maximum of  $f(R)$  when the wavelength is varied. This is because the undulating structure of  $Q_s(R, \lambda)$  are expanded or contracted due to changes in  $n$ , whereas  $f(R)$  remains unchanged.

The particle size distribution function is extracted from the measured  $K_f(\lambda)$  by a deconvolution process because the functional form of  $Q_s(R, \lambda)$  is known. The uniqueness in determination of  $f(R)$  is a critical issue in such a deconvolution process; it simply hinges on the breadth of the wavelength range in measuring the resonance structure of  $K_f(\lambda)$ .  $K_f(\lambda)$ , of course, is obtained from measurement of the intensity ratio  $I(x, \lambda)/I_0(\lambda)$ . In view of the wide dynamic range required of the technique as a means for aerosol filter evaluation, the ratio must be measurable over a wide range of the particle number density  $n$ . The main strength of the light scattering loss mode lies in the fact that the quality of the measured ratio  $I(x, \lambda)/I_0(\lambda)$  can indeed be maintained as the particle number density undergoes steep changes over several orders of magnitude because the ratio depends on the product of  $x$  and  $n$  and the product of  $xn$  can be kept in a narrow range of value by appropriately adjusting  $x$  in response to the changes in  $n$ . Consequently,  $K_f(\lambda)$  can be measured accurately even though the magnitude of  $K_f(\lambda)$  may decrease sharply with decreasing  $n$ .

The procedure for determination of the particle size distribution is to search for a distribution function of definite amplitude, width and maximal radius parameters in such a way that the calculated



$K_f(\lambda)$  best fits the measured  $K_f(\lambda)$ . The search is carried out on a dedicated computer by means of an efficient numerical algorithm which we have devised for this application.

Several two parameter size distribution functions are employed:

Zeroth order log-normal distribution

$$f(R) = (2\pi z^2 R_m)^{-\frac{1}{2}} \exp \left[ -z^2/2 + (\ln R_m - \ln R)^2/2z^2 \right] \quad (4)$$

Schultz distribution (unnormalized)

$$f(R) = (R/R_m)^z \exp \left[ -(z+1)R/R_m \right] \quad (5)$$

Maxwell distribution (unnormalized)

$$f(R) = (R/z)^{M-3} \exp(-R^2/z^2), \text{ where } R_m = z[(M-3)/2]^{\frac{1}{2}} \quad (6)$$

Here  $R_m$  represents the mean or maximal radius and  $z$  the width parameter.<sup>m</sup> It is noted that the actual values of  $R_m$  and  $z$  have different meanings for different distribution functions.

### III. The Experimental Arrangement

Fig. 1 shows schematically the overall arrangement of the experiment. It consists of a source of mineral oil aerosols, two light scattering stations, two collimated continuum light sources, a filter section, a flat field spectrograph with photodetectors, two digital signal processors and a 16-bit microcomputer. The particle source has two generators (a modified Laskin generator and an atomizer), a settling chamber and a flow manifold for arbitrary dilution of the particle suspension with particle-free gas.

The two light scattering stations are basically vacuum-tight chambers of cylindrical shape, equipped with two fused silica windows on the ends. The one on the upstream side of the filter section is short in length, variable from 0.1 to 10 cm, in keeping with a severe loss of the light intensity by scattering at very high particle concentration. The second station is much longer, 134 cm in length, and is located between two wide area mirrors whose orientation can be controlled independently. By changing the relative orientation of the mirrors, the incoming collimated light beam can be steered to make multiple traversals through the chamber. The net effect is to essentially arbitrarily increase the path length  $x$ , as appearing in eq. (1), in response to a sharp decrease in the particle number density in the gas stream after passing through the filter section.

As can be seen in the figure, the light sources employ all-mirror

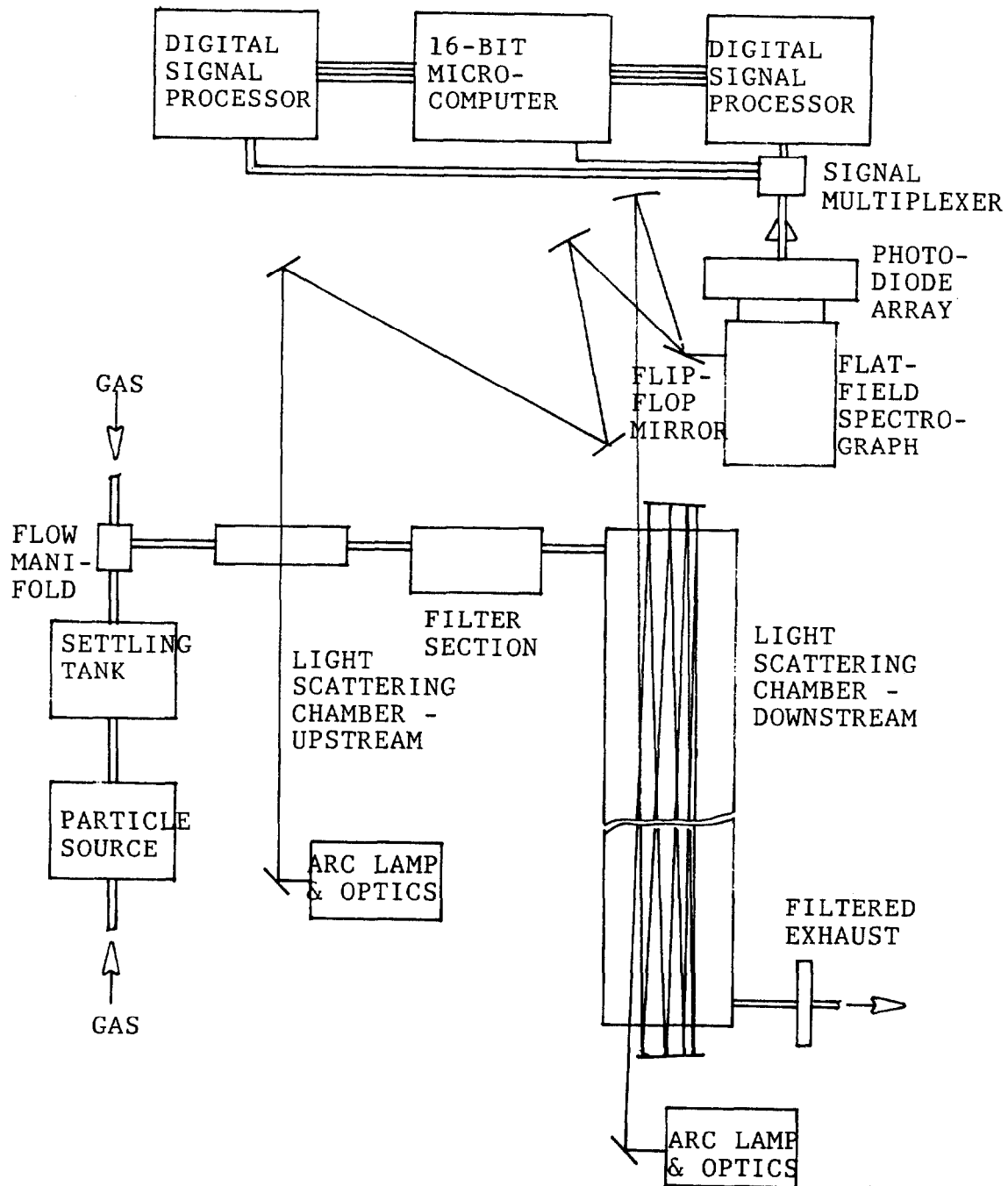


Fig.1. Schematic diagram of the experimental arrangement, consisting of a particle source, two light scattering chambers, a filter section, two continuum light sources, a spectrograph and data processor electronics.

optics in order to produce a highly collimated beam whose beam quality is independent of wavelength over the entire spectral range from 2000 to 9000Å. The xenon arc lamp provides a strong continuum of light with only minor line spectra superposed on it.

Both of the collimated beams terminate at the entrance slit of one spectrograph on a time-shared basis by means of a flip-flop mirror, which can be set at one of the two detented orientations under computer control. The full intensity spectrum is measured with a 1024-element photodiode array detector, which is mounted on the image plane of the spectrograph. The spectrograph provides a flat image plane with a linear dispersion of 360Å/mm.

The intensity spectrum detected by the photodiode array detector is read out in the form of sequential analog voltages corresponding to individual photodiode pixel elements and stored in one of two digital signal processors. Each read-out takes less than 100 msec. After the two light beams are so interrogated, the data stored in the signal processors are moved to the computer under the RS-232C protocol. A full measurement consists of taking  $I_o(\lambda)$ , which is the intensity spectrum seen by the exact same optical system except that the gas glow is free of particles, for each of the two beams and storing the two spectra in the computer as references, followed by measurements of  $I(x, \lambda)$ . Experience shows that the entire experiment can be conducted for hours without measureable changes in  $I_o(\lambda)$  and therefore only occasional updating of  $I_o(\lambda)$  is needed.

The two sets of spectra  $I(x, \lambda)$  and  $I_o(\lambda)$ , corresponding to the two light scattering chambers, are then processed to extract the two attenuation coefficient spectra  $K_f(\lambda)$ . Subsequent numerical searches bring out the particle size distribution functions. The entire process of measurement and analysis takes two minutes at present. It is reasonable to expect that this time can be further reduced at least by a factor of two.

#### IV. Results and Critical Analysis

We will now focus on the measurement of the particle size distribution in the light scattering chamber on the upstream side of the filter section. The particles are droplets of heavy mineral oil. The index of refraction for the oil is needed in order to carry out computation of the total light scattering efficiency  $Q_s(R, \lambda)$ . The measurement of the index over the full wavelength range of interest turned out to be somewhat taxing due to a strong absorption at wavelengths below 3000Å. As a result, we have developed a special instrument for measurement of the index of refraction of liquids. The instrument will be described in another publication but the result for the mineral oil is shown in Fig. 2.

Fig. 3 shows a measured  $K_f(\lambda)$  spectrum for a suspension with

particle number density of  $2 \times 10^7$  particles/cm<sup>3</sup>, as produced by the atomizer. The plot is prepared in such a way that the magnitudes of the  $K_f(\lambda)$  spectrum are shown for 100 different wavelengths and are normalized to the maximum value,  $(K_f)_{\max}$ , of the  $K_f(\lambda)$  spectrum.

The particle number density is determined by two methods: a) counting of particles, as suspended, by means of an ultramicroscope<sup>(1)</sup> and b) counting of the particles which are collected on an electron microscope grid by sweeping out all entrained particles in a volume of gas onto the walls of a container. In the second method, the grid is mounted flush with the inner wall surface of a cylindrical electrostatic precipitator. After a steady flow of the suspension is established through the precipitator section, the flow is stopped and all particles precipitated electrostatically. The collected particles are first exposed to the vapor of osmium tetroxide before examination by electron microscopy. From the known gas volume, surface area and the total number of particles per unit area of the grid, one can deduce the particle number density. This latter method also provides an independent measurement of the particle size distribution function.

Deconvolution of the measured  $K_f(\lambda)$  spectrum of Fig. 3 is carried out by comparing it to a bank of calculated  $K_f(\lambda)$  spectra resident in the computer files. The calculated spectra have been generated by varying the maximal radius and width parameters of a given size

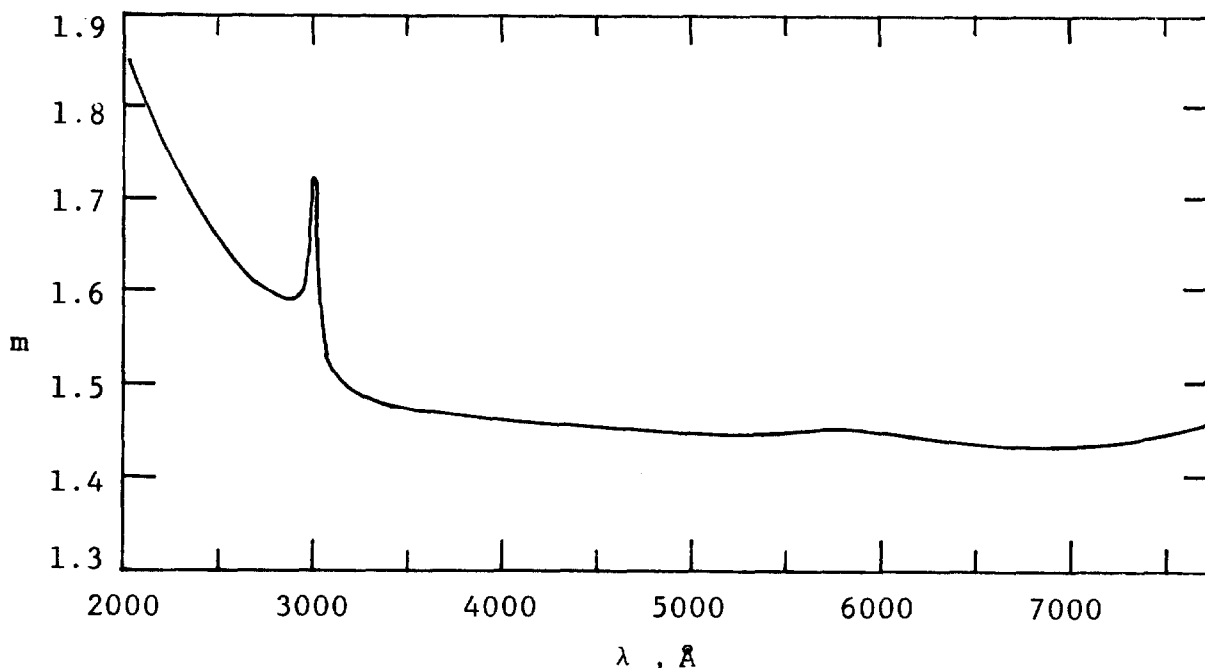


Fig.2. Measured index of refraction of heavy mineral oil as a function of wavelength.

distribution function in the neighborhood of the actual size distribution of the particles used in the experiment. Altogether, five different functions have been considered to represent the particle size distribution and three of them were shown earlier in eqs. (4)-(6). 105 to 132  $K_f(\lambda)$  spectra have been calculated and stored in our computer files for each form of the size distribution function.

The search is conducted by minimizing the absolute difference between the measured and calculated  $K_f(\lambda)$  spectra. The search is broken up into two or three levels of coarseness in the increments of parameters  $R_0$  and  $Z$ . In this way, not only the time for search is significantly reduced, as compared to a sequential search algorithm, but also the precision of the fit can be arbitrarily improved on in

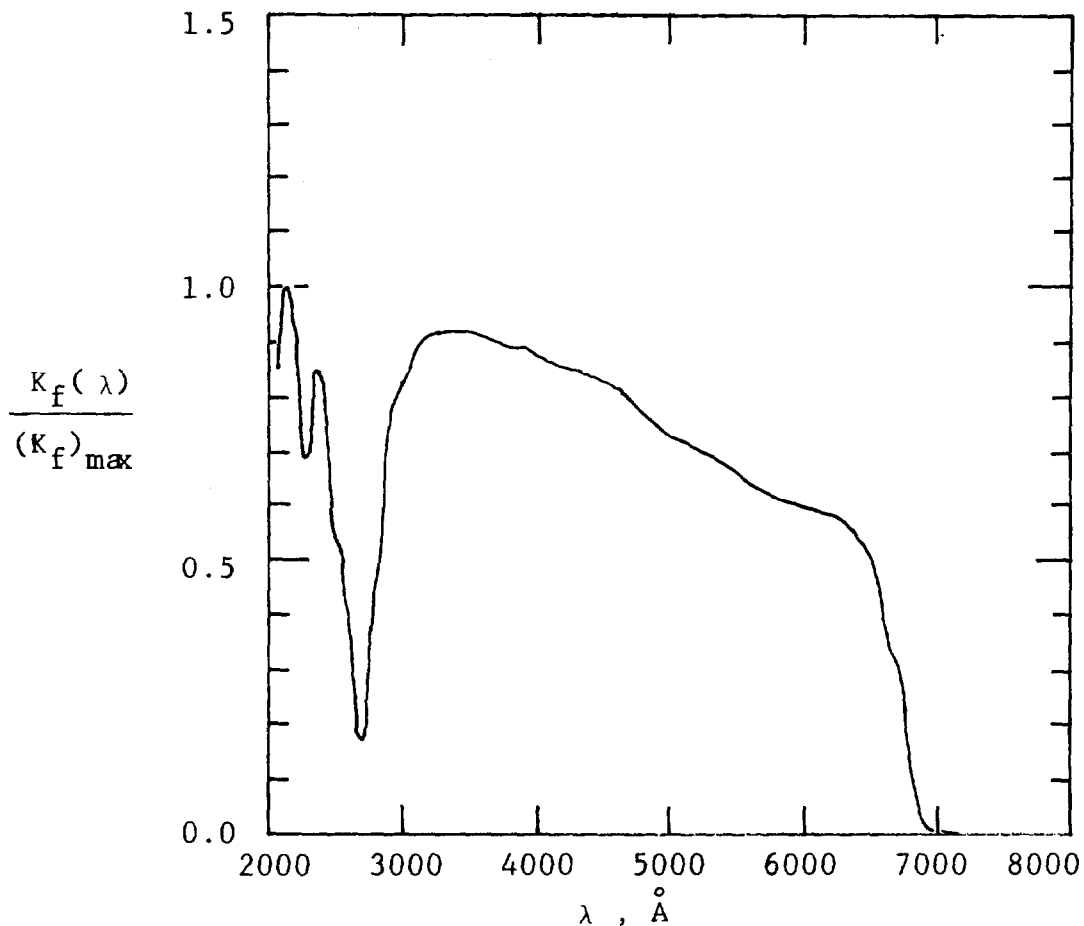


Fig.3. Normalized attenuation spectrum as measured for a suspension of atomized mineral oil drops.

succeeding levels of search, given that the  $K_f(\lambda)$  spectrum has been sufficiently accurately determined.

Fig. 4 shows the resulting particle size distribution function. Also shown in the figure is the result of particle size measurements by electron microscopy based on the sampling procedure employing the technique of the electrostatic precipitation outlined earlier. Agreement is remarkably good between the two results.

In an attempt to evaluate the overall sensitivity of the final determination of the size distribution function to experimental uncertainties, the measured  $K_f(\lambda)$  spectrum has been subjected to a variety of random errors, simulating the shot to shot variations in

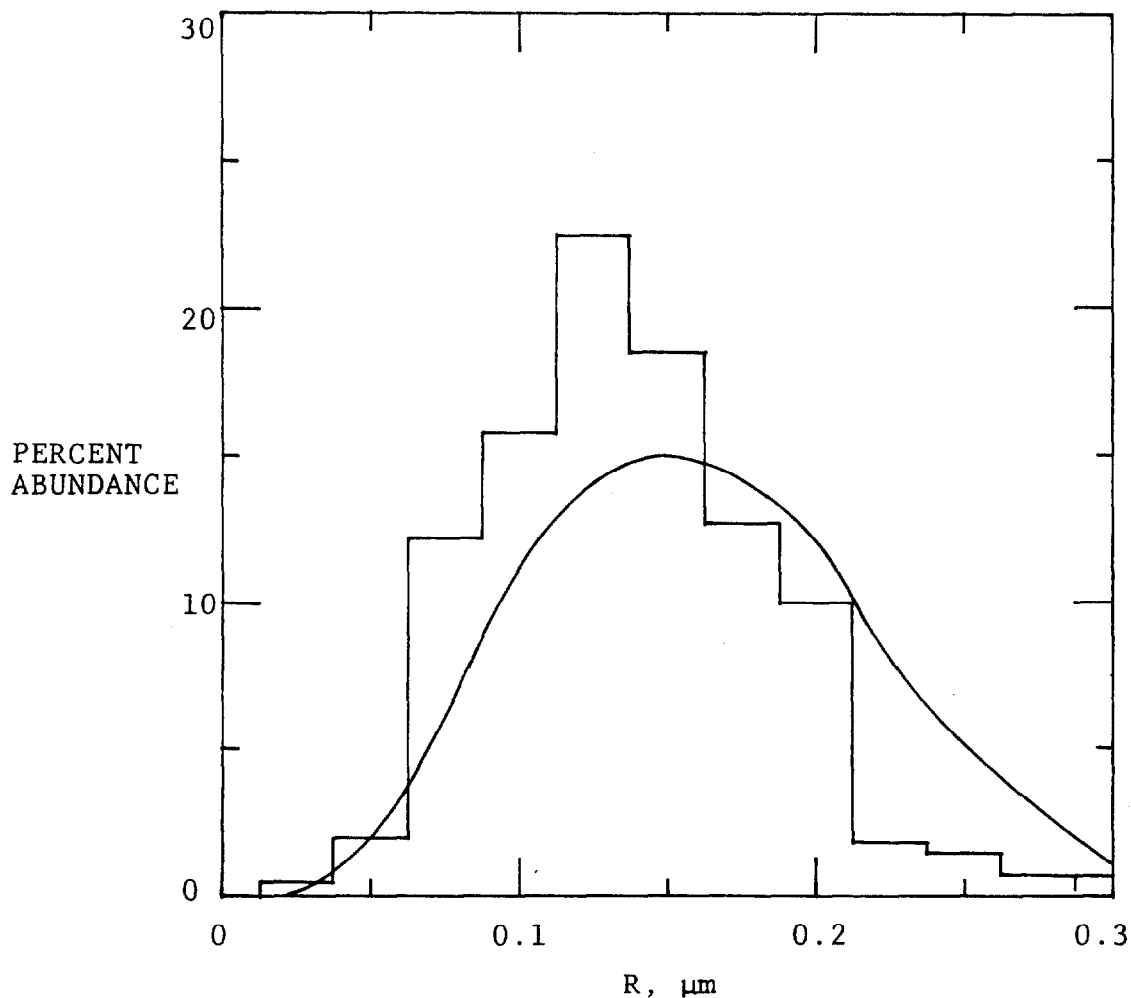


Fig.4. The particle size distribution function as reduced from the measured  $K_f(\lambda)$  of Fig.3, using the Maxwell distribution function. The histogram gives the electron microscopy data.

its measurement. The magnitude of the  $K_f(\lambda)$  spectrum at each given wavelength is subjected to random errors not exceeding a fixed percentage error  $\delta$ . Two white-noise random number generators are used for this purpose, one to choose the size of the number to be added to the measured  $K_f(\lambda)$  spectrum and the other to select its sign. The resulting  $K_f(\lambda)$  spectrum is then processed through the search routine to arrive at a new best-fit particle size distribution function. This is repeated several times for each given  $\delta$ -value in order to determine the range of spread in the best-fit parameters  $R_m$  and  $Z$ . The results of this sensitivity analysis are that for the zeroth order log-normal distribution function, the maximum range of variation in  $R_m$  is  $\pm 2.64$  and  $\pm 7.5\%$  when  $\delta = \pm 2\%$  and  $\pm 5\%$ , respectively. The corresponding spread for  $Z$  shows much the same response.

### V. Conclusions

Our research program on light scattering as a branch of spectroscopy has been described with particular emphasis on implementation of the light scattering loss spectroscopy technique for measurement of the size distribution function of aerosol particles. The technique has been adapted to filter evaluation applications and all aspects of carrying out measurements with the technique have been examined, including its application under real-time conditions. As the evidence presented in the preceding sections demonstrate, the technique is indeed rapid, versatile and information rich in the sense of broad size range coverage and wide dynamic range in particle concentration. In addition, with proper calibrations, one can determine the particle number density as well as the size distribution function. Furthermore, there is ample room for working with more complex forms of the size distribution function, which may have more than two parameters, in order to attain finer details of the particle size distribution.

The author acknowledges valuable assistance of M. Reuter, R. Marlowe, S. H. Kim, R. Millard, J. D. Kim, E. Gretzinger, M. Lee, J. Gregoris and M. Masters. This work has been supported in part by the Chemical Research and Development Center of the U. S. Army.

### References

1. Y. W. Kim, "Development of a New Technique and Instrumentation for Rapid Assessment of Filter Media", Proceedings of the 18th DOE Nuclear Airborne Waste Management and Air Cleaning Conference, Baltimore, 12-16 August 1984, ed. M. W. First (1985). p. 1193

## 19th DOE/NRC NUCLEAR AIR CLEANING CONFERENCE

### DISCUSSION

BERGMAN: A general comment on ensemble scattering, which I think may be applicable to this method, is the non-uniqueness of effectively deconvoluting turbidity spectra or extinction spectra. Namely, for the same spectra you can fit many different particle size distributions. Previous investigators had been well aware of the non-uniqueness of a deconvolution technique for many years. Would you care to comment on how your particular technique of ensemble scattering addresses the problem of non-unique solutions of size distributions?

KIM: The non-uniqueness comes from the meager nature of the experimental data. If you make a measurement at two wave lengths, the non-uniqueness, or ambiguity, in your result becomes enormously multiplied. Our approach exactly addresses that because we are deliberately looking over a very wide spectral range, making 1,024 separate wave length measurements simultaneously. That is to say, we are adding 1,024 boundary conditions which a size distribution function can be fitted to. The function has essentially three characters, two parameters and the nature of the function, so you are trying to solve three unknowns out of 1,024 boundary conditions and therefore a stringent fit can be arrived at. We find non-uniqueness not to be an issue. On the other hand, when you go to experimental methods, where measurements are made at 5 or 6 different laser wave lengths, non-uniqueness becomes a big issue and then you throw in experimental uncertainties right on the top. So, the wealth of information is critical.

BERGMAN: Just to elaborate on that point. Have you tried to fit many different size distributions to the same light scattering spectrum? For example, if you maintain a constant average volume for the particle size distribution while you vary the degree of heterodispersion from monodisperse to heterodisperse, I expect you will see the same light scattering spectra. However, you are absolutely right, the previous work has been restricted to very narrow wave lengths between 400 to 600 nanometers. Increasing the spectrum will resolve some of the ambiguities, but aren't some of the 1,024 boundary conditions redundant?

KIM: I think your points are well made, but I must disagree with you because the measurement is a unique value as you change the wave length of light. It is not measuring it in a more clever way because the physical measuring stick is being changed. When you go through the many different size distribution functions one can decide the best fit for each function. On the other hand, when you look at the chi-square values absolutely, it shows that certain functions fit better than others. That is how we arrived at the Maxwell distribution as being the best fit. What I am really saying, as I mentioned before, is that you are dealing with more than two parameters. By choosing different types of functions, you are introducing a third and fourth additional variable. If you look at the experimental data, the  $K\lambda$  spectrum, they show rather significant details. All the local maxima are real results that come from the fact that the light scattering function has an undulating structure and the size distribution function is scanned



through it as you change the wave length. You run into resonances, i.e., numerous bumps, and the depth of the bump, or how sharp it is will depend on how narrow the size distribution function is. These are the kinds of data that potentially can help accommodate many more independent parameters to deal with the size distribution.

ANDERSON: Your theoretical approach seems to be oriented toward Mie scattering regions. Since filtration interest is restricted to only the portion .01 to .3  $\mu\text{m}$ , how does the Rayleigh and/or Gonz transition affect the interpretation of your Fourier Analyses of the total spectrum? We are looking in the Rayleigh area pretty much where it is a 6th power of the function rather than square. We do not see resonance bumps in the 0.1 - 0.3  $\mu\text{m}$  light scattering patterns because there is a uniform envelope in that area. When you look at your overall theory, I agree with everything you say, but when you look at applications to filter testing, I have reservations.

KIM: Your point is well taken. It is one of the reasons why we are looking at light scattering over a very wide range of wavelengths, with particular emphasis on the very short wavelength end (near 2000 Å). In this way, we can force the Mie parameters into a large value regime and enhance the role of the periodic structure of the total scattering efficiency function. I am curious about your lack of observation of the bumps. How was your experiment done?

ANDERSON: When you are down around 0.1 - 0.2  $\mu\text{m}$  the scattering function is uniform, with the majority of it in the forward direction.

KIM: This is at what wave length?

ANDERSON: This is at the visible wave length which is the same as you are working, 400 to 600 nanometers.

KIM: We are operating with a shorter wave length light source.

ANDERSON: You do not get the pronounced bumps at the other wave length, also.

KIM: I think we are talking about different bumps. I am sure you are referring to the angular dependence.

ANDERSON: That is right.

KIM: The quantity we are dealing with is the total amount of light that is lost in all directions. It involves a spatial integration and that produces the bumps that are indicated here. If you look at the scattering efficiency as a function of the Mie parameter, you see that it behaves like a sort of a damped oscillation. These features are the ones which contain the Rayleigh regime behavior. We are not just limiting our studies to one wave length, or to a narrow range. We are looking at a much longer wave length range where the measuring stick is in fact being changed.

19th DOE/NRC NUCLEAR AIR CLEANING CONFERENCE

ANDERSON: Would you put up the equation you had on earlier? Maybe I am misinterpreting what I saw in your equation. In the very last one,  $K_f$ , is  $R$  is the radius of the particle?

KIM: Right.

ANDERSON: You have a square function in there.

KIM: That's right.

ANDERSON: The Rayleigh theory says it is a 6-power function.

KIM: The scattering efficiency function is conventionally expressed in units of the geometrical cross-section of the particles, so  $\pi R^2$  comes from that. What is left over is still contained in  $Q$  the scattering efficiency function that has the additional size dependence. That is the steep part you are referring to, the very short end of it.

ANDERSON: That is where we are working, down at the steep part.

KIM: I gather that accounts for your concern.

HOLUB: Do you think that your method of deconvolution is better than the traditional iterative methods of Twomey and Maher used in diffusion battery measurements?

KIM: It is better in terms of the time of execution. The attenuation coefficient spectrum takes very large amounts of time to compute and so does any deconvolution scheme. It also is less vulnerable to numerical errors, such as round-offs. Inspection of many calculated spectra helps in developing intuition about the most important features of the relationship between the light scattering techniques and the particle size distribution. We make a quick search and then go through another level of search, and a third. This process is the fastest method we could come up with. We had to provide a distribution function in a minute, or less if we could. It looks as though we can probably push for about 10 seconds in a reasonable fashion.

HOLUB: Do you think that this method could actually replace the other deconvolution approaches?

KIM: I don't have any comments on that. All I can say is that this is our best solution given the boundary conditions that we set up for ourselves.

SCRIPSICK: I am wondering in the vein of Vern Bergmann's and Andy Anderson's questions if it would be possible to do some mathematical experiments looking at different size distributions and how your method would deconvolute them. Would it be able to determine a difference in the region we are interested in for filter testing? If it could, it might go a long way to putting to rest some of the concerns in this area.

## 19th DOE/NRC NUCLEAR AIR CLEANING CONFERENCE

KIM: I think that is a fair question and we have done our share of it. You are really pointing out, I think, the need to look at some of these results. They are forthcoming but at this point we have looked at only these five very well exercised distribution functions and have gone through a fit with all of them, i.e., essentially through a field of about 100 to 150 files for each distribution function. Each distribution function gives you a best fit, as expected, but there is a better fit with some than with others. I think this is something that will take its legitimate course through discussions in the community. On the other hand, as a filter evaluation program, there are some issues still remaining. The dynamic range of the technique is certainly one. I might mention that on the upstream side you may have a distribution function of the type that I showed you, but after going through a filter what will be left in the stream will be very, very small particles at low concentration. Using wavelength of light as a measuring stick, pressure is on the light source to be even shorter in wavelength. When these light sources get to 2,000 - 2,500 Å, the scattered light becomes very hard to find. Therefore, there is a need to find a new light source, which we are also exploring. These are the issues for which we have made significant progress but quite a bit more work needs to be done, and we have to be educated about filters in general.

SCRIPSICK: I have a few more questions of a practical nature. First of all, the time for the rapid method of detection is indicated to be 50-60 seconds for one size distribution, and then you would have to double it in order to do a filter test. Would that take two minutes?

KIM: At present, the measurements, both upstream and downstream of the filter, can be made well under a second. The best fit search takes just under a minute for both when the searches are carried out in parallel. The time needed for the filter to be in the flow stream is well below one minute. We have, in fact, done the best fit searching for five different types of the size distribution functions. Each yields two best-fit parameters but the fit is better with some functions than others. The results from such analysis will be made available in the near future. Now that personal computers are becoming powerful and inexpensive, I don't see the need to burden one computer with both tasks. With two running simultaneously, I expect that 10-20 seconds would be sufficient for both measurements and analysis.

SCRIPSICK: On the order of one minute for a filter test in the worse case. Is that correct?

KIM: Yes.

SCRIPSICK: Also, your system depends on the shape of the particle being circular. Have you looked into the sensitivity of your calculational techniques on the shape of the particles?

KIM: We have been told about this problem by just about everybody we talk to and I have one simple answer. If the

particles are agglomerates, you may see their rotational motion, which is occurring at an extremely high rate. What you are looking at is a time-average contribution. A second point is that electron microscopy shows that agglomerates are not as prevalent with oil drops as among latex aerosols. At high concentration, latex forms very large aggregates. Given the experimental conditions, I am reasonably comfortable with the spherical assumption. It would only add a small adjustment to the analysis scheme.

SCRIPSICK: I was thinking more in terms of a quality assurance test. You use an oil aerosol but in the field you can count on solid particles being irregular.

KIM: I think that is an entirely different problem because the index of refraction has to be dealt with for those particles anyway. I would rather limit my discussion to a situation where an air filter is evaluated by the same type of liquid droplets day in and day out.

## 19th DOE/NRC NUCLEAR AIR CLEANING CONFERENCE

### HEPA FILTRATION AND MONITORING SYSTEM FOR AN UNDERGROUND NUCLEAR WASTE REPOSITORY

P.S. Parthasarthy and J. Shome  
Bechtel National Incorporated  
San Francisco, California

#### Abstract

The design of a HEPA filtration system for the underground areas of a nuclear waste disposal facility involves some unique requirements, normally not encountered in other nuclear facilities. Many of these requirements have been addressed in the design of the Waste Isolation Pilot Plan (WIPP). WIPP is a defense activity of the U.S. Department of Energy and is intended to provide a research and development facility to demonstrate the safe disposal of radioactive wastes resulting from the defense activities and programs of the United States, exempted from regulation by the Nuclear Regulatory Commission.

The primary function of the HEPA filtration system is to minimize the release of radioactive particulate contaminants from the underground facility to the outside environment during and after a postulated nuclear accident. It was established during the design, that the consequences of unfiltered releases from the WIPP facility, during normal operations and accidental occurrences, will be well below the appropriate maximum permissible limits. HEPA filtration for the underground exhaust system is provided solely to mitigate the consequences of any activity release to a level as low as reasonably achievable.

The underground exhaust air stream normally bypasses the filter units. Upon detection of any abnormal radioactivity underground, air is diverted through the HEPA filter units. Filtration mode can be initiated manually or automatically. Manual control is provided locally as well as in a remote central monitoring room.

The main components of the system are:

- A) HEPA filter units consisting of two banks of prefilters and two banks of HEPA filters in series;
- B) Two 10 feet diameter bypass isolation valves;
- C) Underground radiation monitoring system;
- D) Effluent monitoring system;
- E) Exhaust fans.

Some of the concerns addressed during the design were:

- A) Effect of dust generated by underground activities on the HEPA filters;

## 19th DOE/NRC NUCLEAR AIR CLEANING CONFERENCE

- B) Effects of an underground fire on the HEPA filters;
- C) Effect of the time lag between detection of underground radioactivity and initiation of filtration mode, on offsite releases.

An economic analysis was also performed comparing the present system design to a continuous filtration system with no bypass. Results of the analysis are summarized later in this paper.

### Functions of the System

The primary functions of the underground ventilation system at WIPP are:

- A. To provide adequate quantities of fresh air to all underground personnel and equipment.
- B. To maintain an airflow pattern which will preclude movement of potentially contaminated air from areas where waste emplacement operations are performed to areas where construction is in progress.
- C. To minimize the spread of smoke and fire within the underground areas during a postulated fire accident.
- D. To minimize and control the release of airborne radioactive particulate contaminants from the underground facility to the outside environment during and after a postulated nuclear accident.

The focus of this paper will be on the last item listed above.

### System Description

#### General

Storage level in the WIPP facility is approximately 670 meters (2200 feet) below the surface and is served by three shafts.

- A. Construction and salt handling (C&SH) shaft, 3 meters (10 feet) diameter.
- B. Waste shaft, 5.8 meters (19 feet) diameter.
- C. Exhaust shaft, 4.3 meters (14 feet) diameter.

The C&SH shaft is used as the primary air intake to the underground, the waste shaft as the auxiliary air intake and the exhaust shaft is used for the ventilation exhaust. Near the bottom of the C&SH shaft the supply air is split into three streams, one serving the waste storage areas, the second serving the construction areas and the third serving the experimental areas (Fig. 1 and Fig. 2). Air coming down the waste shaft is used to

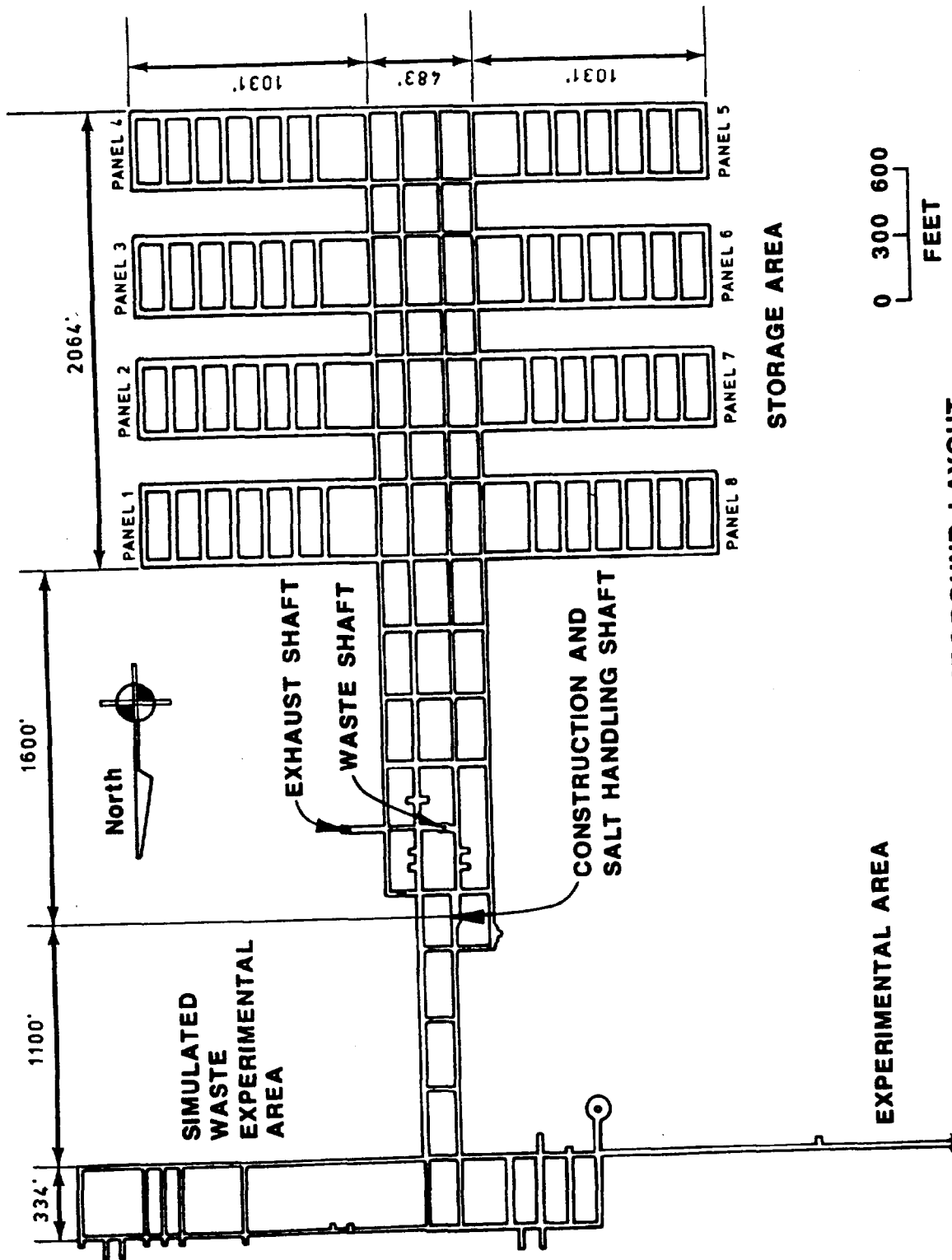


Figure 1 UNDERGROUND LAYOUT





## 19th DOE/NRC NUCLEAR AIR CLEANING CONFERENCE

ventilate only the waste shaft station and the immediate work areas and is then exhausted directly through the exhaust shaft. A common exhaust shaft serves all underground areas.

Construction and waste storage operations will be performed in separate shifts and the bulk of the fresh air will be switched from one area to the other at the end of each shift.

Within the underground facility, ventilation separation is maintained between the waste storage and construction areas. A pressure gradient is established which ensures that air leakage is always from construction areas towards waste storage areas. To facilitate separation of the two sides, a unique sequence of construction, waste emplacement, and backfilling operations will be used. With such sequencing, personnel will not be required to work in the exhaust air stream from the waste storage side.

Three main exhaust fans are located on the surface. In addition, booster fans are provided underground, on the construction side only, to ensure a pressure differential between the waste storage and construction sides.

Each exhaust fan is sized for  $33 \text{ M}^3/\text{sec}$  (70,000 cfm) at a static pressure of 3237 pascals (13.00 inches water gage), to give a total ventilation capacity of  $99 \text{ M}^3/\text{sec}$  (210,000 cfm).

### HEPA Filtration System

It was established by a study<sup>(1)</sup> that the consequences of unfiltered releases from the WIPP underground areas, during normal operations and accidental occurrences, will be well below the appropriate maximum permissible limits. So a HEPA filter system was designed which permits the underground exhaust air stream to bypass the filters during normal operation. HEPA filtration is provided solely to mitigate the consequences of any activity release to a level as low as reasonably achievable. Upon detection of any abnormal radioactivity underground, exhaust air is diverted through the HEPA filters.

The filtration system is housed in the Exhaust Filter Building (Fig. 3). Air is ducted from the exhaust shaft to the building as shown. During normal operation, air flows straight through a 3 meter (10 feet) diameter duct to the outlet plenum and exhausted by the fans to the atmosphere. In the filtration mode, the two butterfly valves in the 3 meter duct are closed and air is diverted through the 1.8 meters (6 feet) duct to the filter inlet plenum. Two filter housings, each of  $14.15 \text{ M}^3/\text{sec}$  (30,000 cfm) capacity, are provided between the inlet and outlet plenums. During the filtration mode the total ventilation exhaust is reduced from the normal flow of  $99 \text{ M}^3/\text{sec}$  (210,000 cfm) to  $28.3 \text{ M}^3/\text{sec}$  (60,000 cfm). Only one out of the three main exhaust fans is required to operate.

All underground activities will cease immediately after switching to the filtration mode. The reduced level of ventilation is adequate to prevent the spread of contamination underground and to support recovery operations.

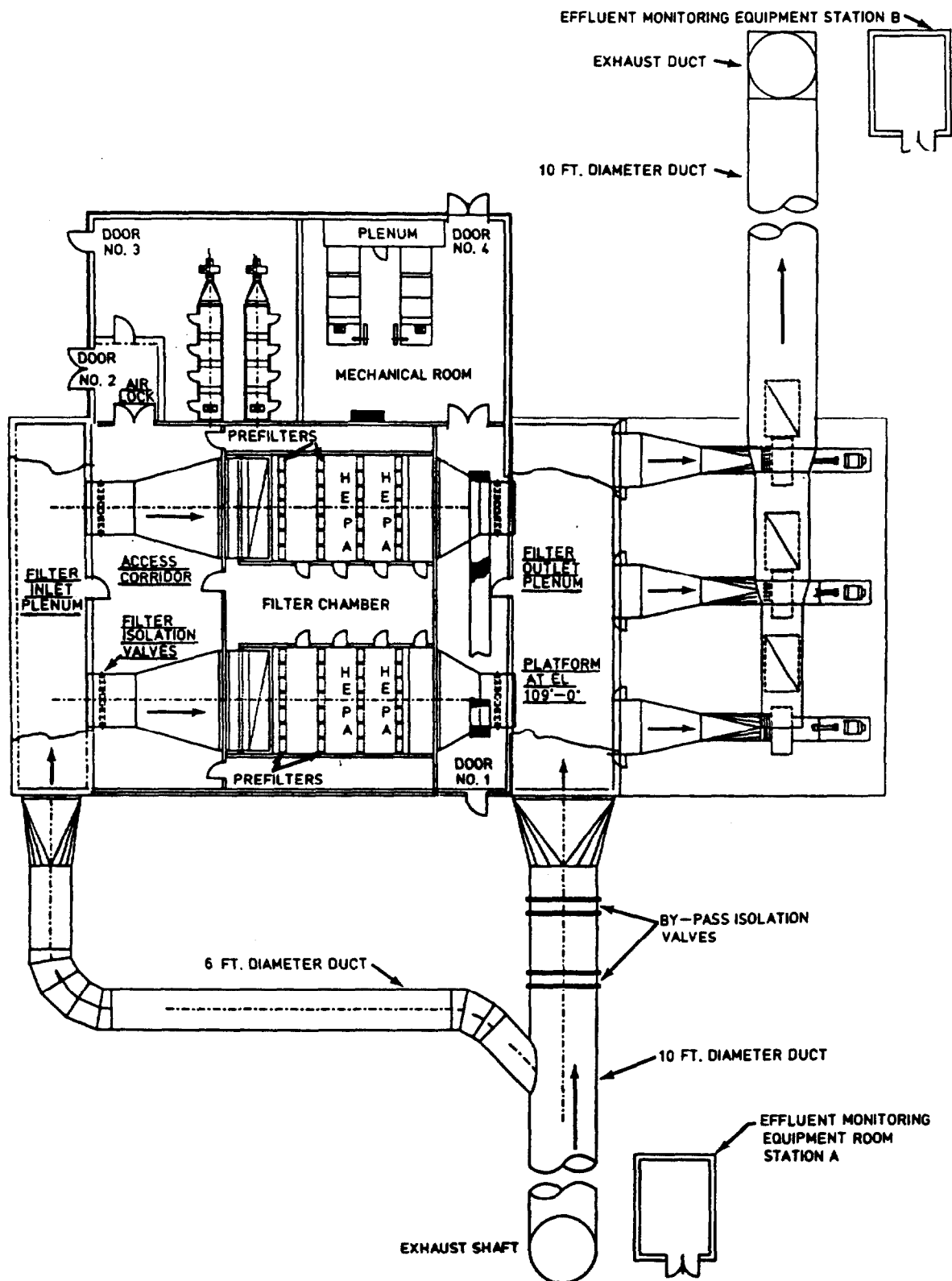


Figure 3 EXHAUST FILTER BUILDING

## 19th DOE/NRC NUCLEAR AIR CLEANING CONFERENCE

Two banks of HEPA filters are provided in series to obtain a decontamination factor of  $10^{-6}$ . Because of high levels of salt dust in the air, the HEPA filters are preceded by two banks of prefilters, a moderate efficiency bank and a high efficiency bank.

### Monitoring System

The monitoring system consists of the following:

- A. Effluent monitoring system consisting of isokinetic probes in the main exhaust duct and monitoring equipment on a nearby skid. The probes are installed at the top of the exhaust shaft and downstream of the HEPA filter units (Fig. 2). The extracted air sample is split into two parallel streams of equal volume. Each stream has a particulate filter. One is viewed by an alpha detector and the other by a beta/gamma detector.
- B. Continuous air monitors (CAM) with alpha and beta-gamma detectors underground.
- C. Non instrumented fixed air samplers (FAS) underground.
- D. Gamma area radiation monitors (ARM) underground.
- E. Differential pressure indicators for each filter bank.
- F. Flow indicators for each exhaust fan.
- G. Status indicators for bypass isolation valves and fan motors.

### Controls

The ventilation system will be automatically switched from the bypass mode to the filtration mode if any of the following events occur:

- A. Detection of airborne radioactive contaminants above a predetermined level by either the alpha or beta CAM associated with the isokinetic probes in the main exhaust duct on the surface.
- B. Receipt of a signal from at least two alpha CAM's, two beta CAM's, or one alpha and one beta CAM in the same underground airstream.
- C. A sustained 15 second loss of signal between the Central Monitoring Room and the local processing unit controlling the valves and fans.
- D. Loss of offsite power.

Items C and D provide a fail safe condition.

Upon receiving an activating signal, the controls automatically divert airflow through the HEPA filter units by closing the bypass isolation

## 19th DOE/NRC NUCLEAR AIR CLEANING CONFERENCE

valves, opening the filter isolation valves and stopping two of the three exhaust fans. Construction side booster fans underground are also stopped at this time.

### Effects of Fire and Dust on HEPA Filters

#### Fire

Smoke particles generated from a fire can rapidly plug HEPA filters and eventually damage them. Lawrence Livermore Laboratory (2)(3) has conducted a number of studies and experiments on this subject. These results could not be directly applied to WIPP because of the considerable distance between the HEPA filters and the potential source of fire underground at WIPP. Also, sufficient data is not available on the concentration and size distribution of smoke particles that would be in the airstream at the time of reaching the HEPA filters. A considerable amount of the smoke particles are expected to settle down in the underground drifts(4).

The Lawrence Livermore studies also indicate that prefiltration is the most promising of the various countermeasures being considered to prolong HEPA filter life. While WIPP does not have a rolling prefilter system referred in these studies, it has two stages of extended media prefilters.

The design basis fire underground consists of the following sequence of events(4):

- A. A 60 gallon diesel fuel tank on an underground vehicle ruptures.
- B. An ignition source sets the diesel fuel and the vehicle on fire.
- C. One stack of drums containing contact handled nuclear waste is involved in the fire. It is assumed that the other rows of drums behind the first row are protected by backfill material.

A computer program(5) that was used for ventilation network analysis on the WIPP project was also used to study the temperature distribution at various points of the network based on the design basis fire. The results indicated that the temperature in the vicinity of the HEPA filters would be less than 37.7°C (100°F). Based on this analysis, fire suppression features were deemed unnecessary for the HEPA filters.

#### Dust

In the WIPP underground facility dust is a major problem, when compared to other nuclear facilities. However, there are two alleviating factors:

- A. The HEPA filter units are part of a standby system and hence will not be exposed to dust laden air at all times.
- B. The filter units are located on the surface and are a long distance away from the source of dust generation. A major portion of the dust generated will settle down in the underground drifts (tunnels) before reaching the surface.

## 19th DOE/NRC NUCLEAR AIR CLEANING CONFERENCE

The key to prolonging the life of the HEPA filters during the filtration mode is to provide an efficient pre-filtration system which will remove most of the dust particles. A study of the available data on dust concentration and particle size distribution in the exhaust air stream was made. Two sources of data available are:

- A. A survey made by the Inhalation Toxicology Research Institute (ITRI) at WIPP<sup>(6)</sup>.
- B. A survey made at the Potash Company of America (PCA) near Carlsbad,<sup>(7)</sup> Table 1.

The surveys indicate that a decrease of nearly two orders of magnitude in concentration occurs as the sampling point is moved away from the mining equipment to the bottom of the exhaust shaft. The PCA survey provides a size distribution and concentration for each size range at the bottom of the exhaust shaft (Table 1).

Table 1 PCA Survey: Dust concentration and particle size distribution at the bottom of the exhaust shaft.

<u>Particle Size</u> <u>Micron</u>	<u>Concentration</u> <u>µg/cft</u>
7 to 11	1.68
3.3 to 4.7	2.39
1.1 to 2.1	3.44
0.43 to 0.65	2.23
0.4 to 0.05	1.19

These data were used to study prefilter and HEPA filter life during the filtration mode. This is a very conservative analysis because,

- A. During filtration mode, no mining activities are scheduled to take place, minimizing dust generation.
- B. During filtration mode the exhaust volume, and hence the velocity in the shaft, are reduced to a third of the normal operating value. This will cause more dust to settle down before reaching the filter units.
- C. PCA data was taken underground at the bottom of the shaft. No credit is taken for any plate out in the shaft, ducts, and the plenum upstream of the filters.

Based on vendor information<sup>(8)</sup> on dust holding capacity and filter efficiency, it was determined that during the filtration mode the prefilters will last approximately 21 days of continuous use before requiring replacement. HEPA filters appear to last for more than 2 years of continuous use (See Tables 2 and 3). They may need replacement for other reasons.

Table 2 Dust removed by various filter banks.

Particle Size Micron	Mod. Effy. Prefilter		High Effy. Prefilter		First Bank		HEPA Filter	
	Removal <sup>a</sup> Efficiency	Weight of Dust Removed $\mu\text{g/cft}$	Removal <sup>a</sup> Efficiency	Weight of Dust Removed $\mu\text{g/cft}$	Removal <sup>a</sup> Efficiency	Weight of Dust Removed $\mu\text{g/cft}$	Removal <sup>a</sup> Efficiency	Weight of Dust Removed $\mu\text{g/cft}$
7-11	98%	1.65	100%	0.03	100%	0.00		
3.3-4.7	80%	1.91	95%	0.46	100%	0.02		
1.1-2.1	60%	2.06	80%	1.10	100%	0.28		
0.43-0.65	40%	0.89	70%	0.94	100%	0.40		
0.4-0.05	10%	0.12	40%	0.43	99.99% <sup>b</sup>	0.64		
TOTAL		6.63		2.96		1.34		

<sup>a</sup> The removal efficiencies indicated above are approximate and are based on values indicated in ERDA Manual 76-21(9), Page 51.

<sup>b</sup> Conservative assumption for this analysis.

**19th DOE/NRC NUCLEAR AIR CLEANING CONFERENCE**

Table 3 Filter life.

	Moderate Effy. Prefilters	High Effy. Prefilters	First Bank HEPA Filters
Design air flow, each cell	1430 cfm	1430 cfm	1430 cfm
Dust loading from Table 2	6.63 $\mu$ g/cft	2.96 $\mu$ g/cft	1.34 $\mu$ g/cft
Dust loading, gm/hour	0.569	0.254	0.115
Dust holding capacity, gms (at final resistance)	270 <sup>a</sup>	130 <sup>a</sup>	2700 <sup>b</sup>
Filter life, hours	475	512	23,478
Filter life, days of continuous use	20	21	978

- <sup>a</sup> Information, courtesy of American Air Filter. Values at 2000 cfm flow rate. Values at 1430 cfm would be higher.
- <sup>b</sup> Information, courtesy of American Air Filter. Result of test using ASHRAE dust without lint.
- All filters are 24"x24"x11 1/2".

## 19th DOE/NRC NUCLEAR AIR CLEANING CONFERENCE

### Filter Bypass Feasibility Study

The study<sup>(1)</sup> evaluated the feasibility of discharging the ventilation exhaust air from the underground storage areas directly to the atmosphere, without continuous filtration.

The two main components of the study were,

- A. Radiological protection analysis and,
- B. Reliability analysis.

The radiological protection analysis evaluated the maximum potential radioactivity releases to the atmosphere. These releases depend on the time lag between the postulated releases of radioactivity to the underground air stream, the detection of the radioactivity by the CAM's or by air sample analysis, and the initiation of the filtration mode of operation. The analysis considered, among other things, delay time between underground detection and release to the atmosphere, and response time of the CAM's. Results of the study indicate that the maximum radioactivity that could be released is within the maximum permissible concentration limits established by 10 CFR 20 and DOE Order 5480.1A.

The reliability analysis considered levels of redundancy in system design, equipment failure rates, test intervals, and average time for repair. The results indicate that for each year of plant operation, the probability that the system will fail to detect and filter abnormal concentrations of radioactivity is less than  $1.24 \times 10^{-3}$ .

### Economic Analysis

During the design of the WIPP facility, a study<sup>(10)</sup> was performed to evaluate if a continuous filtration system would be more economical than a bypass system. A continuous filtration system will be simpler since it will not require any bypass hardware and control needed for switchover from one mode of operation to the other.

The study considered:

- A. Capital costs for each alternative,
- B. Operating and maintenance costs, including filter replacement and disposal costs for the life of the facility and,
- C. Annual energy consumption.

A lifecycle cost analysis was performed using Department of Energy guidelines including discount rates and energy escalation rates. The results indicate that a filtration system with bypass is clearly more cost effective than a continuous filtration system. The major difference is in the filter replacement costs over the life of the facility. Continuous dust loading on the filters from the underground air stream makes filter replacement a very significant factor. Fan energy consumption increases considerably when the filters are in the air stream continuously.



## 19th DOE/NRC NUCLEAR AIR CLEANING CONFERENCE

While significant design changes have occurred since the study was performed in terms of airflow quantities, number of filter housings, etc., the results of the study are still valid in principle.

### Acknowledgements

The support and cooperation of Samuel Chu, Nuclear Engineering Group Supervisor, Bechtel National, Inc. in reviewing this paper is sincerely appreciated. His input on nuclear related matters has been invaluable.

### References

1. Bechtel National, Inc.; "Storage exhaust filter bypass feasibility study"; Document No. 41K510AA-019, Rev 3.
2. Gaskill, J.R., Alvares, N.J., Beason, D.G., Ford H.W., Jr.; "Preliminary results of HEPA filter smoke plugging tests using the LLL full scale fire test facility"; Proceedings of the 14th ERDA Air Cleaning Conference.
3. Alvares, N.J., Beason, D.G., Ford, H.W.; "In-duct countermeasures for reducing fire generated smoke aerosol exposure to HEPA filters"; Proceedings of the 15th DOE Nuclear Air Cleaning Conference.
4. Bechtel National, Inc.; "Design bases fire study, repository level; Document No. 76-F-510-02.01, Rev 3.
5. United States Bureau of Mines; "Mine ventilation simulation system (MNVNTLN); February 1980.
6. Newton, G.J., Cheng, Y., Wong, B.A., Boecker, B.B., "Aerosol measurements in the partially completed underground waste isolation pilot plant; final report", July 1983, Inhalation Toxicology Research Institute.
7. Stinebaugh R.E.; "Results of air samples taken in Potash Company of America"; Sandia Laboratories memorandum Metcalf J.H.; February 10, 1978.
8. Data Received by WIPP Project From American Air Filter, March 1985.
9. Burchsted C.A., Kahn J.E., Fuller A.B.; Nuclear Air Cleaning Handbook; ERDA 76-21.
10. Bechtel National, Inc.; "Storage exhaust filtration system cost study"; Document No. 41-F-510-07, Rev 1.

19th DOE/NRC NUCLEAR AIR CLEANING CONFERENCE

DISCUSSION

HOLUB: Have you measured radon and radon daughter levels? How did you measure the activity levels?

PARTHASARATHY: As far as my information goes, we do not have a radon problem at this time and radon is not being measured at WIPP. An air monitor continuously samples the air stream and any buildup of radioactive particles on the filters will actuate the detectors.

HOLUB: What kind of instrument is used?

PARTHASARATHY: We have detectors for all three forms, alpha, beta, and gamma.

HOLUB: Do you measure continuously on a filter paper?

PARTHASARATHY: Yes, in addition to the continuous air monitors, we have fixed air samplers that collect particles on a filter paper but do not have detectors. The filter papers are taken to the lab and checked on a periodic basis. In addition, we have continuous air monitors with detectors built-in that can automatically turn on the filtration system. Radon detected underground is higher than atmospheric levels above ground.

HOLUB: Yes, I know that Carlsbad Caverns have a pretty high radon concentration.

MURTHY: Your first slide showed that one purpose of the HEPA filters is to "confine radioactivity, if any." Since WIPP is not yet operating, what are the sources of radioactivity now?

PARTHASARATHY: The design is based on having a clean facility during operations, which means all waste is contained and we don't have releases into the airstream. You would only get releases when there is a mechanical breach of a container.

MURTHY: When will WIPP become operational?

PARTHASARATHY: The end of 1988.

MURTHY: You will receive waste at that time?

PARTHASARATHY: Yes, we will receive the first waste in October, 1988.

## 19th DOE/NRC NUCLEAR AIR CLEANING CONFERENCE

### MEASUREMENTS OF REMOVAL EFFICIENCIES PERFORMED ON POWDER METAL AND FIBER METAL CARTRIDGES TO BE USED IN URANIUM ENRICHMENT FACILITIES AND GLOVEBOX EXHAUST DUCTS

\*H.-G. Dillmann

\*\*W. Bier, G. Linder, K. Schubert

\*Laboratorium für Aerosolphysik und Filtertechnik

\*\*Institut für Kernverfahrenstechnik

Kernforschungszentrum Karlsruhe GmbH

Postfach 3640, D-7500 Karlsruhe 1

Federal Republic of Germany

#### Abstract

Development work is described which has been performed on fiber metal filter cartridges used to remove extremely small particles in separation nozzle plants for uranium enrichment. The separation nozzle method is explained. The removal efficiencies measured in filters previously used as well as in new prototypes are indicated.

#### I. Introduction and Summary

Under the separation nozzle method developed by the Karlsruhe Nuclear Research Center, uranium-235 is enriched by centrifugal forces in a semi-circular flow of a gas mixture consisting of uranium hexafluoride ( $\text{UF}_6$ ) and a light gas, i.e. helium or hydrogen /1/. Figure 1 shows a separation nozzle system; its semi-circular wall along which the gas flows, at the present state of the art has a radius of only 50  $\mu\text{m}$ . Due to the chemical

properties of the  $UF_6$ , very fine (sub-micron) particles of  $UF_6$  decomposition products are formed continuously in the gas flow /2/. Therefore, special filters must be used to protect the separation nozzles which, in terms of their performance data, are highly sensitive to dust.

A powder metal filter unit, the filter material of which had originally been fabricated for liquid filtration was built and tested successfully in a technical prototype separation nozzle stage similar to the stages needed in numbers of several hundreds in an enrichment plant.

The developmental work on the separation nozzle method aims at the realization of advanced nozzle systems which are further reduced in size by a factor of two or three (radius of curvature 15-25  $\mu m$ ). This will increase considerably the performance of the separation stages but, on the other hand, will make the nozzle systems more sensitive to dust particles.

Therefore, measurements of removal efficiencies were performed on the existing powder metal filter cartridges using the uranin method /3/ and new upgraded metal filters were developed on the basis of sintered stainless steel fiber mats. First prototype filter cartridges of 2-8  $\mu m$  fiber thickness were tested with the uranin method and removal efficiencies up to 99 % with low pressure drops of 1-2 % were measured.

With the fiber filters even higher removal efficiencies can be achieved by further optimization. This makes this type of filter interesting for other applications, e.g. in glovebox exhaust ducts.

## II. Test of Powder Metal Filter Cartridges in a Separation Nozzle Stage and by the Uranin Method

The separation nozzle stage in which the powder metal filter unit was tested is shown in Figure 2. The feed gas is compressed by a two-stage radial compressor with intermediate and final cooling. The gas enters the separation tubes on which the nozzle systems are mounted from below via the set of filter cartridges. The gas flow through the filter is about  $13\,000\text{ m}^3/\text{h}$ ; the operating pressure which is inversely proportional to the dimensions of the nozzle system, is 0.5 bar for nozzles with a radius of  $50\text{ }\mu\text{m}$  (Fig. 1). The total nozzle length of one separation stage is about 500 meters.

The powder metal filter unit which, on account of the aggressiveness of  $\text{UF}_6$  is made of stainless steel, is shown in Figure 3. It consists of 21 cartridges each having 19 filter tubes of 20 mm diameter and 600 mm length. The filter unit has been optimized for reasons of economy to attain minimum pressure drops of about 1-2 % in the filter and a relatively small filter surface of about  $15\text{ m}^2$ . This implies relatively high face velocities of about 30 cm/s. The filter material has been taken from a fabrication program for liquid filtration; its mean grain size is about  $70\text{ }\mu\text{m}$ , its porosity about 50 %, and the wall thickness is 1 mm. The specific inner surface of the filter is  $1500\text{ cm}^2/\text{cm}^3$ .

The results of endurance tests of the stage with the filter and, for reasons of comparison also without the filter, are shown in Figure 4. By operation without the filter it was demonstrated that due to the permanent deposition of very small amounts of powder particles in the nozzle system the mass flow through the nozzle decreases slightly but steadily. When operating the stage with the filter no change in the mass flow was measured within the limits of accuracy over a test period of 2000 hours. Hence sufficiently long service lives of at least several years can be expected for separation nozzle stages.

# 19th DOE/NRC NUCLEAR AIR CLEANING CONFERENCE

In order to examine the filter more closely with regard to the removal mechanism and the development of improved filters which will be described in the next chapter, single filter cartridges similar to those shown in Figure 3 were measured with the uranin method which has already been described repeatedly at this conference /3/.

Compared with the normally applied aerosol filter testing methods, this method yields the most conservative results because the spectrum of particles is very narrow and lies around 0.2  $\mu\text{m}$ . The measured results have been presented in Table 1 and Figure 5.

Table 1: Decontamination factors of sintered metal powder cartridges from various suppliers. (See also Fig. 5)  
Test aerosol: uranin

	Volume Flow $\text{m}^3/\text{h}$	Decontamination Factor	Removal Efficiency %
P1	100	1.44	30
	200	1.37	27
	300	1.29	23
	400	1.22	16
	500	1.1	10
P2	100	1.3	24
	200	1.2	17
	300	1.29	22
	400	1.29	22
	500	1.22	18
P3	200	1.35	26
	400	1.28	22
	600	1.17	15

## 19th DOE/NRC NUCLEAR AIR CLEANING CONFERENCE

It became apparent that under comparable conditions only removal efficiencies of up to approximately 30 % had been attained. This did not come as a surprise because, as mentioned before, the filter material had been taken from liquid filtration where removal efficiencies greater than 99 % have been attained only for particles greater than 10 to 15  $\mu\text{m}$ . This means that the filter unit with only comparatively low removal efficiencies for the particle sizes of approximately 0.2  $\mu\text{m}$  used in the uranin method is sufficient in practical application of the separation nozzle process where the dust particles are much smaller.

The particles deposited in the nozzles during the test run of the stage without filter (Fig. 4) result from the continuous decomposition of very small amounts of the  $\text{UF}_6$ ; at first the decomposition products have the size of one or two molecules. Then, by agglomeration with other decomposition molecules in the gas flow, they grow and, without a filter provided, can reach only a certain size before they are deposited in the curved nozzle by means of the centrifugal forces. For the nozzles of a 50  $\mu\text{m}$  radius used in the test run, this maximum particle size can be calculated to be about 0.01  $\mu\text{m}$ ; for particles of this size the nozzle would act as a total filter barrier.

The good results of the powder metal filter unit (Fig. 4) which filters out all particles smaller than 0.01  $\mu\text{m}$  can only be explained by diffusion effects taking place at relatively high face velocities and in multiple filtration.

During growth the decomposition particles which touch the inner surface of the filter (approx. 1000  $\text{m}^2$ ) are deposited by diffusion and they stay at the wall due to van der Waals forces. Thus the filter prevents the particles from growing and obviously they do not reach sizes of about 0.01  $\mu\text{m}$  at which they would be deposited in the nozzles downstream of the filter. The probability of contact between growing particles and the inner filter surface is greatly enhanced by the fact that the total gas flow is pumped through the filter every three seconds (multiple filtration). This

## 19th DOE/NRC NUCLEAR AIR CLEANING CONFERENCE

holds for short circuit operation of one stage and for plant operation with the stages, each equipped with a filter, connected in series and the gas flowing from stage to stage.

Table 2 contains the removal efficiencies calculated for multiple filtration comprising 1, 10, 100, and 1000 runs.

Table 2: Removal efficiencies calculated for multiple filtration. 1, 10, 100, and 1000 filtrations.

$\eta/1$	$\eta/10$	$\eta/100$	$\eta/1000$
10	65	99.99	100
1	9.5	63	99.99
0.1	0.99	9.5	63
0.01	0.099	0.99	9.5

### III. Development and Testing of Improved Filters on the Basis of Sintered Stainless Steel Fiber Mats

As mentioned earlier, developmental work on the separation nozzle method aims at reducing the nozzle size by a factor of two or three (radius of curvature 15-25  $\mu\text{m}$ ). This will increase considerably the performance of the separation stage. On the other hand, the reduction in size will make the nozzle more susceptible to dust particles.

Therefore, new upgraded metal filters were developed on the basis of stainless steel fiber mats. The thickness of the fibers was varied from 8  $\mu\text{m}$  down to 2  $\mu\text{m}$ . Figure 6 shows one of the first



prototype cartridges. As cut fiber particles have to be avoided, sintered fiber material was used. This also simplifies the fabrication of filter cartridges. The wall thickness of the sintered fiber mats is 0.3 mm, the mean porosity about 65 %.

A major improvement has been achieved by pleating the sintered filter cartridges and thus increasing the filter surface. Actually, a fiber filter material has a greater specific surface compared to a grain material of the same weight fabricated from powder metal, and it enhances the number of particles removed by diffusion. In the material tested here, the specific surface of  $7000 \text{ cm}^2/\text{cm}^3$  is about 5 times larger than in the powder metal filter.

The results obtained from measurements performed with the uranin method on these fiber filter cartridges are shown in Table 3 and in Figure 5.

Figure 7 shows the respective pressure losses of the filter cartridges at 1 bar and with air as the testing gas.

The measured results show that fiber filter cartridges under comparable conditions yield much higher (up to 99 %) removal efficiencies than powder metal cartridges. The removal efficiencies could be further improved by implementing certain developments, e.g. an increase in the fiber areal weight or an increase in the area subjected to the flow which would result in lower face velocities.

Considering that a removal efficiency of only 30 % of the powder filter was sufficient to protect the 50  $\mu\text{m}$  radius nozzle from all dust particles below 0.01  $\mu\text{m}$  in size, it is supposed that a considerably higher removal efficiency, i.e. between 90 and 99 %, as measured with the filters of 2  $\mu\text{m}$  fiber thickness, should suffice to protect the smaller advanced nozzles with a radius of 15-25  $\mu\text{m}$ .

**19th DOE/NRC NUCLEAR AIR CLEANING CONFERENCE**

Table 3: Decontamination factors of fiber metal filter cartridges, measured with uranin as the test aerosol.  
(See also Fig. 5)

Fiber Diameter Type	Volume Flow m <sup>3</sup> /h	Decontamination Factor	Removal Efficiency %
F1: 8 μm	100	5	80
	200	4.5	78
	300	3.3	70
	400	2.99	66
	500	4.2	76
F2: 4 μm	100	10.6	91
	200	8.4	88
	300	7.0	86
	400	6.4	84
	500	6.1	83
F3: 2 μm	100	26.2	96
	200	21	95
	300	14	93
	400	12	91
	500	11	90
F4: 2 μm	100	630	99.8
	200	41	98
	300	73	99
	400	112	99.1

Consequently, a complete filter unit identical to the prototype filters made of 2 μm fiber mats was ordered and is currently being fabricated by industry. Filter testing in the separation nozzle stage with a process gas of UF<sub>6</sub> and helium will be performed in early 1987 when the advanced separation nozzles will be available.

#### IV. Prospects

For the fiber filters even higher removal efficiencies than the measured 99 % can be achieved by further optimization of the depth of pleats of the filter mats, by improvement of the geometric configuration, and by variation of the layer thickness of the fibers. This makes this type of filter interesting in other applications.

Use of these corrosion and temperature resistant filter cartridges with high removal efficiencies for particles with diameters in the sub-micron range is optimum, e.g. in fuel element fabrication plants, (trains of boxes) if fire aerosols have to be removed. Another advantage offered by fiber metal filters is that they act as automatic barriers to flames. This means that the propagation of flames is avoided by passive measures.

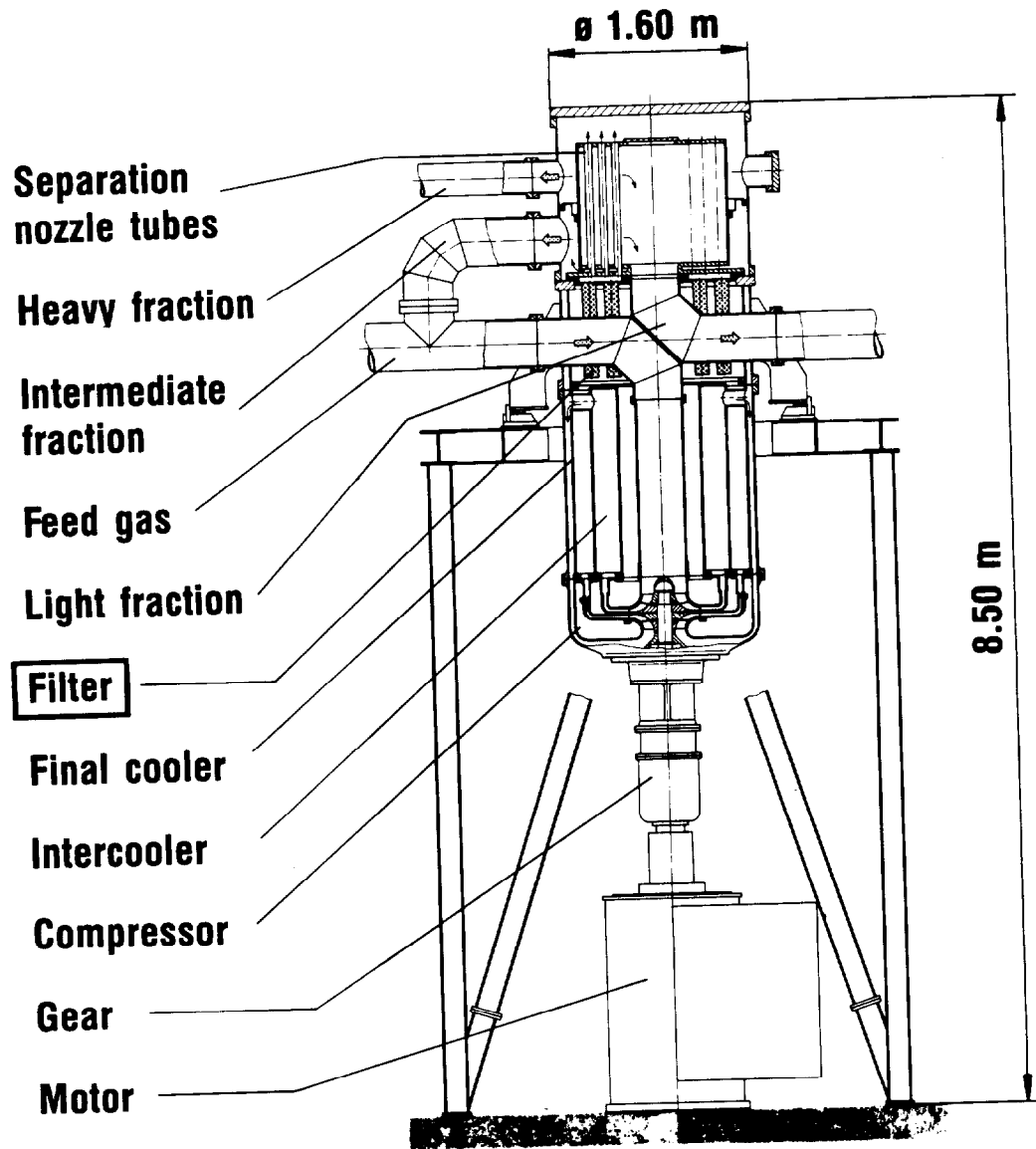
Moreover, these all-metal filter elements can be cleaned and hence - unlike the previously used fiber glass filters - are suitable for repeated use.

#### V. References

- /1/ BECKER, E.W.; BIER, W.; BLEY, P.; EHRFELD, W.; SCHUBERT, K.; SEIDEL, D.:  
"Development and Technical Implementation of the Separation Nozzle Process for Enrichment of Uranium-235".  
AIChE 1982 Winter Meeting, Orlando, Florida, USA, March 2, 1982.
- /2/ BECKER, E.W.; BIER, W.; HAGMANN, P.; MIKOSCH, F.:  
"Bedeutung der radiolytischen Selbstzersetzung von Uranhexafluorid bei der Anreicherung von Uran-235 nach dem Trenndüsenverfahren."  
KfK-Bericht 3332, Kernforschungszentrum Karlsruhe GmbH, (April 1982).
- /3/ DILLMANN, H.-G.; PASLER, H.:  
"Experimental Investigations of Aerosol Filtration with Deep Bed Fiber Filters".  
CONF 820 833, p. 1160 (1983).



Fig. 1: Separation nozzle system for the enrichment of uranium-235. A gas mixture of uranium hexafluoride and a light gas enters the nozzle from the left side and is expanded along the curved wall. At the present state of development, the radius of the curved wall is 50  $\mu\text{m}$ .



kfk

S1.55.883 IKVT

Fig. 2:  
Separation nozzle stage SR33 for the enrichment of Uranium 235

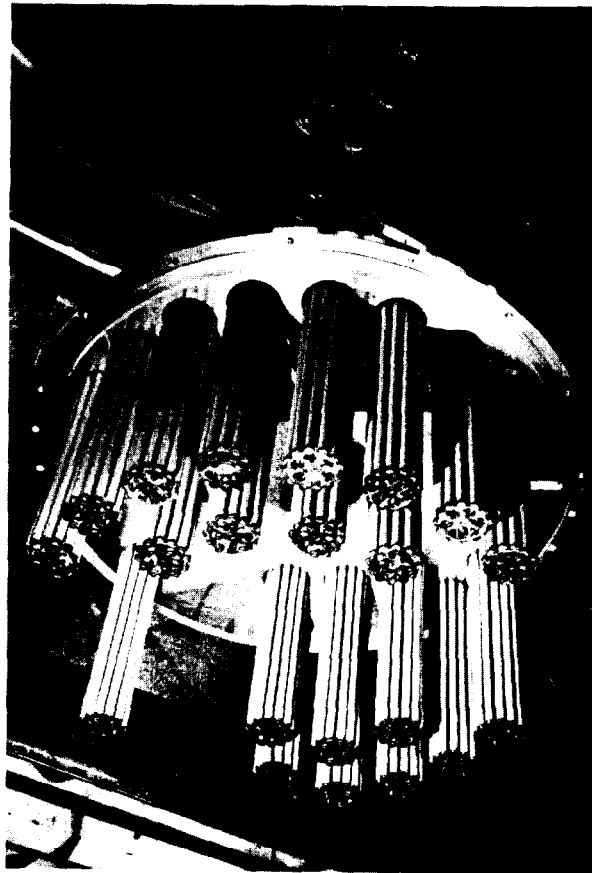
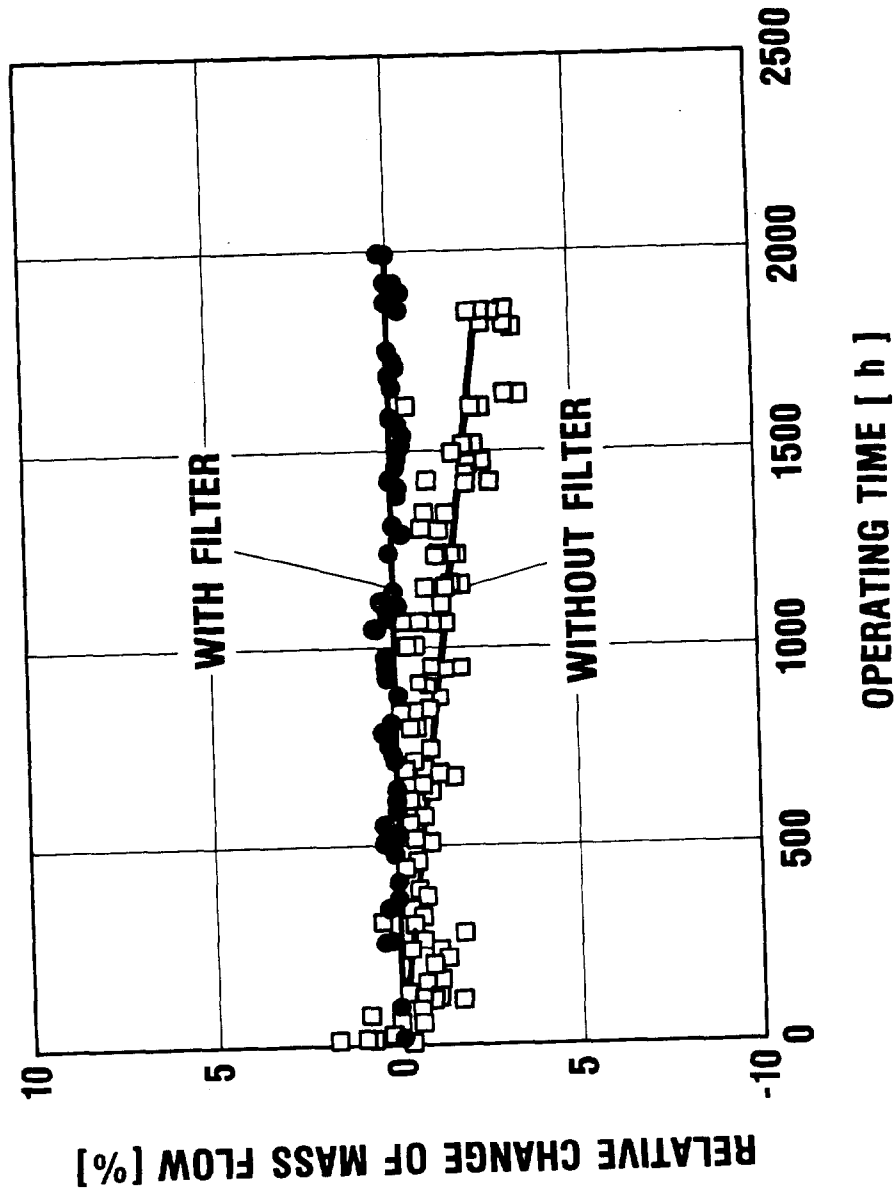


Fig. 3: Filter unit with sintered powder metal cartridges as used in the prototype separation stage (shown in Fig. 2) to protect the separation nozzle systems from the very fine particles (submicron range) formed in small amounts in the process gas.



K4.632.686 IKVT

Fig. 4: ENDURANCE TEST OF A SEPARATION NOZZLE STAGE

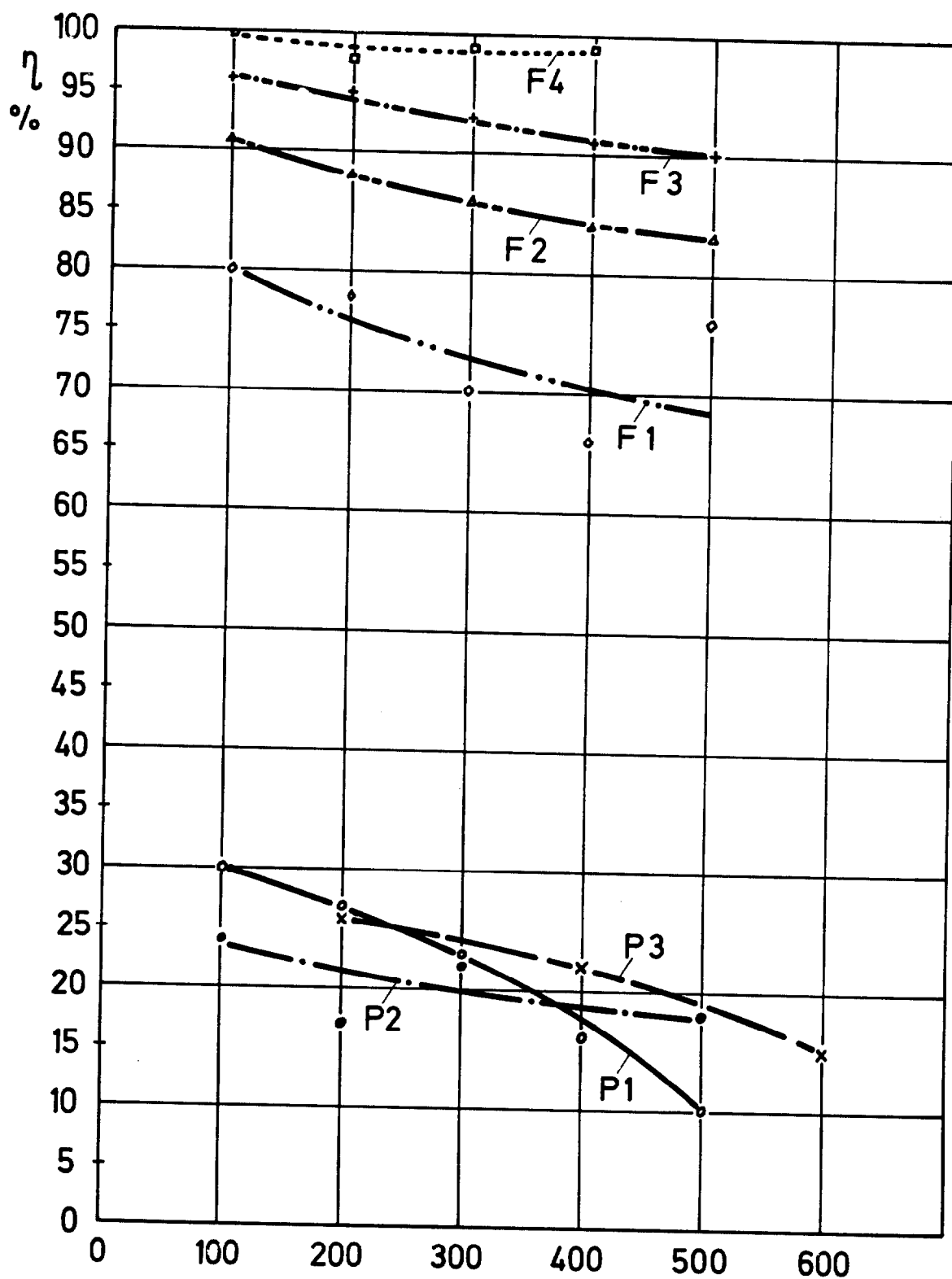


Fig. 5: Removal efficiencies of powder and fiber filter cartridges as a function of air flow, measured with uranin as the testing aerosol.



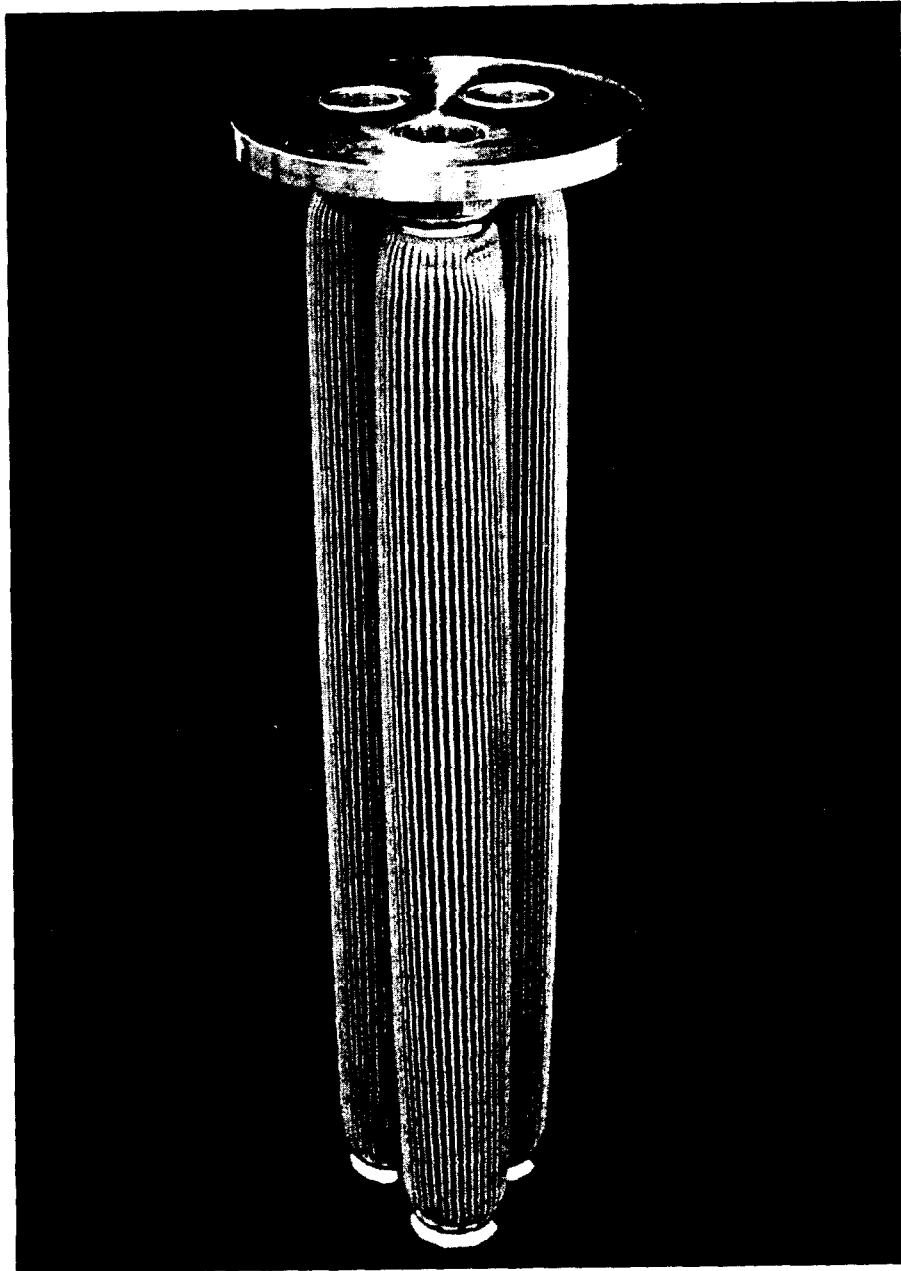


Fig. 6: Prototype of a 2  $\mu$ m stainless steel fiber filter cartridge.

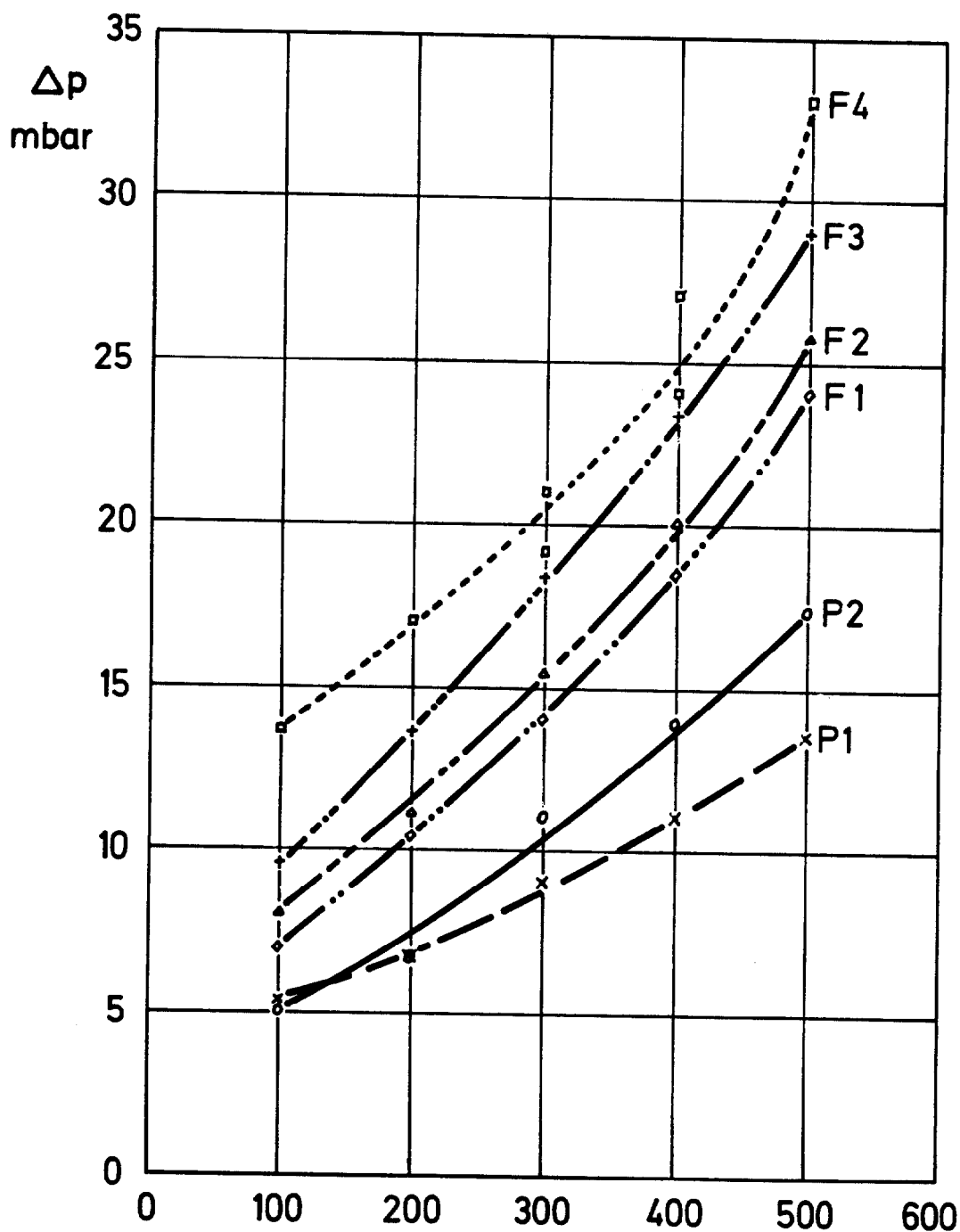


Fig. 7: Pressure drop of powder (P1-P3) and fiber (F1-F4) filter cartridges as a function of air flow.  $\text{m}^3/\text{h}$

KfK LAF 86

## 19th DOE/NRC NUCLEAR AIR CLEANING CONFERENCE

### EXPERIMENT ON A MULTILAYER TYPE AIR FILTER FOR THE FILTRATION OF SODIUM AEROSOL \*

N.Otake and O.Nozaki  
Nippon Muki Co.,Ltd.  
Yuki,Ibaraki-Ken, JAPAN

#### Abstract

An emergency air filter system of FBR was developed by using a multilayer type filter to protect the function of HEPA filter from clogging due to loading of sodium aerosol. To examine the effect of loading of sodium aerosol on the filter system, sodium aerosol consisting of sodium oxides and the related compound was supplied to the filter system. Several parameters to determine the effectiveness of the multilayer type filter were surveyed. It was confirmed that the emergency air filter system of FBR consisting of the multilayer type filter - a medium filter - HEPA filter with standard size (610mm×610mm) in series could hold 800 g-Na at 1.5 kPa without clogging.

#### 1. Introduction

The present work was carried out to develop a pre-filter for a high efficiency particulate air (HEPA) filter for an emergency air filter system of a Fast Breeder Reactor (FBR). The emergency filter system is required to remove sodium oxide aerosol released in an event of the posulated accident of FBR.

Sodium aerosol, when generated in the air, may consist of  $\text{Na}_2\text{O}$ ,  $\text{Na}_2\text{O}_2$ ,  $\text{NaHCO}_3$ ,  $\text{Na}_2\text{CO}_3$ , or their mixture according to the condition of atmosphere. The sodium aerosol, if collected by HEPA filter, may cause clogging of the air filter so that the function of air cleaning system will be lost. It was recommended by Kitani et al. that the loading capacity of HEPA filter should be limited to 1 mg-Na/cm<sup>2</sup>.<sup>(1)</sup> Jordan reported 16 mg/cm<sup>2</sup> at 5 kPa for 2.6 m<sup>2</sup> glass fiber filters.<sup>(2)</sup> McCormack et al. reported 2.7 ~ 16 mg/cm<sup>2</sup> at 5 kPa for HEPA filters.<sup>(3)</sup> Thus, the problem of severe clogging of air filter by sodium aerosol should be solved.

For example, a sand bed filter was developed by a group of KfK in West Germany.<sup>(4)</sup> On the other hand, McCormack et al. reported that none of the pre-filter tested were effective in increasing the sodium oxide/hydroxide holding capacity by the combination of pre-filters and HEPA filters.<sup>(3)</sup>

This work is concerned with the filtration of sodium aerosol by applying a multilayer type filter to the filter system without a special blower with the strong sucking force or to install many filters for a large surface area in ventilation systems. The multilayer type filter consists of a few layers of perforated filters by which sodium aerosol may be holded without clogging and can protect the function of HEPA filter.

The emergency air filter system for a FBR, considering one unit of system, is possible to design as shown in Fig. 1, in which the system consists of a multilayer type filter, a medium filter, a HEPA filter and

---

\* This work was performed under contracts between the Power Reactor and Nuclear Fuel Development Corporation and Nippon Muki Co.,Ltd.

a charcoal filter, respectively. Thus, the HEPA filter is protected by the multilayer type filter and medium filter.

The effectiveness of the multilayer type filter was investigated with respect to kind of filter media, opening diameter, opening area ratio and intervals among layers. Another important subject in the test was to evaluate the effect of humidity.

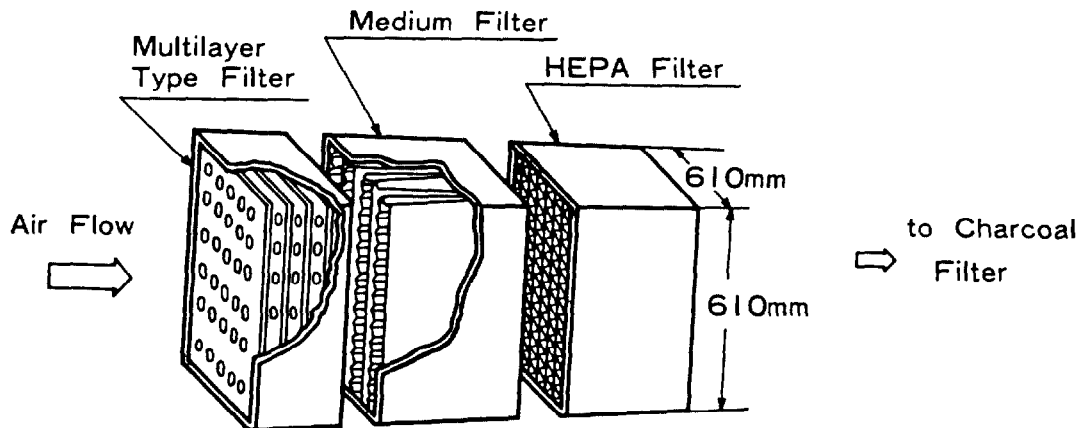


Fig. 1 A filter assembly developed for an emergency filter system of FBR.

## II. Experimental

### Test apparatus

The test apparatus is shown in Fig. 2. Filter units with standard size (610 mm X 610 mm) were installed singly or in series. The apparatus consists of filter system, a burning pan for sodium aerosol generation, a blower, ducts and measurement systems. The blower can suck 77 m<sup>3</sup>/min at 5 kPa of static pressure. The concentration of aerosol was monitored by Sibata digital dust counter which could measure the scattered light intensity of white light at 50° from the direction of light beam propagation.

### Particle size analysis

The particle size distribution of sodium aerosol was analyzed by sampling the aerosol on meshes of an electron microscope by a thermal depositor and the particles on the meshes were analyzed by Carl Zeiss-TRZ 3 particle size analyzer.

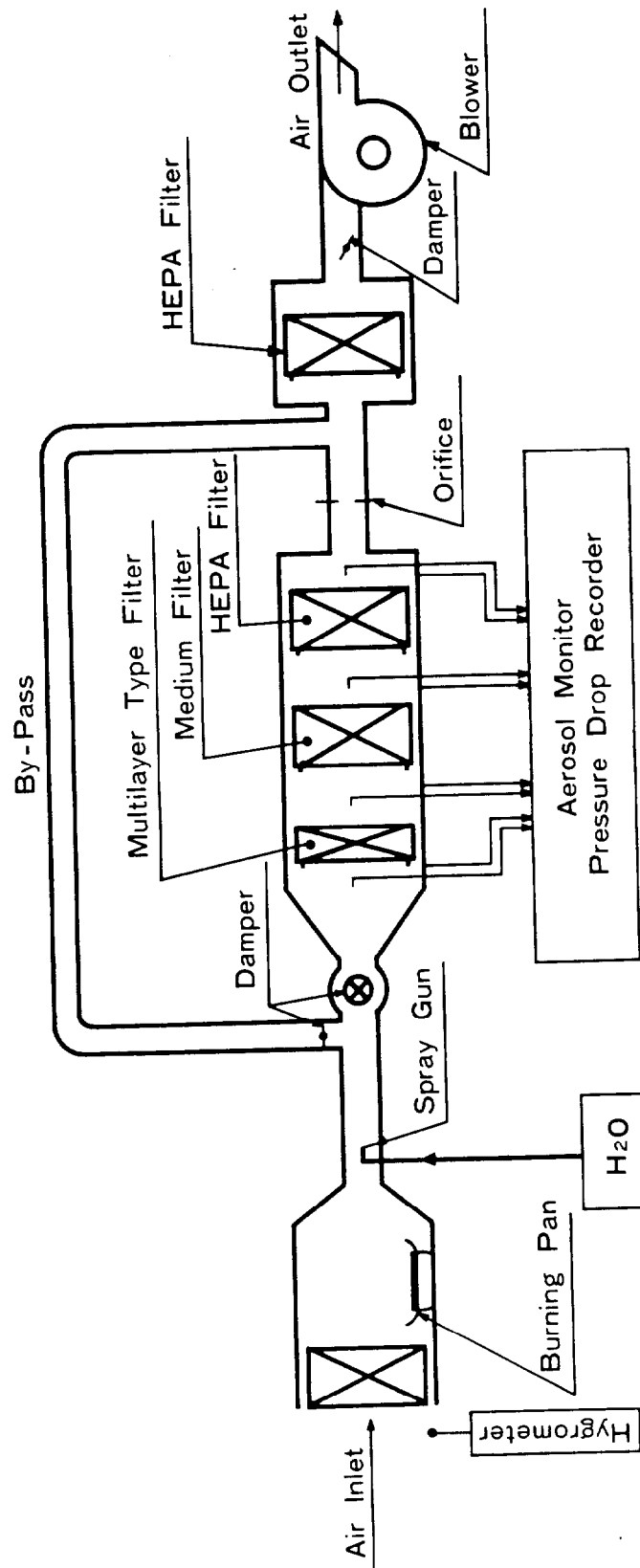


Fig. 2 Sodium aerosol test apparatus.

## 19th DOE/NRC NUCLEAR AIR CLEANING CONFERENCE

### Sodium analysis

The amount of sodium trapped on filters was analyzed by atomic absorption spectroscopy. The values of Na on each filter were used to obtain the average removal efficiency of aerosol.

### Medium filter

The specification of medium filter is given in Table 1.

Table 1 The specification of medium filter.

Filter Media	: High Silica Content Fiber
Filter Size	: 610 <sup>H</sup> × 610 <sup>W</sup> × 290 <sup>D</sup> (mm)
Air Flow Capacity	: 28 m <sup>3</sup> /min
Initial Pressure Drop	: 17 kPa maximum
Removal Efficiency	: 45 % minimum(0.3μmDOP)

### Multilayer type air filter

Fiber media such as stainless steel, Zirconia, alumina, alumina-silica and high silica content glass were investigated for the multilayer type filter to remove sodium aerosol. As a whole, high silica content glass mat was selected from view points of high loading of sodium oxide aerosol and disintegration due to corrosion by sodium hydroxide. Fig. 3 shows a configuration of multilayer type filter with the diagonal stagger perforation of round hole (stagger angle 45°). The opening were arranged so as to meet flat part of the neighbor layer alternately. Diameter of openings and opening area ratio are connected with an equation regarding pitches of openings as follows,

$$R = 157 D^2 / P^2 \quad (1)$$

where

D : diameter of openings  
P : center to center pitch  
R : opening area ratio.

The condition for openings on a layer to meet the filter media of the neighbor layer is given as  $P > 2D$  and the maximum value is about 39 %. In this work, the opening area ratio was taken less than 30 %.

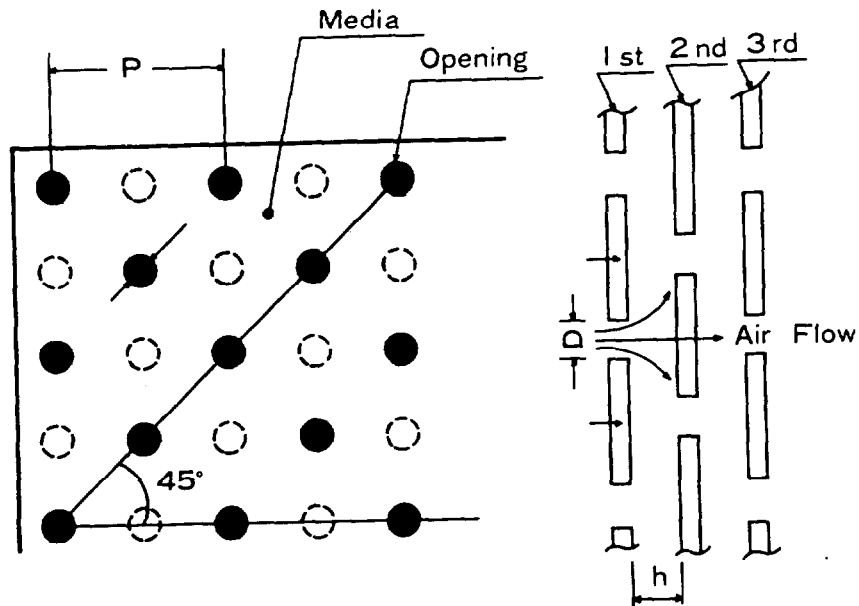


Fig. 3 45° Staggered Cutting

As to the diameter of openings, a range of 10 ~ 35 mm was taken for the practical usage. Table 2 shows the experimental parameter for diameter of openings, opening area ratios and number of openings.

Table 2 Experimental parameter of media.

Opening Area Ratios & No. of Openings		Diameter of Opening	10mm $\phi$	15mm $\phi$	20mm $\phi$	25mm $\phi$	30mm $\phi$	35mm $\phi$
※ 10%	Number of Opening		450	200	128	72	50	32
	Opening Ratio(%)		9.5	9.5	10.8	9.5	9.5	8.3
15	Number of Opening		722	338	162	128	72	50
	Opening Ratio(%)		15.2	16.1	13.7	16.9	13.7	12.9
20	Number of Opening		968	450	242	162	98	72
	Opening Ratio(%)		20.4	21.4	20.4	21.4	18.6	18.6
25	Number of Opening		1152	512	288	200	128	98
	Opening Ratio(%)		24.3	24.3	24.3	26.4	24.3	25.3
30	Number of Opening		—	648	338	242	162	128
	Opening Ratio(%)		—	30.8	28.5	31.9	30.8	33.1

※ Approximate opening area ratio.

# 19th DOE/NRC NUCLEAR AIR CLEANING CONFERENCE

On the other hand, the interval among layers was another factor. The effectiveness of intervals among layers were investigated according to Table 3.

Table 3 Setting of various intervals among layers.

Type of Multilayer	Interval Among Layers			
	1st	2nd	3rd	4th
A	20	20	20	20
B	30	20	20	10
C	45	20	20	10
D	70	20	20	10
E	25	20	15	10
F	40	30	20	10

(mm)

## Filter system design

At first, a prior condition was given by a relation between the maximum holding capacity of sodium aerosol as Na and the maximum pressure drop regarding a HEPA filter at flow rate of 28 m<sup>3</sup>/min. The holding capacity was taken as 200 g from the condition of 1 mg-Na/cm<sup>2</sup> and the pressure drop was 0.5 kPa, i.e., a standard value for exchange of HEPA filter in industries.

Table 4 A strategy of a filter system for an emergency filter system for FBR.

Filter Unit Item		Pre-Filter	Middle Filter	Final Filter	Total
		Multilayer Type Filter	Medium Filter	HEPA Filter	
Pressure Drop	Initial (kPa)	X <sub>1</sub>	0.15	0.25	X <sub>1</sub> + 0.4
	Final (kPa)	Y	0.50	0.50	1.50
Sodium Aerosol Holding Capacity (g) *		X <sub>2</sub>	130	200	X <sub>2</sub> + 330

\* Na base



The data on the medium filter were obtained experimentally by using sodium aerosol under a condition of 16.5 °C, 41 % R.H. and flow rate of 28 m<sup>3</sup>/min. The concentration of aerosol was 0.6 ~ 0.8 g/m<sup>3</sup> as Na. The data is shown in Fig. 4, where  $\eta_0$  is the value by Sibata digital dust counter. The amount of Na on the filter was determined by sodium analysis mentioned above. Thus, the maximum pressure drop was taken as 0.5 kPa and the corresponding aerosol holding capacity of Na as 130 g-Na for the medium filter.

The overall relation among filter units are shown in Table 4, in which each role of medium and HEPA filters are given respectively. The overall maximum pressure drop was taken as 1.5 kPa. From the table, it is required that the multilayer type filter should be designed properly with respect to pressure drop.

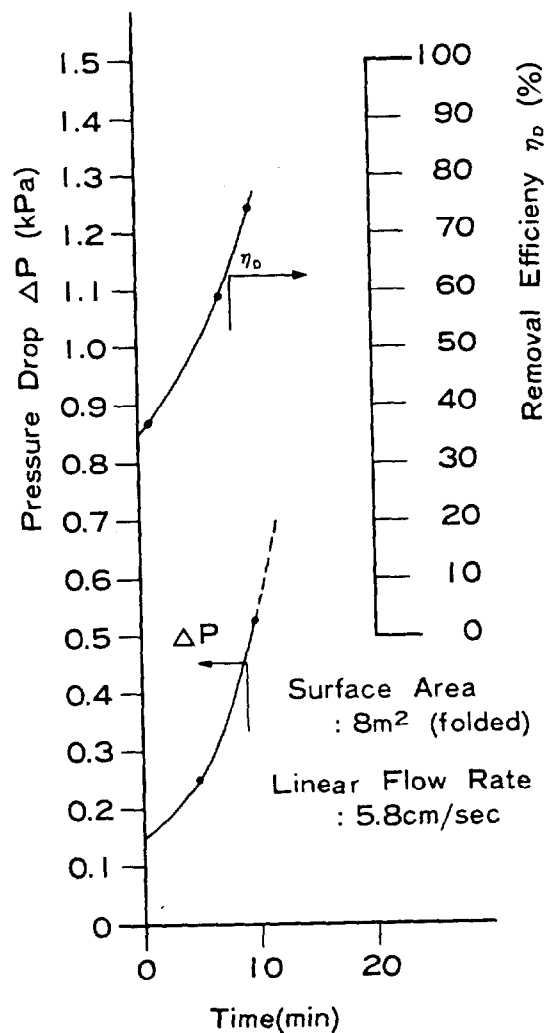


Fig. 4 The change of pressure drop and removal efficiency by high silica content fiber mat as a function of time (Medium filter).

III. ResultOpening area ratio

The initial pressure drop for the multilayer type filter of five layers was investigated as a function of opening diameter and opening area ratio at the flow rate of 28 m<sup>3</sup>/min. The result is shown in Fig. 5. From the figure, it is seen that the pressure drop is mainly determined by opening area ratio. The diameter of opening did not give much influence on the pressure drop. From Table 4, it was required that the highest pressure drop at the initial condition should be less than 0.4 kPa. From Fig. 5 the value corresponds to 20 % for opening area ratio.

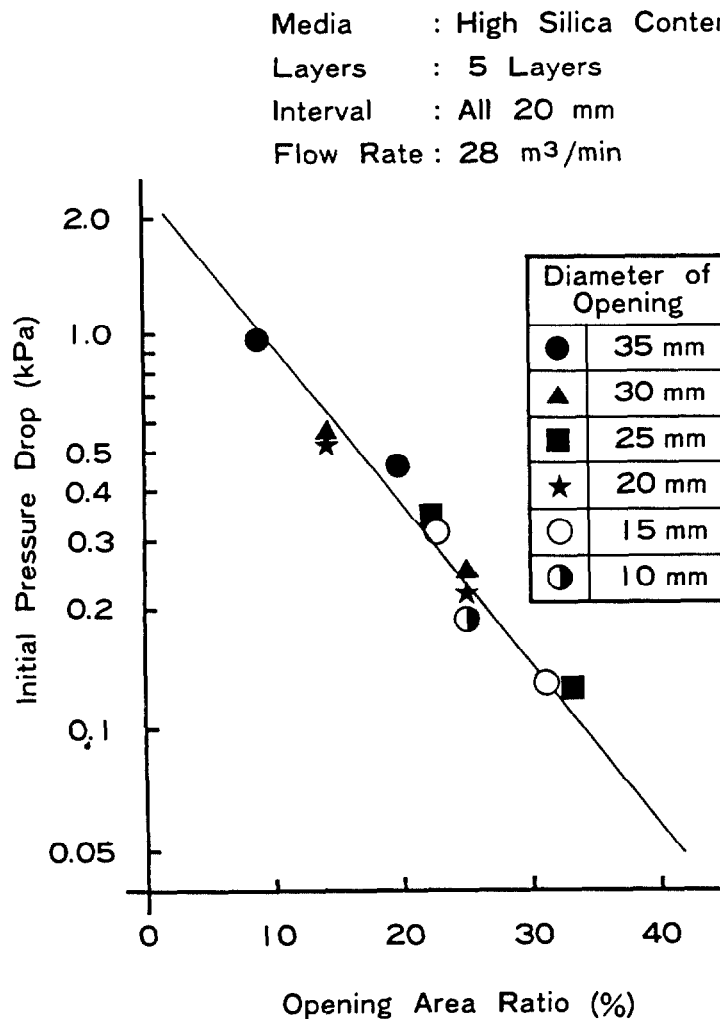


Fig. 5 The pressure drop as a function of opening area ratio.




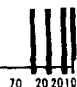


Diameter of opening

The effect of diameter of opening on the removal of sodium aerosol was examined. If the diameter of opening was smaller than 15 mm, the opening was clogged due to loading of sodium aerosol. So the diameter of opening was decided to fix 20 mm.

Intervals among layers

With a constant value of 20 % as the opening area ratio, the intervals among layers were set as shown in Table 3. The pressure drop for the types of A ~ F in Table 3 is given in Table 5.

Table 5 The initial pressure drop on several combination of multilayer at a room condition.

Run No.	Intervals of Layer(mm)	Flow Rate	Initial Pressure Drop
53-15	Air Flow →  A	28 $\frac{m^3}{min}$	0.338 kPa
53-16	→  B		0.345 kPa
53-17	→  C		0.348 kPa
53-18	→  D		0.357 kPa
53-20	→  E		0.39 kPa
53-21	→  F		0.375 kPa

Sodium aerosol

It was tried to generate sodium aerosol uniformly as much as possible by feeding sodium metal on buring pan manually in reference to the dust counter. Fig. 6 shows the data in which the concentration of sodium aerosol was relatively constant at the inlet of multilayer type filter. The average concentration of sodium aerosol was  $0.6 \sim 0.8 \text{ g/m}^3$  as Na. The difference of sodium concentration before and behind filter gave the removal efficiency.

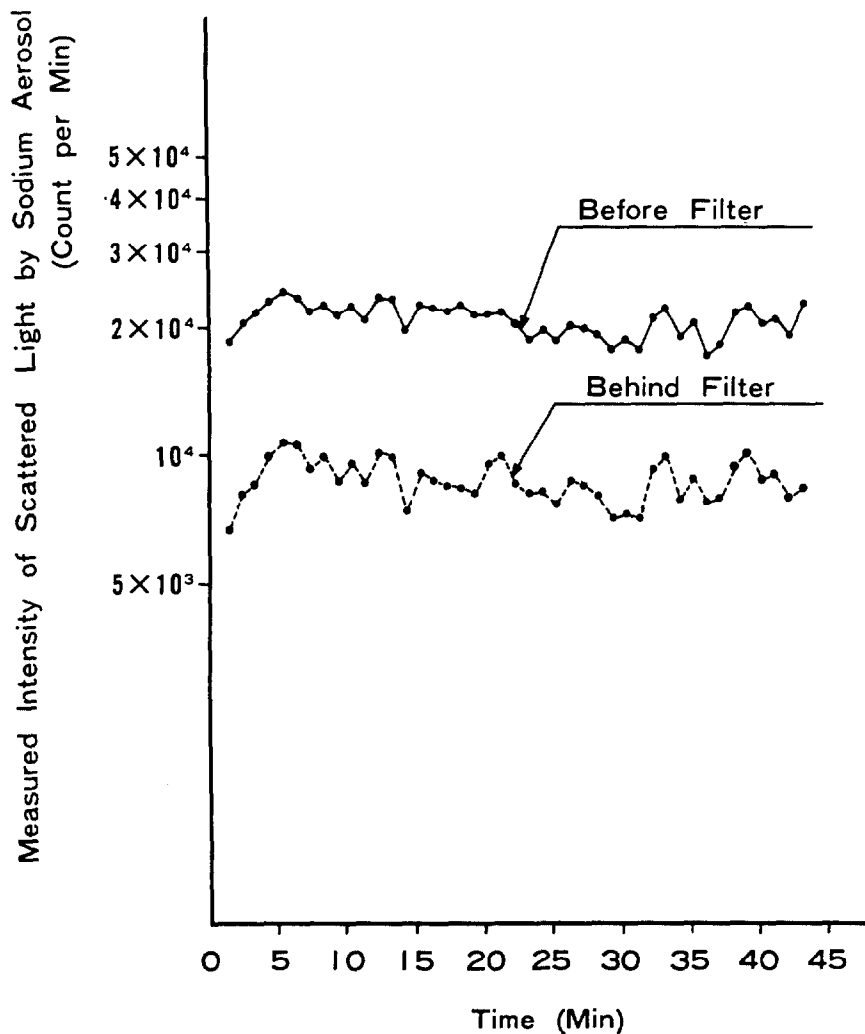


Fig. 6 Intensity of scattered light of sodium aerosol before and behind the multilayer type filter during run (Run 53-14).

Fig. 7 shows the photograph taken by an electron microscope. The particle size distribution was characterized with CMD (count median diameter) as  $0.29 \mu\text{m}$  and geometric deviation  $\sigma_g = 1.6$ .

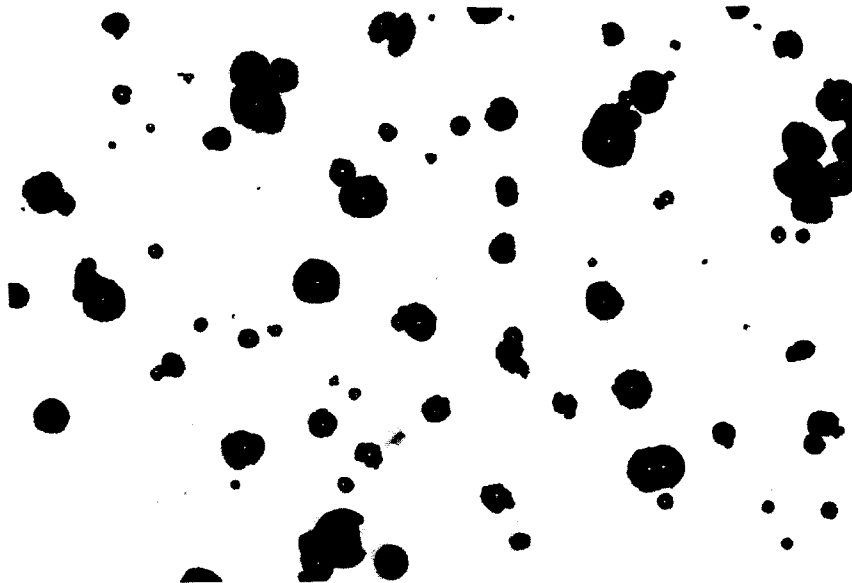


Fig. 7  
Sodium Oxide Aerosol  
Electron Microscope  
( $\times 21656$ )  
CMD =  $0.29 \mu\text{m}$   
 $\sigma_g = 1.6$

The appearances of trapped sodium aerosol on the first and second layers of the multilayer type filter is shown in Fig. 8. The sodium compound was distributed uniformly over the first layer, but it scattered on the second layer as lumps corresponding to openings of the first layer. On the downward layers after the second one, it was slight and uniform. It was noticed that the color of it was yellowish in dry condition, but white in a wet condition.

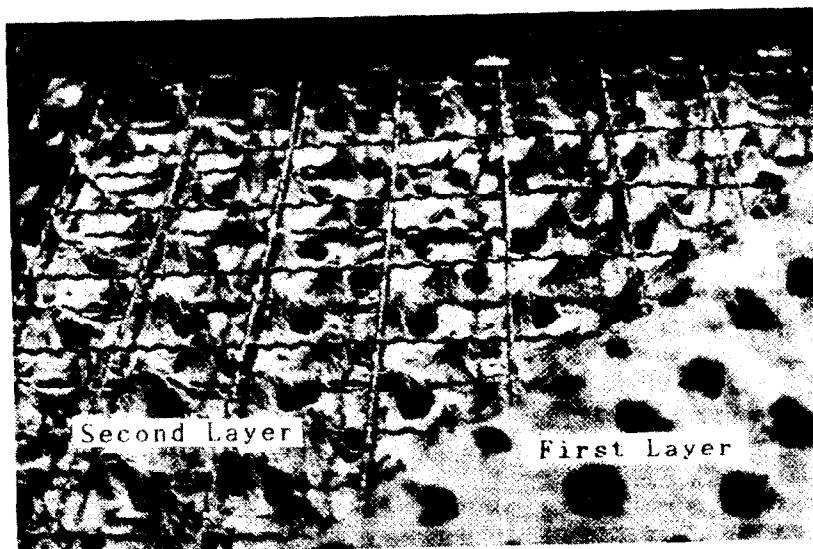


Fig. 8  
Distribution of sodium  
aerosol on filter.

Sodium aerosol trapping on layer

## a) Monolayer

Using monolayer of the same filter media, two runs were carried out to investigate the removal efficiency of sodium aerosol as a function of flow rate. One run was done at linear flow rate of 155 cm/sec which was corresponding to the first layer of multilayer type filter with 0.3 m<sup>2</sup> in area if it had no opening. The other was done at 5.8 cm/sec by setting the medium filter with 8 m<sup>2</sup> in area. The test results are shown in Fig. 9 for the former test and Fig. 4 for the latter one. It is seen from the figures that the removal efficiency increases with flow rate. At 0.7 kPa, the plane filter could trap sodium aerosol as much as about 16 g of Na per one filter unit or 5 mg-Na/cm<sup>2</sup>. While the folded filter could trap about 150 g of Na per one unit or 1.9 mg-Na/cm<sup>2</sup>.

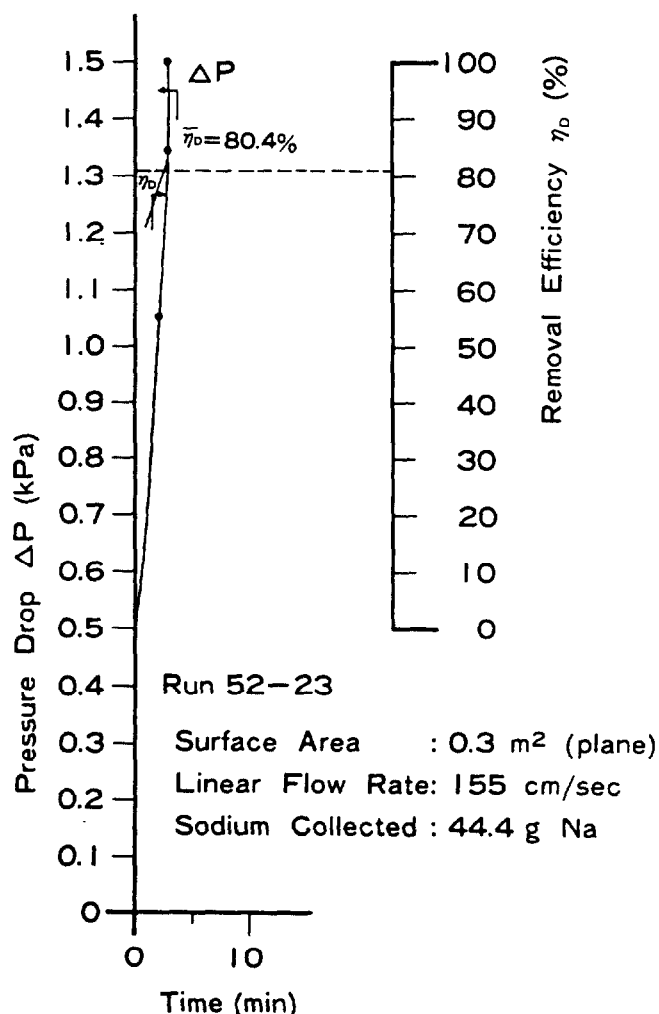




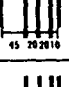
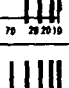
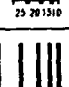

Fig. 9 The change of pressure drop and removal efficiency by high silica content fiber mat as a function of time (One layer of the multilayer type filter with no opening).

## b) Multilayer

The runs for removal of sodium aerosol using several multilayers were carried out under  $28 \text{ m}^3/\text{min}$  up to  $0.7 \text{ kPa}$  of pressure drop. The results are shown in Table 6 and Fig.10. From Fig.10 it is seen that the first layer could trap  $68 \sim 158 \text{ g-Na}$  per layer or  $18 \sim 42 \text{ mg-Na/cm}^2$  under  $155 \text{ cm/sec}$  of linear flow rate. These values are quite different from the case of monolayer in Fig. 9 in spite of the same linear flow rate, i.e.  $5 \text{ mg-Na/cm}^2$ . It is considered that although most of aerosol would pass through openings in the first layer, a portion of aerosol might pass the filter media and the aerosol would be filtered efficiently as much as  $100 \%$  due to very low flow rate.

On the other hand, the second layer could trap sodium aerosol efficiently because of high air flow rate during passing through openings of the first layer: One mechanism is by filtration through filter media and the other is by inertia collision on the surface of filter media on which sodium aerosol was deposited. When sodium aerosol is loaded gradually on the second filter media, the air jets would be enlarged around the clogged portions.

Table 6 Result of Na loading on each layer.

Run No.	Intervals of Layers(mm)	Temp. (°C)	R.H. (%)	1 st (g)	2 nd (g)	3 rd (g)	4 th (g)	5 th (g)	Total (g)	Total Feed (g)	$\eta$ %
53-15	Air Flow →  A	11	50	156.5	196.0	78.6	41.1	47.3	519.4	694.4	74.8
53-16	→  B	6.5	54	112.4	233.2	82.7	54.1	47.2	529.6	1052.9	50.3
53-17	→  C	9	59	108.0	108.0	74.0	87.5	128.0	505.5	604.7	83.6
53-18	→  D	14	68	68.0	52.8	41.3	33.0	28.8	223.9	313.6	71.4
53-20	→  E	6.5	62	104.0	145.5	75.0	58.3	46.7	429.5	672.1	63.9
53-21	→  F	6.5	62	82.0	102.0	40.5	44.2	40.3	309.5	918.4	33.7

$$\% \eta = \frac{\text{Total Loading (g)}}{0.8 \text{ g/m}^3 \times 28 \text{ m}^3/\text{min} \times \text{Time (Min)}} \times 100$$

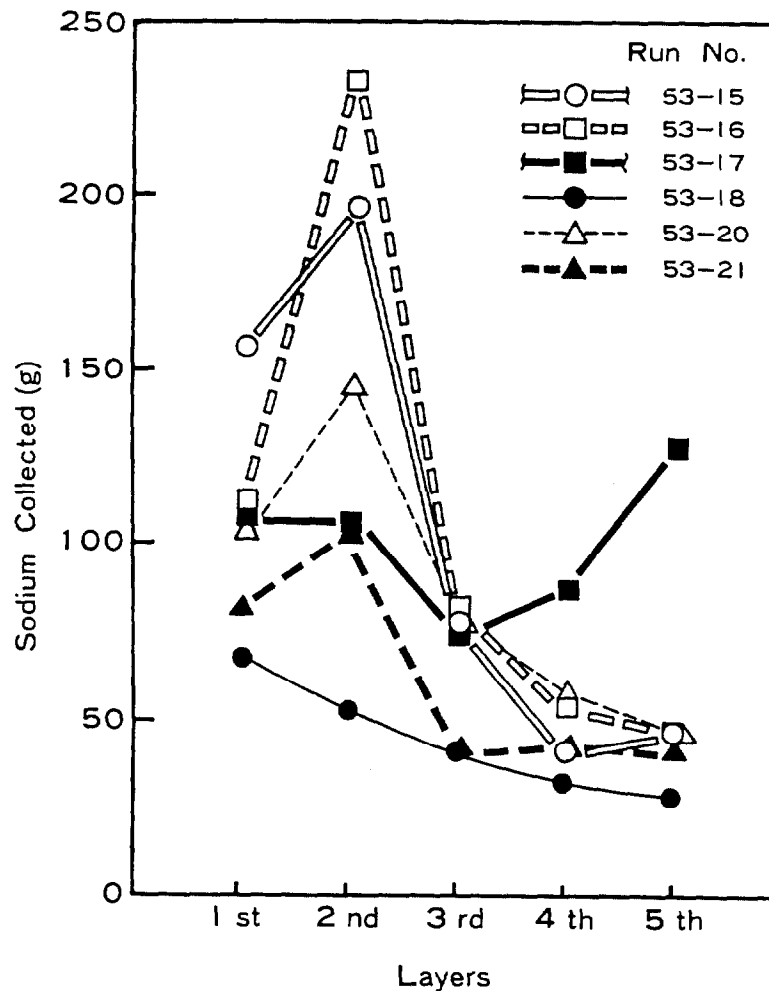


Fig.10 Results of Na loading on each layer.

The controlling factor of the pressure drop was examined by applying metal plates with openings by arranging them according to Table 3. The type A showed 0.3 kPa and the type F 0.32 kPa. This means that the pressure drop mainly arises by air flow through openings, but not by collision of air jet onto the plate. It is estimated that the increase of pressure drop may be arisen by clogging of openings by sodium aerosol. So that, it is necessary to evaluate not only the removal efficiency of aerosol, but also the pressure drop. It is found that the second layer contributes effectively towards the solution of high holding of sodium aerosol with low increase of pressure drop. In other words, if tried to distribute sodium aerosol equally over every layer, the aerosol deposited worked to clog the openings of layers. From the results, the interval among the layers was taken 20 mm equally, because it gave better effectiveness and also simplicity for manufacturing.



# 19th DOE/NRC NUCLEAR AIR CLEANING CONFERENCE

## Effect of humidity

The effect of humidity on the emergency air filter system of FBR was concerned. The test was carried out for the overall filter system. The results are shown in Table 7. The increase of pressure drop was given as a function of time in Fig.11. The overall pressure drops with loading of sodium aerosol on the filter system are summarized in Fig.12 with respect to the absolute humidity. It is found that the higher the absolute humidity, the lower the increase of pressure drop. From the result, it is concluded that the minimum loading of sodium aerosol is 800 g-Na per one filter system. The effect of water droplets on the filter system was also examined. Water droplets could reduce the increase of pressure drop definitely as shown in Fig.13.

Table 7 Na aerosol loading test.

	Run No.	Temp. (°C)	R.H. (%)	D.P. (°C)		Multilayer Type Filter	Medium Filter	HEPA Filter	Total
In Normal Air	53-1	22.5	74	17.5	Na Loading (g)	527.5	179.6	274.9	981.0
					$\eta_w$ (%)	53.7	39.5	$\approx 100$	
	53-3	26.5	34	9.1	Na Loading (g)	616.3	199.1	120.1	935.5
					$\eta_w$ (%)	65.9	62.4	$\approx 100$	
	53-14	11.5	90	9.6	Na Loading (g)	623.9	148.8	231.3	1,004.0
					$\eta_w$ (%)	62.1	39.1	$\approx 100$	
	53-22	6.5	62	0	Na Loading (g)	392.7	277.1	152.2	822.0
					$\eta_w$ (%)	47.8	64.5	$\approx 100$	

19th DOE/NRC NUCLEAR AIR CLEANING CONFERENCE

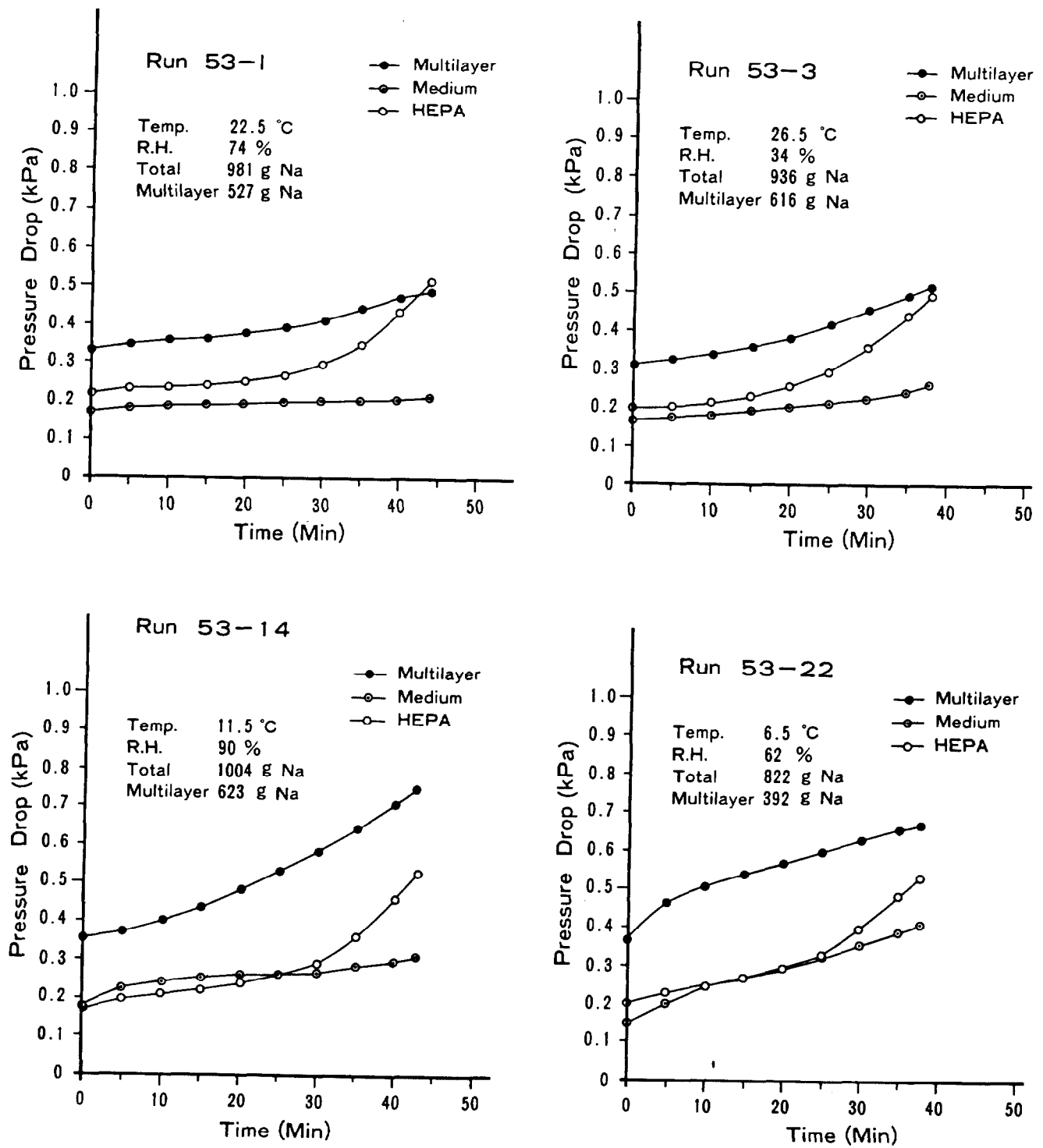


Fig. 11 The change of pressure drop as a function of time.

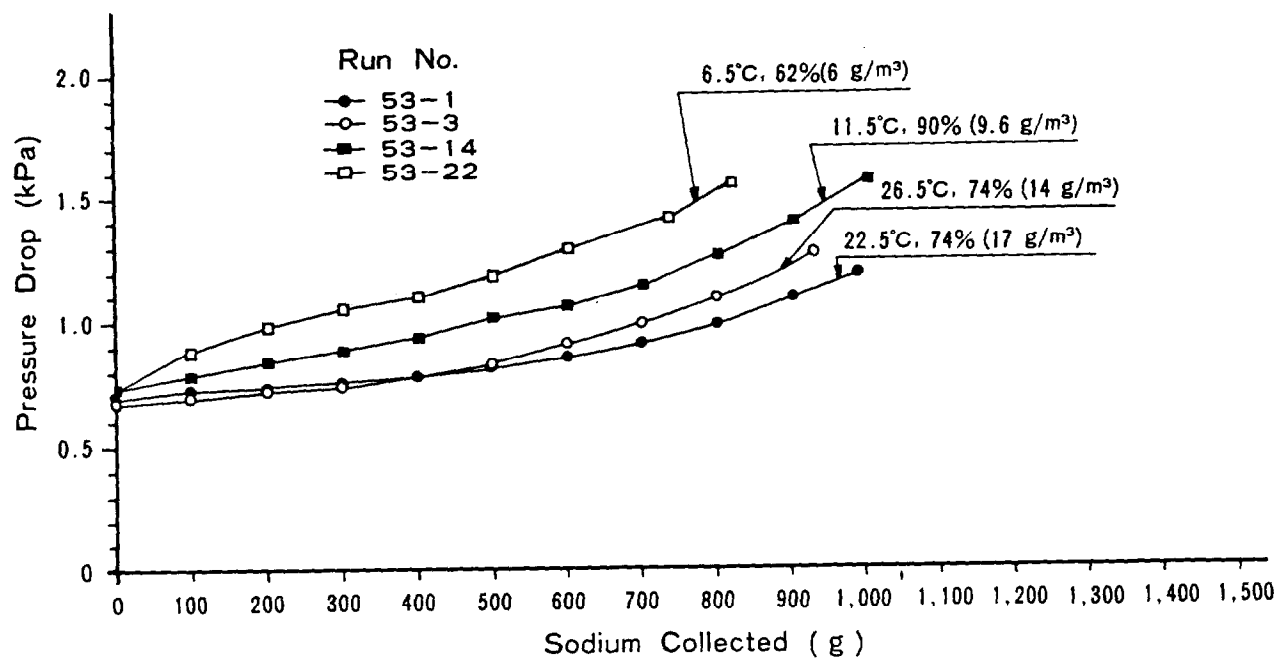


Fig. 12 The change of pressure drop during loading of sodium aerosol.

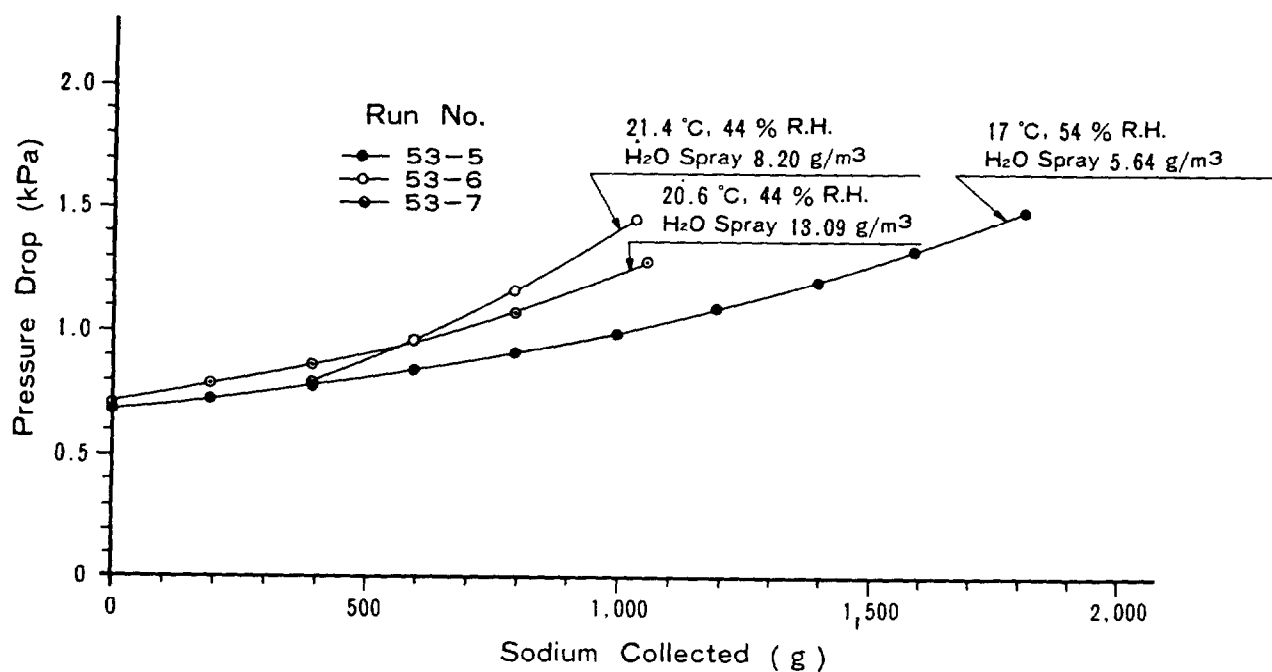


Fig. 13 The change of pressure drop during loading of sodium aerosol.

## 19th DOE/NRC NUCLEAR AIR CLEANING CONFERENCE

### IV. Summary

- (1) A filter system consisting of a multilayer type filter - a medium filter - a HEPA filter with standard size (610mm X 610mm) were examined to develop an emergency air filter system of FBR, where the multilayer type and medium filters are for protection of HEPA filter.
- (2) High silica content glass fiber was selected for the filter media for the multilayer type filter as well as the medium filter.
- (3) A series of run were carried out for the design of multilayer type filter to remove aerosol effectively. The filter consisted of 5 layers of fiber mat with openings of 20 mm in diameter and opening area of 20 %.
- (4) The high humidity reduced the increase of pressure drop of the filter system.
- (5) It was confirmed that an emergency air filter system of FBR consisting of a multilayer type filter - a medium filter - a HEPA filter with standard size as 610mm X 610mm in series could hold 800 g-Na at 1.5 kPa of the overall pressure drop.

### Reference

- (1) Private communication with Dr. Kitani, S., Messrs. Uno, S., Takada, J., and Takahashi, K. of Japan Atomic Energy Research Institute. (1972)
- (2) Jordan, S., Alexas, A., Lindner, W., Filtration of Sodium Fire Aerosol, Trans. Am. Nucl. Soc., 24, 526 (1977)
- (3) McCormack, J. D., Hilliard, R. K., and Barreca, J. R., Loading Capacity of Various Filters for Sodium Oxide/Hydroxide Aerosols, Proceeding of 15th DOE Nucl. Air Cleaning Conf.,
- (4) Bohn, L., Jordan, S. and Schikarski, W.: Experiments on Filtration of Sodium - Aerosol by Sand-Bed-Filters, CONF-740401, 461 (1974)

## 19th DOE/NRC NUCLEAR AIR CLEANING CONFERENCE

### DEVELOPMENT AT THE KARLSRUHE NUCLEAR RESEARCH CENTER (KfK) OF REMOTELY OPERATED FILTER HOUSINGS AND FILTER ELEMENTS FOR REPROCESSING PLANTS

K. Jannakos, H.J. Becka, G. Potgeter, - IT  
J. Furrer - LAF II  
Kernforschungszentrum Karlsruhe  
Federal Republic of Germany

#### Abstract

Under the Reprocessing and Waste Treatment Project (PWA) development work is carried out at the KfK on fabricating and testing remotely operated filter housings and filter elements for wet and dry aerosol retention. The remotely operated filters are used mainly to clean gaseous effluents containing a high portion of radioactive aerosols, e.g. for cleaning dissolver offgases from reprocessing plants.

Development work on the remotely operated filter housings has produced a third generation of filter housings which are modular in design so that in an accident parts of the housing and of the remote handling mechanism, respectively, can be replaced by remote operation using a crane and a manipulator.

The development of filter elements for aerosol retention started from the rectangular design via a quasi-circular design to a polygonal filter element for dry aerosol retention. This filter element is suited for gas flows up to 3000 m<sup>3</sup>/h and temperatures up to 200 °C. It can be replaced by remote handling and compressed to about one third of its volume so that the waste volume can be minimized.

Remotely operated filter elements with circular packed fiber glass (single ring layer filter) are used for wet aerosol retention. The packed surface available with a packing thickness of about 50 mm governs the maximum gas flow achievable. It has been the goal of development work to optimize the packed surface for a specified size of the filter element in order to keep low the number of filter units needed to purge a gas flow. Two variants of filter elements have been developed, the double ring layer filter and the star-shaped layer filter.

The technical development of the filter elements has now been completed but testing is still going on, above all as regards remote handling, tightness, decontamination factor for various offgas parameters (humidity, temperature, pressure, NO<sub>x</sub>), corrosion, and under accident conditions.

#### I. Introduction

For cleaning offgases carrying a high activity inventory in nuclear facilities - e.g. the dissolver offgas in reprocessing - special filters and remote handling devices are needed which

## 19th DOE/NRC NUCLEAR AIR CLEANING CONFERENCE

guarantee a high removal efficiency largely verifiable, are safe in operation and amenable to remotely operated replacement, packaging and removal of the loaded filter elements from the site.

Considering the development work underway as well as planning work on a reprocessing plant in the Federal Republic of Germany, development of suitable filters and remote handling devices for cleaning the dissolver offgas of large reprocessing plants was started in 1975 under the Reprocessing and Waste Treatment Project (PWA). The objectives included:

- Development and testing of a remotely operated filter housing for accommodation of aerosol and iodine filter elements inclusive of the necessary handling devices.
- Development and testing of filter elements capable of remote replacement for retaining total volume flows of aerosols and iodine of up to 3000 m<sup>3</sup>/h.

Some of the development work, mainly that part related to filter housings and remote handling, was already reported in 1980 at the 16th DOE Nuclear Air Cleaning Conference (1).

The technical development has meanwhile been completed. Testing of the improved filter housing and filter elements is still going on, above all as regards remote handling, tightness, removal efficiency for various offgas parameters (e.g. humidity, temperature, pressure, NO<sub>x</sub>), accident conditions, and corrosion phenomena.

In this report the remotely operated filter housing and the filter elements are described and operating experience accumulated until now on remote handling, readiness for operation, corrosion and sealing behavior is presented.

### II. Remotely Operated Filter Housing

In the course of development work concentrating on special applications three generations of filter housings have been developed. They differ mainly in their remote handling and maintenance concepts which had been worked out for the filter cell depending on the status of development work.

Figure 1 shows the filter housing of the third generation. It consists of the vessel with the hinged lid and clamping mechanism. The vessel is of vertical design. The connections for gas inlet and outlet and for cleaning the inner housing wall and monitoring the tightness of the filter element seat are provided on the vessel. The filter element is installed in the vessel in such a manner that it ensures a gastight isolation between the upstream and downstream air faces. The filter element can be passed by the flow either axially or radially, depending on the type of the filter element (iodine or aerosol filter) used.

The filter housing is suited for accommodating filter elements capable of retaining iodine, wet and dry aerosols. The lid and clamping mechanism are the same in all filter elements; only at the filter housing minor modifications are necessary. Figure 1 shows an

1500

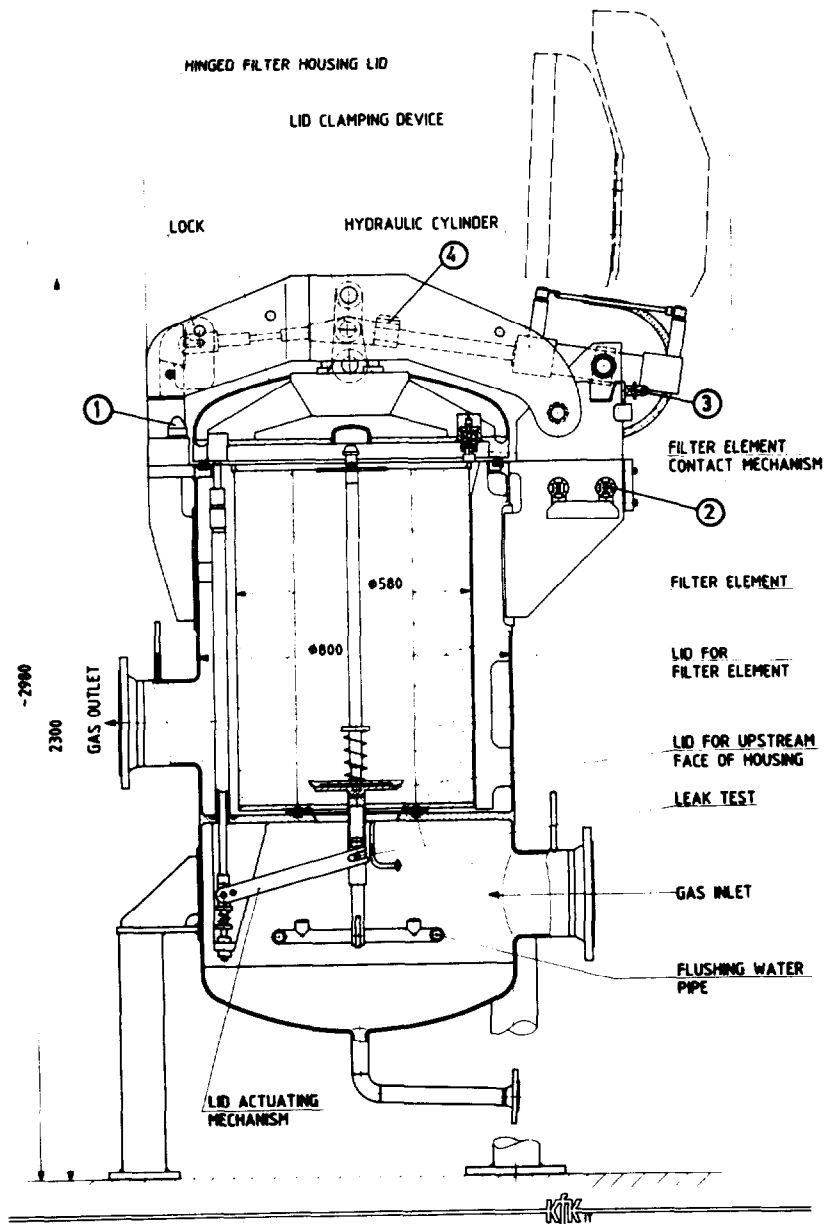


FIGURE 1  
REMOTELY OPERATED FILTER HOUSING WITH HEPA FILTER

aerosol filter element. The filter housing can be optionally provided with a lock mechanism in order to avoid that the downstream face of

## 19th DOE/NRC NUCLEAR AIR CLEANING CONFERENCE

the filter housing becomes contaminated during filter changeout. The locking plate of the filter housing at the inlet of the filter element is automatically controlled via an actuating bar from the lid of the housing. The aperture towards the filter element is open when the lid of the housing is closed and closed when the lid of the housing is opened.

The clamping mechanism (carrying the lid of the housing) is installed at the housing in such a manner that it can be hinged and is actuated hydraulically. When the housing lid is closed the clamping mechanism is the first part that contacts the locking hook. The lid does not yet contact the sealing of the housing. As the movement of the hydraulic piston continues, the contact mechanism gets locked, the lid is moved vertically downwards via the elbow lever joint and the guide bolts and pressed onto the sealing. When the hydraulic piston has reached its end position the elbow level joint is above the central axis and self-supporting. This means that the lid of the housing remains closed in the absence of hydraulic pressure. The filter element is pressed by the lid via plate spring gaskets. These also serve to compensate fabrication tolerances or elongations of the filter element during operation. The maximum possible clamping force for the lid and filter element is about 100 kN. A maximum of 40 kN is required. About 20 kN each are needed for the lid of the housing and the filter element. The total clamping force or the individual clamping forces for the lid and filter element, respectively, can be optionally indicated at the operator's panel. This indication supplies valuable information about the condition of the sealing of the housing and the pressure applied to the filter element.

The hydraulic system for opening and closing of the housing lid is outside the filter cell. Only two lines of about 10 mm outer diameter lead to the filter housing.

The inner diameter and the height of the filter housing can be adapted to the requirements. To this day filter housings of up to 790 mm inner diameter and 840 mm inner height have been tested. The filter housings have been designed for the pressure range of 0 to 2.5 bar absolute pressure. Figure 2 shows the filter housing installed in the test bench.

The description above applies to all three generations of filter housings. For the third generation the lid and the hydraulic cylinder have been designed in conformity with the status of the handling technique developed for the German reprocessing plant in such a manner that they can be replaced remotely in case of failure. It can be noted in Fig. 3 that a crane and a heavy load manipulator are required to equip the filter cell. This equipment is adequate for filter cells accommodating a large number of filter housings.

Should the hydraulic cylinder fail, the hydraulic lines equipped with rapid action couplings are decoupled from the housing with the heavy load manipulator, the fastening bolts for the hydraulic cylinder are withdrawn and laid down in the magazine and the hydraulic cylinder is lifted with the crane, removed and posted out. A new hydraulic cylinder is mounted in the reverse order.



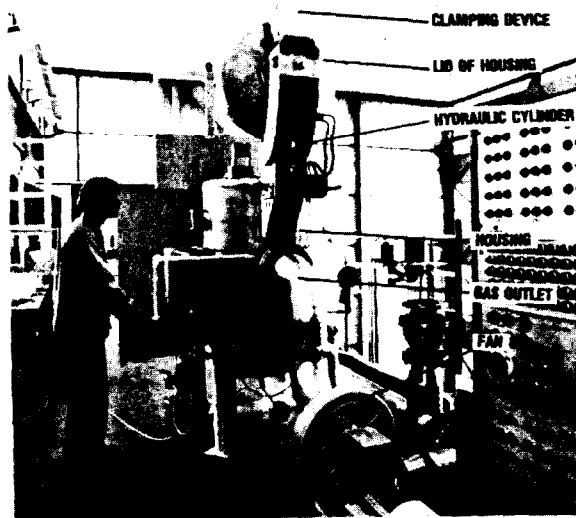


FIGURE 2  
TEST FACILITY  
FILTER HOUSING WITH OPEN LID

Figure 4 shows the withdrawal of the fastening bolt for the hydraulic cylinder and Fig. 5 shows the removal of the disassembled cylinder during the phase of testing.

If the mechanism at the housing lid fails, it is replaced together with the clamping device. The lid in the contacted state (Fig. 1) is dismounted as follows: The two fastening screws (<sup>1</sup>) are screwed out with a screwdriver provided at the manipulator (thus relieving the clamping device), the two fastening bolts (<sup>2</sup>) are withdrawn and the hydraulic lines decoupled. A transport device is coupled to the lid using the crane and the manipulator so that the lid can be lifted and removed (Fig. 6). The repaired or the new lid is mounted on the housing in the reverse order.

The sealing between the lid and the housing which is attached to the housing is replaced remotely using a special device.

The third generation of filter housings has been tested since early 1986. Testing has related mainly to remote handling because the clamping mechanism and the filter housing had been tested already sufficiently for the first and second generations.

The first generation of filter housings (Fig. 7) has been designed in such a way that in case of failure of the mechanism of the lid the latter can be opened and closed with an emergency lever operated by the crane (without locking). After the loaded filter element has been withdrawn and the inner housing surfaces cleaned the mechanism of the lid can be repaired either in situ by staff wearing protective clothes or the lid can be dismounted from the

HYDRAULIC CYLINDER

MANIPULATOR GRAB

FASTENING BOLT  
OF HYDRAULIC CYLINDER

431

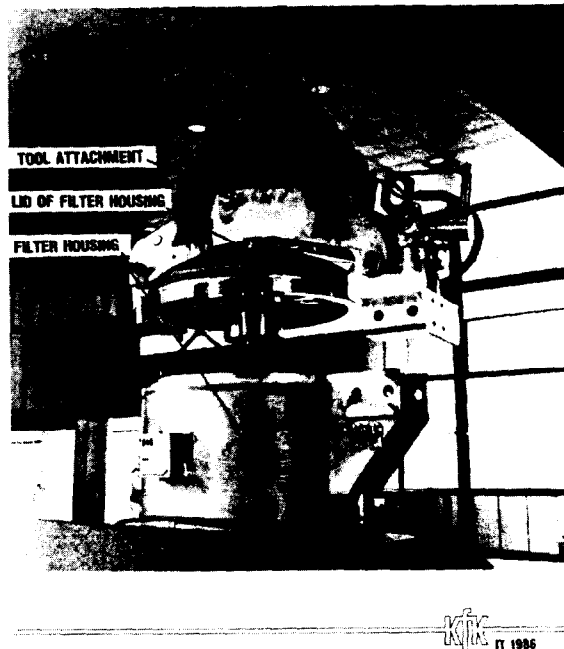


FIGURE 6  
FILTER HOUSING  
REMOTELY OPERATED LID REMOVAL

housing and repaired outside the filter cell. This design of the housing is particularly suited for small filter systems which can be cleansed and taken out of service before the filter cell is entered.

The filter housings of the first generation have undergone a sufficient amount of testing since 1978 with iodine and aerosol filter elements (three filters). The offgas values (temperature, pressure, iodine and  $\text{NO}_x$  fractions, aerosols, steam) selected for the filter testing phase resembled largely those which are expected to occur in the dissolver offgas of a reprocessing plant.

Since 1984 housings of this type have been used together with HEPA and fiber pack filters in the PAMELA (vitrification pilot plant for HLLW) facility which started active operation in 1985. According to information received from the operator, DWK, they have so far performed well with a high decontamination factor (fiber pack filter =  $3 \times 10^3$ , two HEPA filters in series  $> 10^5$ ).

As the filter housing can be readily handled, there have been no errors in handling so far. No wear and corrosion phenomena have been visible although the filter housings have been made from the usual stainless steel, material No. 1.4541. The sealing of the housing consists of a silicon mixture resistant to  $\text{NO}_x$ , steam and  $\text{HNO}_3$ . Following the initial permanent deformation of the sealing (about 5%) no further changes have been detected.

## 19th DOE/NRC NUCLEAR AIR CLEANING CONFERENCE

In the filter housings of the second generation (Fig. 8), developed for a specific purpose, the vessel of the filter housing has been screwed to the bottom of the filter cell. The bottom of the filter cell has been made as shielding so that the radiation emanating from the gas lines and the loaded filters is adequately attenuated and work can be performed in the filter cell. The lid of the filter housing which is likewise provided with a shielding of the same thickness as the bottom of the cell, is installed on the cell bottom. Emergency handling devices as used for the first and third generations of housings can be dispensed with because the filter cell can be entered in protective clothes for doing repair work. This filter design has been tested since 1980 using the same offgas values as in the first filter generation (two filters). No differences have been observed in filter handling, corrosion, wear, removal efficiency and reliability, compared with the first generation of filter housings.

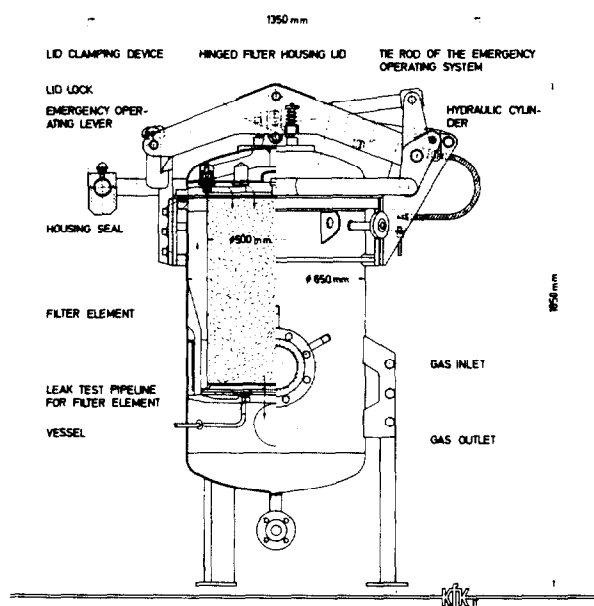


FIGURE 7  
REMOTELY OPERATED FILTER HOUSING  
WITH IODINE FILTER ELEMENT  
(VERTICAL DESIGN)

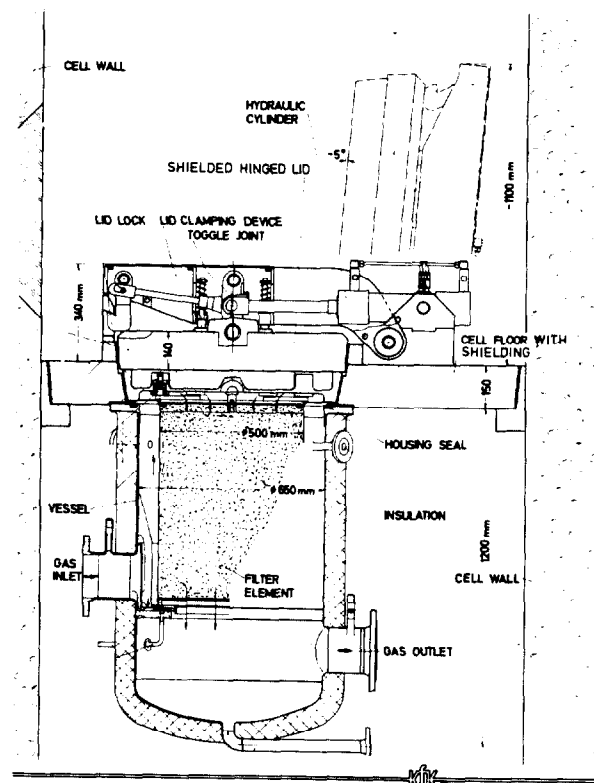


FIGURE 8  
REMOTELY OPERATED "SUSPENDED"  
FILTER HOUSING WITH SHIELDING  
AND THERMAL INSULATION

### III. Filter Element for Aerosols (HEPA)

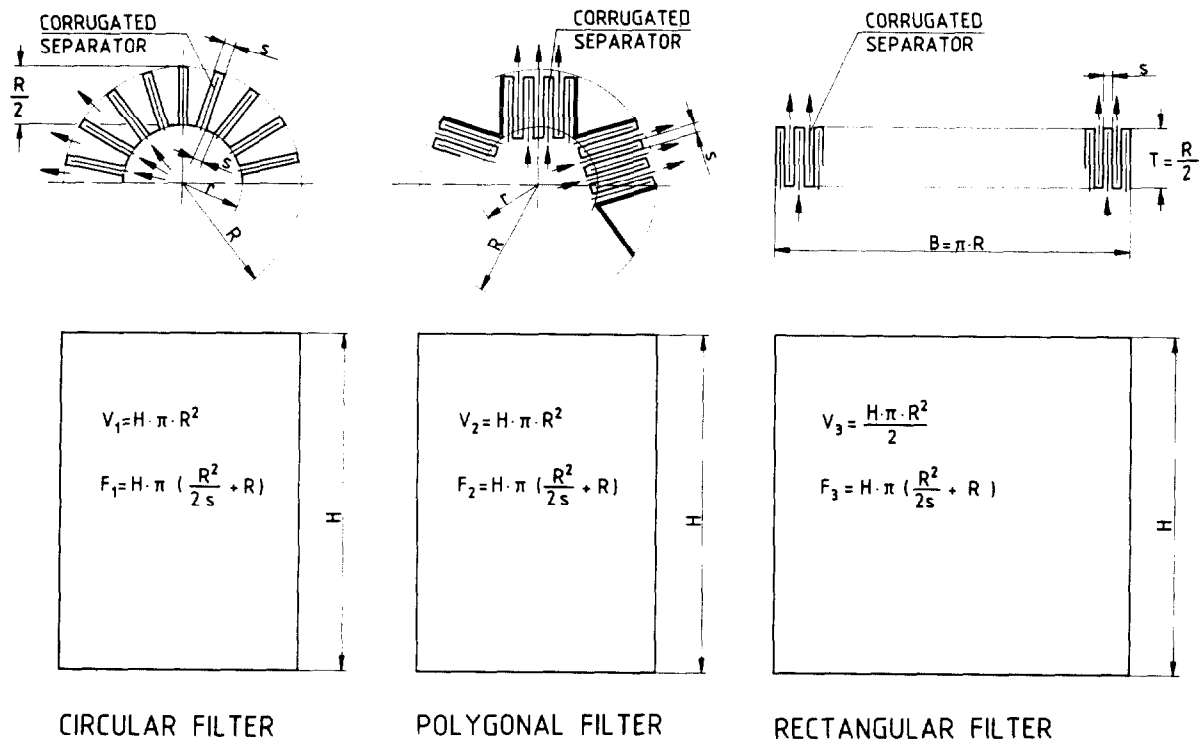
To retain aerosols in offgases carrying a high portion of radioactive aerosols, e.g. dissolver or vessel offgas in reprocessing, filter elements are needed which largely meet the following conditions:

## 19th DOE/NRC NUCLEAR AIR CLEANING CONFERENCE

- a) Operating conditions: The filter elements shall be resistant to
- high permanent temperatures of about 150 °C,
  - pressure variations,
  - acid,
  - NO<sub>x</sub> and iodine.
- Moreover, they shall ensure
- a high permanent removal efficiency,
  - a good and verifiable seat of the sealing.
- b) Handling conditions: The filter elements shall have the following characteristics:
- mechanical protection from damage from outside (transport, installation) and from inside (gas entrained particles),
  - adequate strength,
  - capability of remote handling.
- c) Conditions regarding ultimate disposal and rentability: The filter elements shall have the following characteristics:
- small volume of waste (compressible),
  - low weight (minimum amount of stainless steel material),
  - large paper filter surface and small filter volume (low number of filters),
  - convenient fabrication (little machining of individual components).

### III.1 Generalities

Until this date rectangular filter elements (about 140 mm width, about 270 mm height) have been used in the Federal Republic of Germany to filter offgases carrying a high fraction of radioactive aerosols, e.g. the dissolver offgas in pilot and testing facilities. These rectangular filter elements are screwed to a pentagonal stainless steel frame and sealed so that they make up a quasi-circular filter element. In terms of the paper surface available, the sealing, the required weight of the stainless steel mass and the compression, this design is highly unfavorable. Therefore, a new filter element has been developed which meets largely all requirements indicated under III. As the circular shape is the most favorable with a view to remote handling and ultimate disposal, it has been adopted. In order to be able to transfer to the new filter element the good results in operation and removal efficiency which had been obtained during operation and in many years of testing quasi-circular filter elements, the paper quality, the paper format, the spacing of pleats, the spacers and the packing density have been maintained so that only a new polygonal filter paper support has been developed. The polygonal filter element combines the advantages of the circular and rectangular filter elements in an optimum manner. The surface of the filter paper (Fig. 9) is of the same size with the radius (R), height (H) and spacing of pleats (s) specified in advance. However, no spacers can be provided in the circular filter element in the pleats, which are open towards the outside, because the distances between the paper pleats undergo radial changes. Also preliminary pressing of the filter paper, as performed in the rectangular filter element in order to make the block more stable, cannot be practiced. In the polygonal filter element both disadvantages can be avoided.



$r = 145$   
 $R = 290$   
 $H = 820$   
 $F_1 = F_2 = F_3$

FILTER PAPER SURFACE FOR CIRCULAR FILTER  $F = H \left[ \frac{2 \cdot \pi \cdot r}{s} (R - r) + 2 \cdot \pi \cdot r \right]$   
 CONDITION FOR MAX. FILTER PAPER SURFACE  $\frac{dF}{dr} = 0 \rightarrow r = \frac{R+s}{2}$

FIGURE 9  
COMPARISON OF SIZES AND ARRANGEMENT OF FILTER  
PAPERS OF VARIOUS FILTER ELEMENTS

The conditions to be met for a maximum filter paper surface of circular and polygonal filter elements, respectively, with the external radius specified, is  $dF/dr = 0$ . The paper surface is

$$F = H \left[ \frac{2 \pi r}{s} (R - r) + 2 \pi r \right]$$

where:

- F = filter paper surface,
- r = inner radius of the filter,
- R = outer radius of the filter,
- H = filter height.

## 19th DOE/NRC NUCLEAR AIR CLEANING CONFERENCE

In order to satisfy the condition above,  $r$  must be approximately  $R/2$  [precisely  $r = (R+s)/2$ ]. For this value the paper surface is

$$F = H\pi \left( \frac{R^2}{2s} + R \right)$$

Consequently, with the values given for the filter radius and filter height, it depends solely on the spacings between the pleats. Considering the filters used and tested until now, it has been chosen to lie between 2.5 and 4 mm.

Figure 9 shows for the same filter paper surface the true scale size of a circular, a polygonal and a normally used rectangular filter element.

It can be expected (the relevant tests have not yet been completed) that the polygonal filter element behaves more favorably as regards tearing and blowing out of the filter paper exposed to fluctuations in pressure and mass, compared to the currently used rectangular filter element, because it is made up of smaller individually supported paper surfaces.

### III.2 Description of the Polygonal Filter Element

The polygonal filter element, Fig. 10, consists of the filter paper and the frame. The frame is made up of a bottom and a lid connected with each other by a supporting tubular structure. The seat gasket is glued to the bottom and fastened in addition by a holding ring. Both faces of the gasket (glued and contacting faces) are monitored for tightness during operation. The force from the lid to the bottom gasket is transmitted via the supporting structure. The filter paper provided is endless and glued at both ends: It is divided into five filter chambers by the V-spacers; the inner and outer surfaces of these chambers are of the same width. To provide better protection under conditions of pressure and gas mass fluctuations, the filter paper is contacted with the help of the V-spacers and glued to the latter. The lower front faces of the filter paper and the V-spacers are embedded into a special sealant on the sheet metal bottom and sheet metal lid, respectively. Except for the installed condition, the bottom opening for gas inlet is always closed so as to be largely tight with the help of the locking plate which is closed automatically by gravity.

As a protection against damage from outside a screen has been provided in front of the filter surfaces. Figures 11 and 12 show a polygonal filter element for a maximum gas flow of about 3000 m<sup>3</sup>/h. Dimensions of this filter element: diameter 580 mm, height 900 mm. The surface of the filter paper is 35.4 m<sup>2</sup> for  $s = 2.8$  mm; this gives a maximum face velocity of the gas of 2.4 cm/s. The filter element weighs about 30 kg. The maximum pressure loss of the not loaded filter element, without locking plate, is about 25 mm WC for a gas flow of 3000 m<sup>3</sup>/h.

In order to find out whether the filter element is capable of withstanding higher temperatures, leading e.g. to tearing of the paper as a result of deformation of the frame in the axial direction,

19th DOE/NRC NUCLEAR AIR CLEANING CONFERENCE

the frame was heated to 200 °C in a furnace. No damage of the filter element was observed up to this temperature level.

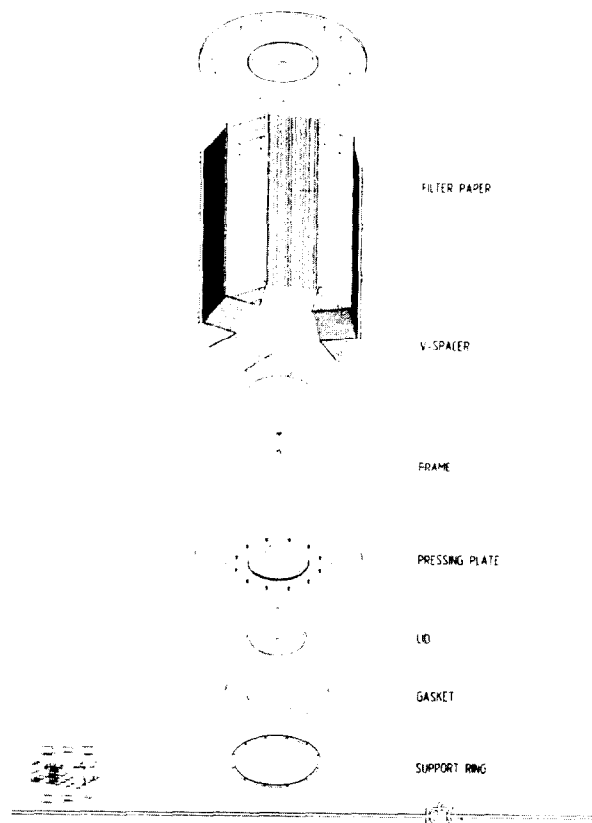


FIGURE 10  
POLYGONAL FILTER ELEMENT (HEPA)

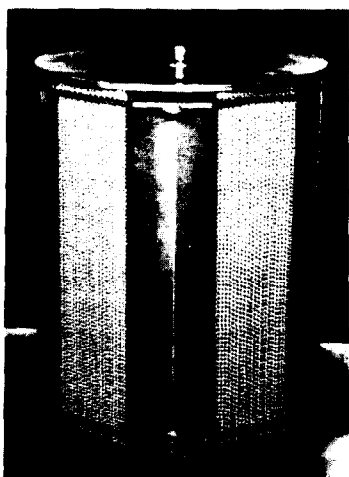


FIGURE 11  
POLYGONAL FILTER ELEMENT (HEPA)  
TOP PLAN VIEW



FIGURE 12  
POLYGONAL FILTER ELEMENT (HEPA)  
INVERTED PLAN VIEW



## IV. Filter Elements for Wet Aerosol Retention

## IV.1 Generalities

To filter wet aerosols from offgases having high contents of radioactive aerosols, remotely operated filter elements with fiber glass packings are used. In the Federal Republic of Germany single ring layer filters with fiber glass packing are used to filter radioactive offgases from pilot and test facilities upstream of the HEPA filters (Fig. 13). The gas face velocity is limited (about 6 -8 cm/s) in order to achieve optimum operating conditions (low pressure loss, high removal efficiency).

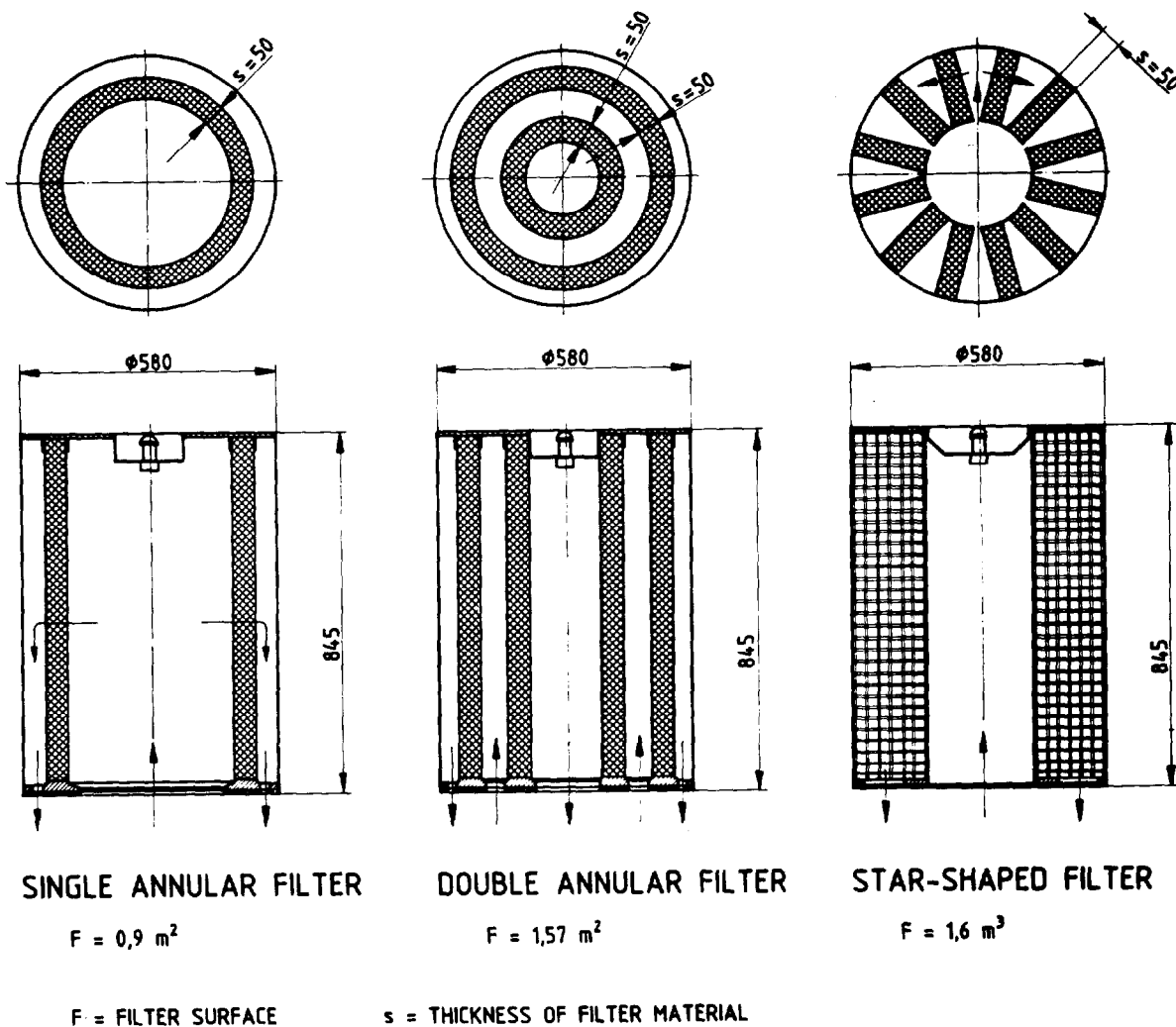


FIGURE 13  
 PACKED FIBER MIST ELIMINATOR  
 COMPARISON OF THE FILTER SURFACES

Consequently, for a given gas flow the number of the filter units required is dependent on the filter surface of the fiber glass packing available. The number of filter units should be kept as low as possible. In the single ring layer filters the filter surface depends only on the filter height provided that the diameter is defined in advance. However, if standard waste drums are used for ultimate disposal, the filter height is limited to 850 mm. In order to optimize the filter surface for a given volume of the filter element, two further solutions have been elaborated, namely a double ring layer filter and a star-shaped layer filter.

Figure 13 shows for comparison of the three alternatives the filter surfaces available for identical external sizes of the filter elements, as well as the schematic layout of the three solutions. The single ring layer filter has been tested under cold conditions in the PASSAT facility since about 1978 and under active conditions in the PAMELA facility since 1985. The decontamination factor is  $3 \times 10^3$ .

#### IV.2 Double Ring Layer Filter

The double ring layer filter, Fig. 14, is composed of the filter frame and the filter material. The filter material consists of glass fibers and is identical with the filter material used in the proven single-ring layer filter. The layer thickness is about 50 mm. The filter frame is made up of the bottom to which the gaskets of the seats have been mounted similar to the mounting in the HEPA filters, the jacket, the lid and the tubular structure connecting the lid with the bottom. The contact forces for the gaskets of the seats are transmitted to the bottom via the tubular structure. To support the fiber glass layers concentric stainless steel screens, cylindrical in shape, have been fastened between the bottom and the lid. The non-filtered air flows from the bottom into the annular space between the two fiber glass ring layers, passes them in the radial direction and leaves the filter element towards the bottom through the central opening and the external annular gap. Water nozzles have been provided below the gas inlet annular gap so that the fiber glass layers in the filter housing can be flushed.

The main disadvantage of this filter element consists in three times sealing required with respect to the filter housing: two gaskets between the inflowing and outflowing gas and one between the filter element jacket and the filter housing in order to avoid a high contamination of the inner surfaces of the filter housing. The main advantage consists in the easy mounting of the filter layers. The filter element has not yet been tested.

#### IV.3 Star-shaped Layer Filter

The star-shaped layer filter, Fig. 15, consists of the filter frame and the filter material. The filter material is composed of glass fibers and is identical with the filter material of the proven single-ring layer filter. The layer thickness is about 50 mm. The filter frame is made up of the bottom to which the gaskets are mounted as in the HEPA filter, the jacket, the lid and the inner

tube which transmits to the bottom the forces needed to press the sealing. To support the fiber glass layers, star-shaped stainless steel screens have been installed between the jacket and the inner tube. To flush the fiber glass layers, a nozzle system has been installed at the filter element and connected to the water pipe of the filter housing when the filter element is inserted into the filter housing.

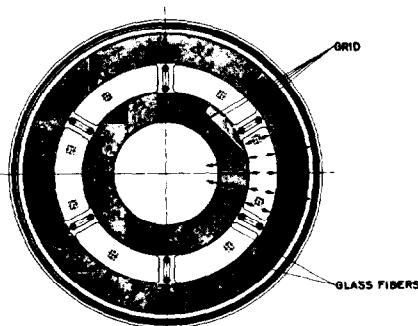
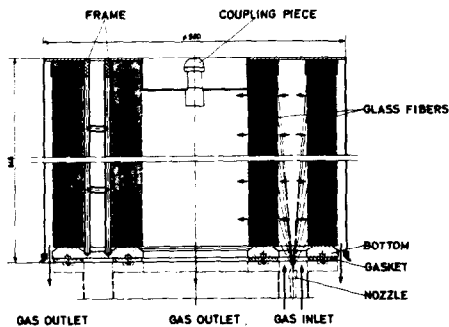


FIGURE 14  
PACKED FIBER MIST ELIMINATOR

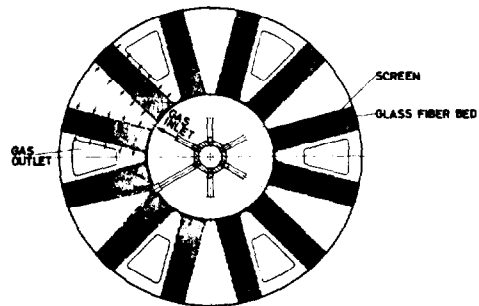
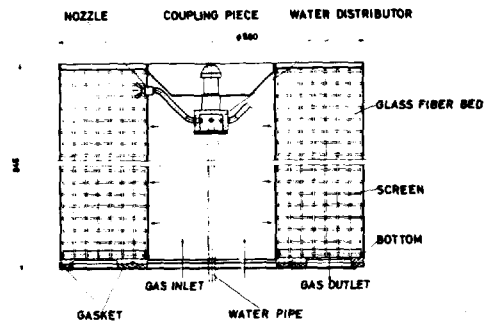


FIGURE 15  
PACKED FIBER MIST ELIMINATOR

The unfiltered air flows from bottom (Fig. 15) through the centric bottom opening into the filter element and through the longitudinal gaps of the filter element to the filter layers, passes them and leaves the filter element flowing downwards through the openings in the bottom provided for this purpose. The filter element is equipped with a gasket between the inflowing and out-flowing gas and a gasket between the filter element jacket and the filter housing in order to avoid excessive contamination of the inner surfaces of the filter housing.

The main disadvantages of this filter element is the costly provision of the stainless steel screen as well as the requirement of stuffing the filter material. The main advantage consists in simple sealing and force transmission to the sealings. The filter element has not yet been tested.

## 19th DOE/NRC NUCLEAR AIR CLEANING CONFERENCE

### References

- (1) Jannakos, K., Lange, W., Potgeter, G., Furrer, J., Wilhelm, "Selected solutions and design features from the design of remotely handled filters and the technology of remote filter handling. Previously operating experience with these components in the PASSAT facility," Proceedings of the 16th DOE Nuclear Air Cleaning Conference, Vol. 1, 317 (1980)
- (2) Furrer, J., Wilhelm, J.G., Jannakos, K., "Aerosol and iodine removal system for the dissolver offgas in a large fuel reprocessing plant," Proceedings of the 15th DOE Nuclear Air Cleaning Conference, Vol. 1, 494 (1978)
- (3) Jannakos, K. et al., Furrer J., Wilhelm, J.G., "PASSAT - eine prototypische Abgasfilteranlage. Beschreibung und bisherige Betriebserfahrungen," KfK-Nachrichten 3/79

## 19th DOE/NRC NUCLEAR AIR CLEANING CONFERENCE

### CLOSING COMMENTS OF SESSION CO-CHAIRMAN ETTINGER

We have had a look at unique applications of filtration and new approaches to filter testing. It has been a varied discussion ranging from waste disposal to sodium aerosols to uranium enrichment facilities. There have been unique concerns identified, ranging from remote operations, to a standby automated system, to a filter system where you can reuse the filters and meet corrosion and resistance requirements. The speakers have expressed a lot of concern about humidity and temperature effects. I think the message is that people are looking at new approaches to filtration. They range from a multi-layer approach, to the use of powders or fibers for filtration, and the drawing on other technologies such as liquid filtration. Also, some of the papers are concerned with very basic physics principles as related to the application of test methods using light scattering and fluorescence spectroscopy. An important consideration is how to adopt some of the new methods to produce new filter test methods and new filtration techniques. The two go together because we need new test methods to go with new filtration procedures. We also have to learn how to apply some of the new methods to reduce the harmful effects of humidity and temperature. That will permit us to design better filters, the aim of two of our speakers. It has been a very interesting and informative session.